SESSION 6

RECENT ADVANCES IN NUCLEAR TECHNIQUES AND INSTRUMENTATION

From Fertilizer to Food: Tracing Nitrogen Dynamics in Conventional and Organic Farming Systems Using ^{15}N Natural Abundance

P.M. Chalk[1,*], C.T. Inácio[2], and A.M.T. Magalhães[2]

ABSTRACT

Synthetic nitrogen (N) fertilizers differ markedly from organic N fertilizer sources in relative isotopic composition at natural abundance levels ($\delta^{15}N$). The objective of this paper is to provide an overview of the applications of $\delta^{15}N$ techniques to study the dynamics of synthetic fertilizers, animal excreta and composts in the soil-plant-atmosphere continuum. However, isotopic fractionation processes often complicate the interpretation of results. These fractionation processes and the factors affecting the $\delta^{15}N$ signatures of organic N fertilizers are reviewed. Published data from short-, medium- and long-term experiments with annual crop rotations and in pastures subject to organic N inputs are also examined and analyzed with respect to changes in delta nitrogen-15 ($\delta^{15}N$) signatures of the soil, the crop or pasture, the soil biota and leachates. The use of $\delta^{15}N$ to differentiate organic and conventional plant products is briefly covered. There are few data on the dynamics of N during the storage of animal excreta or the composting of agricultural wastes as shown by $\delta^{15}N$ values in the organic, inorganic or gaseous N phases. The major N loss process is ammonia (NH_3) volatilization. Reviewed data show significant relationships between bulk $\delta^{15}N$ signatures of stored manure and cumulative NH_3 loss or bulk $\delta^{15}N$ of livestock manure composts and N concentration. These significant relationships suggest that $\delta^{15}N$ may have wider applications in estimating the efficiency of N conservation during storage or composting. In addition, the combined use of bulk $\delta^{15}N$ and delta oxygen-18 ($\delta^{18}O$) signatures of nitrous oxide (N_2O) evolved during storage and composting, together with the isotopomer-derived site preference of N_2O, are emerging technologies for identifying N_2O production pathways. $\delta^{15}N$ in combination with appropriate statistical analysis is a promising diagnostic tool for differentiating organic and conventional plant products.

Key words: *animal excreta, compost, crop rotations, delta ^{15}N, isotopic fractionation, pastures.*

INTRODUCTION

In conventional farming systems the use of both synthetic and organic N fertilizers is permitted, whereas in organic systems only organic N sources may be used as fertilizer. The principal organic N fertilizer sources are animal excreta (manure and urine) and composts which may be derived from both animal wastes and crop residues. Organic fertilizer may also consist of human excreta or composts made from household or municipal wastes, including sewage sludge, but domestic- or municipally-derived organic fertilizers are not considered in this paper.

There are fundamental differences between synthetic and organic N fertilizer sources with respect to their ability to supply N for crop growth. Organic N sources must be biologically mineralized to inorganic N before they become available for plant uptake, whereas synthetic N fertilizers (ammonium and nitrate salts) are highly soluble in water and are readily available for plant uptake. Urea is the principal synthetic N fertilizer used in agriculture, and it is also quickly taken up by plants following its rapid enzymatic hydrolysis to ammonium in soil. Therefore, organic N fertilizers are often referred to as slow-release N sources, and are considered to be somewhat better synchronized with crop demand for N. However, organic fertilizers contain a mixture of both organic and mineral (NH_4^+ and NO_3^-) forms of N.

Both organic and synthetic sources are subject to several N loss processes which reduce their effectiveness to supply N for plant growth. Animal excreta must be collected and stored in intensive animal feeding operations before application to crops or pastures, and gaseous N losses (NH_3, N_2O, N_2, and other oxides of N (NO_x)) may occur during storage. Similar loss processes may occur during the composting of agricultural wastes. Nitrogen losses may occur following N fertilizer application to soil either via gaseous N emissions or nitrate leaching. Therefore it is important to estimate the N fertilizer use efficiency, and where possible to quantify the N loss pathways of synthetic and organic fertilizer sources during each phase of the continuum.

The use of the ^{15}N stable isotope is a basic tool for studying the dynamics of N in farming systems (Chalk, 1997). Both naturally-occurring differences in the relative abundance of ^{15}N in N sources, or the use of N sources artificially-enriched in ^{15}N can be used to trace the fate of fertilizer N. The literature on the application of ^{15}N to study N dynamics in animal excreta or compost-amended soils was reviewed by Dittert, Georges and Sattelmacher (1998) and Chalk, Magalhãese and Inácio (2013), respectively. The emphasis of these reviews was on quantifying post-application N use efficiency and N transformations in soil, rather than on N transformations prior to soil application i.e. during storage or composting. The objective

1 International Atomic Energy Agency, Wagramerstrasse 5, PO Box 100, 1400 Vienna, Austria
2 EMBRAPA-Soils, National Center of Soil Research, Brazilian Agricultural Research Corporation, Rua Jardim Botânico 1024, Rio de Janeiro, Brazil
* E-mail address of the corresponding author: chalkphillip@gmail.com

L.K. Heng, K. Sakadevan, G. Dercon and M.L. Nguyen (eds), Proceedings — International Symposium on Managing Soils for Food Security and Climate Change Adaptation and Mitigation. Food and Agriculture Organization of the United Nations, Rome, 2014: 339–348

TABLE 1. $\delta^{15}N$ signatures of animal diets and excreta

Animal	Diet	$\delta^{15}N$ (‰)			Reference
		Diet	Faeces	Urine	
Jersey cow	Pasture	+0.6	+2.6	–1.6	Steele and Daniel (1978)
Angus steer	Silage	+0.6	+2.1 to +2.5	–2.1 to –2.8	
Llama	Alfalfa	+0.4	+3.3	+0.1	Sponheimer *et al.* (2003)
	Bermuda grass	+5.8	+8.8	+3.7	
Swine	Not specified	+1.7 ± 1.0	+2.4 ± 0.9	–0.1 ± 1.1	Mariappan *et al.* (2009)
Dairy cow	Silage[1]	+1.8 to +8.4	+4.2 to +8.8	–0.9 to +4.1	Cheng *et al.* (2011)

[1] Nine individual silages were made from forage grasses (3 types), red clover, red clover mixed with corn or oats in different proportions

of the present paper is to provide an overview of the applications of the ^{15}N natural abundance technique to trace N transformations that occur during pre- and post-application of animal excreta and composts. The application of $\delta^{15}N$ to differentiate organic and conventional foodstuffs is only briefly covered, as this topic was comprehensively reviewed for plant products by Inácio, Chalk and Magalhães (2013).

Units of ^{15}N concentration

Stable isotopic values close to the natural abundance of the designated isotope are expressed by the notation (δ) in units of parts per thousand (per mil or ‰) relative to the international standard for that element (Chalk, 1995). Since N has only two stable isotopes (^{14}N and ^{15}N), then:

$$\delta^{15}N\ (‰) = \{[(^{15}N / {}^{14}N)_{sample} / (^{15}N / {}^{14}N)_{standard}] - 1\} \times 1\,000 \quad (1)$$

where the international standard is atmospheric N_2 ($\delta^{15}N$ = 0‰, by definition).

The $\delta^{15}N$ value can be either negative or positive depending whether it is depleted or enriched in ^{15}N relative to the standard.

Stable isotopic values of artificially-enriched samples are expressed as absolute abundance in units of atom $\%\,^{15}N$ (Chalk, 1995).

$$\text{Atom } \%\,^{15}N = (\text{number of } ^{15}N \text{ atoms / total number of } ^{15}N + {}^{14}N \text{ atoms}) \times 100 = [^{15}N / (^{14}N + {}^{15}N)] \times 100 \quad (2)$$

Thus as can be seen from Equation 2, it is incorrect to substitute atom $\%\,^{15}N$ for the $^{15}N/^{14}N$ ratio in Equation 1, as is sometimes seen in the earlier literature (e.g. Selles and Karamanos, 1986), and although a close approximation will be obtained it will nevertheless be an underestimate (Chalk, 1995).

Since the absolute ^{15}N abundance of atmospheric N_2 is 0.3663 ± 0.0004 atom % (Junk and Svec, 1958) then:

$$^{15}N \text{ enrichment (atom } \%\,^{15}N \text{ excess)} = \text{atom } \%\,^{15}N - 0.3663 \quad (3)$$

It is quite common in the literature to see atom $\%\,^{15}N$ incorrectly designated as ^{15}N enrichment. Atom % excess values are used to trace the pathways of ^{15}N-enriched fertilizers added to soil.

The relationship between the $^{15}N/^{14}N$ ratio and atom $\%\,^{15}N$ is given by:

$$^{15}N/^{14}N = \text{atom } \%\,^{15}N/(100 - \text{atom } \%\,^{15}N) \quad (4)$$

For atmospheric N_2:

$$^{15}N/^{14}N = 0.3663/(100 - 0.3663) = 0.00367647$$

$\delta^{15}N$ signatures of synthetic and organic fertilizers

Synthetic N fertilizers (ammonium salts and urea) are derived from ammonia (NH_3) produced by the Haber-Bosch process, which involves the catalytic reduction of atmospheric N_2 at high temperature and pressure by H_2 derived from methane or natural gas. Therefore the $\delta^{15}N$ signatures of synthetic fertilizers are expected to be close to that of atmospheric N_2 (0‰ by definition). A review of published data (Inácio, Chalk and Magalhães, 2013) shows that synthetic N fertilizers have slightly positive or negative $\delta^{15}N$ values within the range of –3.9 to + 5.9‰.

Organic N fertilizers are generally naturally enriched in the stable isotope ^{15}N compared with synthetic N fertilizers. A review of published data (Inácio, Chalk and Magalhães, 2013) shows that total N in manures and composts varies with $\delta^{15}N$ values in the range of +2.0 to +16.7 and +4.9 to +45.2‰, respectively. Animal excreta consist of both solid (dung) and liquid (urine) components, except for poultry where there is no urinary component. Dung and urine components often show marked differences not only in the relative amounts and N concentrations, but also $\delta^{15}N$ signatures.

Steele and Daniel (1978) reported that dairy and beef cattle urine was depleted in ^{15}N relative to the animal diet while manure was enriched (Table 1). Sponheimer *et al.* (2003) reported similar data for llamas, with faeces enriched in ^{15}N relative to both low- and high-protein diets, whereas urine was depleted in ^{15}N (–2.1‰) relative to the low-protein diet, but was not significantly different from intake $\delta^{15}N$ on the high protein diet (Table 1). Mariappan *et al.* (2009) similarly reported swine urine depleted in ^{15}N relative to diet and faeces (Table 1). More recently, Cheng *et al.* (2011) reported both positive and negative $\delta^{15}N$ values for the urine of dairy cows, while manure was always positive (Table 1). Urine was invariably depleted in $\delta^{15}N$ relative to diet, while faeces were either similar to or enriched in $\delta^{15}N$ relative to diet (Cheng *et al.*, 2011). A highly significant positive linear relationship was found between the $\delta^{15}N$ values of the feed (range of +2 to +8.5‰) and faeces (range of +4 to +9‰) (Cheng *et al.*, 2011).

Organic fertilizers contain both organic and inorganic [ammonium (NH_4^+) and nitrate (NO_3^-)] forms of N. The inorganic N concentrations are generally low compared with the total N of the manure or compost, but $\delta^{15}N$ values can be quite variable (Table 2). The inorganic N fraction is often enriched in ^{15}N compared with the total N, indicating non-uniform labelling due to isotope fractionation processes. The unusually high $\delta^{15}N$ values for inorganic N in cattle feedlot manure (Kim *et al.*, 2008; Table 2) may be indicative of substantial N losses during storage.

TABLE 2. Concentration and ^{15}N natural abundance of total and inorganic forms of N in organic N fertilizers

Material	N fraction	N concentration[1] (g/kg)	$\delta^{15}N$[1] (‰)	Reference
Cattle manure	Total	4.4–10.7[2]	+7.9[3]	Choi *et al.* (2006)
	NH_4^+	0.001–0.067[2]	+9.9[3]	
	NO_3^-	0.007–0.009[2]	+16.6[3]	
Cattle feedlot manure (sawdust bedding)	Total	9.5	+11.4	Kim *et al.* (2008)[4]
	NH_4^+	2.0	+39.8	
	NO_3^-	0.22	~+26	
Swine manure compost	Total	23.1 (1.2)	+15.3 (0.2)	Yun *et al.* (2011)
	NH_4^+	0.33 (0.014)	+12.5 (1.3)	
	NO_3^-	0.12 (0.008)	+22.6 (0.1)	

[1] Data in parentheses are standard deviations of the mean
[2] Range of values over 4 yr
[3] Mean values over 4 yr
[4] Data are time zero at the beginning of composting for 90 d

TABLE 3. Discrimination factors (ε) for some N cycle processes

Process	Discrimination factor (‰)	
	Högberg (1997)[1]	Robinson (2001)
Ammonification (organic N → NH_4^+)	≈0	0–5
Nitrification ($NH_4^+ \rightarrow NO_2^- \rightarrow NO_3^-$)	15–35	15–35
Ammonia volatilization ($NH_4^+ \rightarrow NH_3\uparrow$)	29	40–60
Denitrification ($NO_3^- \rightarrow NO_2^- \rightarrow N_2O\uparrow \rightarrow N_2\uparrow$)	0–33	28–33
N_2O and NO production during NH_4^+ oxidation		35–60
Biological N_2 fixation	0–2	0–6
Inorganic N assimilation by plants	0–20	0–19 (NO_3^-)
		9–18 (NH_4^+)

[1] Values given as α were converted to ε by Equation 8

Isotopic fractionation processes affecting the $\delta^{15}N$ signatures of organic N fertilizers

Units

Isotopic fractionation can occur as a result of physical (e.g. diffusion), chemical (equilibria or ion exchange) or biological (enzymatic) processes. It can be expressed by the fractionation factor (α) where $\alpha = \delta_A / \delta_B$ in an equilibrium reaction, where A is a reactant and B is a product. Isotopic fractionation can also be expressed as discrimination (Δ or ε) in units of per mil (‰).

$$\varepsilon(‰) = (\delta_s - \delta_p)\,[1 + (\delta_p\ 1\ 000)] \quad (5)$$

where δ_s is substrate and δ_p is product

An approximation of the above equation is

$$\varepsilon(‰) = \delta_s - \delta_p \quad (6)$$

The fractionation factor (α) is approximated by:

$$\alpha = (\varepsilon\ /1\ 000) + 1 \quad (7)$$

or

$$\varepsilon = (\alpha - 1) \times 1\ 000 \quad (8)$$

Thus for a fractionation factor (α) of 1.020, ε of the product = –20‰ relative to the substrate (Högberg, 1997).

Processes

Fractionation factors for all physical, chemical and microbially-mediated transformations of N in soil are significant, especially NH_3 volatilization, nitrification and dissimilatory NO_3^- reduction (biological denitrification) (Högberg, 1997; Robinson, 2001). These three processes are the major N transformations affecting the natural ^{15}N isotopic composition of the principal organic N fertilizers, animal wastes and composts. Nitrogen isotope discrimination (ε) factors for the major N cycle processes (Högberg, 1997; Robinson, 2001) are given in Table 3.

Volatilization of NH_3 involves several steps (i–iv) in which isotopic fractionation can occur (Högberg, 1997):

(i) Equilibrium effect (A ↔ B in solution)

$$^{14}NH_3 + {}^{15}NH_4^+ \leftrightarrow {}^{15}NH_3 + {}^{14}NH_4^+$$

NH_4^+ is more enriched with ^{15}N than NH_3 at equilibrium. i.e. = α = 1.020 – 1.027

(ii) Kinetic effects

1. Diffusion of NH_3 in solution to the site of volatilization (α ≈ 1 000)
2. Volatilization of NH_3 (α = 1.029)
3. Diffusion of NH_3 away from the site of volatilization (α ≈ 1 000)

The compound effect of these processes on the net fractionation can be large (Högberg, 1997) since α for equilibrium effect and for volatilization of ammonia are greater than 1.02. Ammonia volatiliza-

tion is quantitatively the most significant N loss process during storage of animal excreta, the voiding of excreta on grazed pastures and during the composting of agricultural wastes.

The first step in nitrification, the enzymatic oxidation of $NH_4^+ \rightarrow NO_2^-$ was shown to have a large fractionation factor (1.015 to 1.036) in pure cultures of *Nitrosomonas* (Högberg, 1997). Thus a decrease in NH_4^+ concentration with a concomitant increase in its $\delta^{15}N$ signature and the production of NO_3^- relatively depleted in ^{15}N all point to active nitrification (Wrage *et al*., 2004). According to Högberg (1997) the second step in nitrification ($NO_2^- \rightarrow NO_3^-$) is not normally rate-limiting and should therefore not lead to further fractionation. However, this is frequently not the case in urine patches and during the composting of animal excreta where the oxidation of nitrite is inhibited by the high pH resulting in the temporary accumulation of nitrite (e.g. Clough *et al*., 1998; Sasaki *et al*., 2006).

Denitrification can be a significant fractionation process during the storage of animal excreta and the composting of agricultural wastes. The overall process or so-called "total denitrification" ($NO_3^- \rightarrow NO_2^- \rightarrow N_2O\uparrow \rightarrow N_2\uparrow$) has a fractionation factor of 1.028 – 1.033 (Robinson, 2001) although Högberg (1997) gives a much wider range (Table 3). Robinson (2001) also shows a large discrimination factor for N_2O and NO produced during nitrification, of the same order of magnitude as for NH_3 volatilization (Table 3).

N_2O production pathways have been investigated using the dual isotope measurements of $\delta^{15}N$ and $\delta^{18}O$ of the N_2O emitted from soil (e.g. Yamulki *et al*., 2000). Several studies have reported that $\delta^{15}N$ values of soil-emitted N_2O can be as low as –56‰ and as high as +3‰, with $\delta^{18}O$ values varying between –21‰ and +57‰ (Yamulki *et al*., 2001; Bol *et al*., 2003). The $\delta^{15}N$ values of soil-emitted N_2O are thus lower than the corresponding tropospheric (+18.7‰) and stratospheric (+21.3‰) values (Yamulki *et al*., 2001; Bol *et al*., 2003). Nitrous oxide produced by nitrification or denitrification in soils is depleted in ^{15}N relative to its substrate (NH_4^+ and NO_3^-, respectively), but as noted above, the fractionation is larger for nitrification-derived N_2O. Therefore, a shift in N_2O production from nitrification to denitrification increases both $\delta^{15}N$ and $\delta^{18}O$ values up to 20–50‰ and 10–25‰, respectively (Yamulki *et al*., 2001; Bol *et al*., 2003). However, if urine is the main source of nitrification, a shift in the $\delta^{15}N$ signature (but not in the $\delta^{18}O$ signature) would be expected, because the oxygen in urea [$CO(NH_2)_2$] would be hydrolyzed to CO_2 (Yamulki *et al*., 2001).

When N_2O is further reduced to N_2 during total denitrification, $\delta^{15}N_2O$ becomes more enriched relative to the N_2 product. Thus simultaneous measurements of the $\delta^{15}N$ signatures of emitted N_2O and N_2 permits the amount of $N_2O \rightarrow N_2$ to be calculated, and hence improves estimates of the relative contribution of nitrification and denitrification to total N_2O emissions from soils (Bol *et al*., 2003).

The intramolecular distribution of N isotopes in N_2O is an emerging tool for defining the relative importance of microbial sources of this greenhouse gas (Sutka *et al*., 2006). Since N_2O has two N atoms within the asymmetric molecule (central and outer N), ^{15}N is distributed across three principal isotopomers, $^{15}N^{15}NO$, $^{15}N^{14}NO$, $^{14}N^{15}NO$. A technique developed by Sutka *et al*. (2006) enables the individual measurement of $^{15}N^{14}NO$ and $^{14}N^{15}NO$. The difference in $\delta^{15}N^{\alpha}$ and $\delta^{15}N^{\beta}$ is the so-called site preference ($SP = \delta^{15}N^{\alpha} - \delta^{15}N^{\beta}$, where $\delta^{15}N^{\alpha}$ and $\delta^{15}N^{\beta}$ represent the $^{15}N/^{14}N$ ratios at the centre and outer N atoms, respectively). The difference in the site preference for N_2O from hydroxylamine oxidation (~33‰) and nitrite reduction (~0‰) found in a pure culture study (Sutka *et al.,* 2006) can be used to differentiate the relative contributions of nitrification and denitrification to N_2O emissions. Yamulki *et al.* (2001) considered that site preference can provide a more fundamental and sensitive analysis of N_2O sources and production processes compared with the bulk $\delta^{15}N$ analysis of N_2O.

Factors affecting the $\delta^{15}N$ signatures of organic N fertilizers

Storage of animal excreta

Many types of storage facilities for animal excreta exist on farms worldwide. In the UK, the principal types of storage facilities for dairy, cattle and swine excreta are middens (piles or heaps with a permeable or impermeable base), slurry tanks (below or above ground) constructed of steel or concrete, and lagoons with pervious or impervious linings (Nicholson and Brewer, 1997).

Hristov *et al.* (2009) and Lee *et al.* (2011) studied the cumulative amounts and $\delta^{15}N$ signatures of NH_3 emitted from dairy manure during simulated storage under laboratory conditions. $\delta^{15}N$ values of NH_3 volatilized increased quadratically ($r^2 = 0.92$; ***$p < 0.001$) from –31‰ (1 d) to –15‰ (14 d) while the $\delta^{15}N$ of total N remaining in manure also increased quadratically ($r^2 = 0.96$) from +5.6 to +7.2‰ (Hristov *et al*., 2009). A highly significant positive linear relationship was observed between cumulative NH_3 loss and the $\delta^{15}N$ signature of the stored manure ($r^2 = 0.76$; ***$p < 0.001$) over the range of $\delta^{15}N$ in manure of 4 to 8‰ (Hristov *et al.,* 2009).

Ammonia volatilization was most significant during the first 2–3 d of storage and 90 percent of emitted NH_3 came from the urine component of the faeces as a consequence of rapid urea hydrolysis (Lee *et al*., 2011). A sigmoidal curve ($r^2 = 0.96$, ***$p < 0.001$) best described the $\delta^{15}N$ of volatilized NH_3 during incubation for 30 d (Lee *et al*., 2011). NH_3 was highly depleted in $\delta^{15}N$ at the beginning of the manure storage process, and $\delta^{15}N$ values of manure reached a plateau which coincided with the decline in NH_3 volatilization. Therefore, $\delta^{15}N$ of volatilized NH_3 is a promising tool for estimating cumulative ammonia losses during storage of animal excreta, but further testing is required with different excreta under different and more realistic conditions of storage.

The earthen anaerobic lagoon is a common method of on-farm storage of feedlot runoff and slurries from dairy and pig barns in mid-western USA. Mariappan *et al.* (2009) studied the spatial and temporal concentrations and $\delta^{15}N$ signatures of total N and NH_4^+ within 13 anaerobic lagoons of variable volumes receiving dairy (one), cattle (two) and swine (eleven) wastes. $\delta^{15}NH_4^+$ varied from +2.0 to +59.1‰, was spatially uniform within the top 1.5 m of the lagoon, and was not statistically different from the total $\delta^{15}N$ value. Based on comparisons with feed and fresh manure and urine, most ^{15}N isotopic fractionation occurred after excretion and was affected by management and environmental factors (Mariappan *et al*., 2009). $\delta^{15}NH_4^+$ enrichment increased when NH_3 volatilization increased with increasing seasonal temperatures, and lagoons that were frequently pumped out and refilled with fresh waste were not characterized by the high $\delta^{15}N$ values normally associated with animal wastes. Wastes must mature in lagoons in order to develop high levels of $\delta^{15}NH_4^+$ enrichment (> +10‰) (Mariappan *et al.,* 2009).

Composting of agricultural wastes

The $\delta^{15}N$ signature of corn silage increased by +7.9‰ during aerobic-thermophilic composting (Lynch, Voroney and Warman, 2006; Table 4). Composting created a more homogeneous bulk $\delta^{15}N$ signature compared with the feedstock, as seen by the lower sub-sample standard deviation (Table 4). Kim *et al.* (2008) similarly observed an increase in the $\delta^{15}N$ signature of cattle manure composted with sawdust bedding of +4.2‰, and of +3.4‰ for manure composted with rice hull bedding (Table 4).

TABLE 4. Natural ^{15}N abundance in agricultural wastes and derived composts

Residue	δ^{15}N (‰)	Reference
Corn silage	+0.3 ± 1.3	Lynch, Voroney and Worman (2006)
Corn silage compost	+8.2 ± 0.4	
Cattle manure	+7.6	Kim *et al.* (2008)
Cattle manure + rice hull[1] compost	+11.0	
Cattle manure	+11.4	
Cattle manure + sawdust[2] compost	+15.6	

[1] δ^{15}N of rice hull = +4.9 ± 0.1‰

[2] δ^{15}N of sawdust = +1.7 ± 0.2‰

According to Lynch *et al.* (2006), the observed compost δ^{15}N enrichment is attributable to a combination of fractionation mechanisms, including microbial isotope discrimination during N turnover, a shift to more complex N compounds, and fractionation during NH_3 volatilization, with the relative contributions being unknown. Kim *et al.* (2008) reasoned that NH_3 volatilization would be the dominant process in the early thermophilic stage of composting of cattle manure due to the fast hydrolysis of the high concentrations of urea in livestock excreta, followed by slow or insignificant increases in δ^{15}N in the latter stages. This hypothesis remains to be tested.

Kim *et al.* (2008) observed an increase in the δ^{15}N of NH_4^+ from +30.2 to +41.7‰ in manure + rice hull compost, and from +39.8 to +47.8‰ in the manure + sawdust compost, while the δ^{15}N of NO_3^- fluctuated during composting within the approximate range of +25 to +45‰. Based on both the temporal changes in the concentrations and isotopic signatures of NH_4^+ + NO_3^-, Kim *et al.* (2008) concluded that loss of NH_4^+ in the early stages of composting through NH_3 volatilization and nitrification, and loss of NO_3^- in the latter stage (after 60 d) through denitrification were the primary reasons for the increase in δ^{15}N in the composted manure.

There are presently no data available on the δ^{15}N values of NH_3 emissions during composting. However, a weak negative linear relationship was observed between N concentrations and δ^{15}N values of livestock manure composts (r^2 = 0.16; *p < 0.05) over the range of 10 to 35 g·N/kg and δ^{15}N of +9 to +22‰ (Lim *et al.*, 2010). It would be expected that treatments designed to conserve N during composting would exert a strong influence on the δ^{15}N values of volatilized NH_3 and hence compost N concentrations and δ^{15}N values, but data are not yet available.

In contrast to the lack of data for NH_3 there are a few measurements on the natural ^{15}N abundance of N_2O formed during composting. From 0.5 to 1.6 percent of total N was emitted as N_2O during the composting of livestock waste in turned and static piles, respectively, with the δ^{15}N signature of N_2O increasing markedly from –23.1 to –0.2‰ (Yoh *et al.*, 2003). The bulk δ^{15}N signature of N_2O produced during thermophilic composting of cow manure with orchard grass increased from –20 to –15‰ between day 14 and day 45 (Maeda *et al.*, 2010), but then suddenly decreased at day 45 to reach –35‰ at day 56. The isotopomer methodology was applied to identify the sources of N_2O emissions. It was found that denitrification was the main source of N_2O following the turning of the compost pile, with a concomitant reduction in the concentrations of NO_2^- and NO_3^-. An increased value in site preference indicated that nitrification, which occurred mainly in the surface of the pile, partially contributed to N_2O emissions between the turnings (Maeda *et al.*, 2010).

δ^{15}N *s*ignatures of soils, crops, soil biota and leachates under organic and conventional fertilizer regimes

Soils and plants

Experiments of short- (42 to 157 d, medium- (4 to 12 yr) and long-term (30 to 91 yr) duration have been carried out either in the glasshouse or field to compare the temporal changes in the concentrations and δ^{15}N signatures of total soil N and crop N uptake

TABLE 5. N concentration and natural ^{15}N abundance of N fertilizer sources and crop N in short-term pot and field experiments with animal excreta, composts and synthetic N fertilizer

Crop / scale/ duration	N fertilizer source				Plant material			Reference	
	Type[1]	Total N (g/kg)	N rate (kg/ha)	δ^{15}N (‰)	Part	Total N (g/kg)	N uptake (g/plant)	δ^{15}N (‰)	
Maize/ pot / 70 d	C		0				1.83	+6.3	Choi *et al.* (2002)
	U	451	150	–2.3 ± 0.2	Above ground		3.00	+6.0	
	SMC	20.6	150	+13.9 ± 0.2			3.44	+6.7	
Chinese cabbage / pot / 42 d	SMC	25.3	0	+16.2	Outer leaf[3]	24.3		+14.1	Yun and Ro (2009)
			0.5[2]			31.1		+22.2	
			1.0[2]			40.9		+24.5	
			1.5[2]			48.4		+24.4	
Maize / field / 157 d	C		0		Grain	19 ± 1		+6.3 ± 0.3	Szpak *et al.* (2012)
	AS	211 ± 1	700	–0.7 ± 0.1		16 ± 0		+5.8 ± 0.2	
	CD	24 ± 6	75	+13.9 ± 0.6		16 ± 0		+8.1 ± 1.6	
	SG	82 ± 9	200	+38.1 ± 0.6		15 ± 1		+21.2 ± 0.2	

[1] C — control; U — urea; SMC — swine manure compost; AS — ammonium sulphate; CD — camelid dung; SG — seabird guano

[2] Unit is g/kg

[3] Lsd (*p < 0.05) between N rates; Total plant N = 2.1 g/kg; δ^{15}N plant material = 1.0‰

under animal excreta, composts and synthetic N fertilizer regimes. A range of annual crops in short-term (single season) experiments or in medium- to long-term crop rotations has been used.

Short-term (single season) experiments

Choi *et al.* (2002) found large differences in the $\delta^{15}N$ signatures of urea and swine manure compost treatments applied at the same N rate in a pot experiment, which were reflected in the $\delta^{15}N$ signatures of the foliage of maize at day 30. However, these differences were short-lived and converged to the initial $\delta^{15}N$ value of total soil N of +6.9 ± 0.3‰ after 70 d, despite the increasing N uptake from control, to urea to compost treatments (Table 5).

Yun and Ro (2009) found a highly significant positive linear relationship between the N uptake of Chinese cabbage in a pot experiment and the N application rate of swine manure compost, which had a $\delta^{15}N$ value of total N of +16.2‰. There were small differences in the N concentrations between outer (older) and inner (younger) leaves, and the N concentration increased with N rate (Table 5). However, the $\delta^{15}N$ values were significantly higher for outer compared with inner leaves, which often exceeded the $\delta^{15}N$ value of the total N of the applied compost (Table 5). This apparently anomalous result was due to the non-uniform $\delta^{15}N$ label between the organic and inorganic components of the compost. The higher $\delta^{15}N$ values of the compost NH_4^+ and NO_3^- pools exerted a stronger influence than the total compost N.

In contrast to the previous short-term pot experiments, the $\delta^{15}N$ signatures of maize grain in a field experiment mirrored the $\delta^{15}N$ signatures of the organic N inputs (Szpak *et al.*, 2012). The grain in the ammonium sulphate treatment had a lower $\delta^{15}N$ value than the control, while the grain in the dung and guano treatments had much higher $\delta^{15}N$ signatures than the control (Table 5). The authors claimed that the guano had the highest $\delta^{15}N$ value (+38.1 ± 0.6‰) for an organic N fertilizer reported to date (2012), but Choi *et al.* (2007) previously reported similar values of +40.1 ± 3.4‰ and +45.2 ± 4.1‰ for two compost samples.

Medium-term crop rotations

Choi *et al.* (2006) applied variable rates of swine manure slurry, cattle manure and urea to a soil in each of four yr (Table 6). There were no significant effects on surface soil total N or its ^{15}N natural abundance compared to the control. In contrast, Zhao, Maeda and Ozaki, (2002) found the annual addition of swine manure compost for six yr increased both total soil N and its natural ^{15}N abundance compared with the control at site 1, while at site 2 annual addition of cattle manure for 12 yr resulted in increasing soil total N and its $\delta^{15}N$ signatures with increasing rates of manure (Table 6).

Long-term crop rotations

Total soil N did not differ between control and animal manure treatments after 91 yr (Bol *et al.*, 2005), whereas it was significantly higher in the manure treatment compared with the control after 42 yr (Gerzabek, Haberhauer and Kirchmann, 2001), and between livestock manure compost and the control after 30 yr (Nishida *et al.*, 2007). In addition, total N either decreased (Gerzabek, Haberhauer and Kirchmann, 2001) or remained unchanged over time in the control or synthetic N fertilizer treatments (Nishida *et al.,* 2007), whereas it increased in manure and compost treatments (Table 7). These differences are most likely due to differences in climatic and edaphic factors as well as the intrinsic differences in the characteristics and rates of addition of the organic N sources.

The $\delta^{15}N$ signatures of total N in surface soil (Table 7) did not differ significantly between control and manure treatments (Gerzabek, Haberhauer and Kirchmann, 2001) but they were higher in manure (Bol *et al.*, 2005), compost and ammonium sulphate treatments (Nishida *et al.*, 2007). The last crop of sugar beet (1985) also had higher $\delta^{15}N$ values in the tops of the manure (+6.5‰) compared with the control (+2.0‰) treatment (Bol *et al.*, 2005). Nishida *et al.* (2007) found that the $\delta^{15}N$ signatures of total N in surface soil decreased in the control and ammonium sulphate treatments over time, but increased in the compost treatment (Table 7). Therefore there were no consistent trends in the relative long-term temporal changes in total soil N and the corresponding $\delta^{15}N$ signatures (Table 7). How-

TABLE 6. N concentration and natural ^{15}N abundance of annual fertilizer amendments and total N in surface soil in medium-term field experiments (crop rotations) with animal excreta, composts and synthetic N fertilizer

Annual fertilizer amendment					Soil					
Type[1]	Time (yr)	Total N (g/kg)	N rate (kg/ha)	$\delta^{15}N$ (‰)	Depth (cm)	Total N (g/kg)		$\delta^{15}N$ (‰)		Reference
						Initial	Final	Initial	Final	
C	6		0		0–20		3.8		+6.6[2]	Zhao, Maeda and Ozaki, (2002) Site 1
SMC		56.0	800	+14.3			5.5		+9.6[2]	
CM	12	25.3	163	+19.1			4.8		+9.4[2]	Zhao, Maeda and Ozaki, (2002) Site 2
			325				4.9		+10.3[2]	
			650				5.8		+10.4[2]	
C	4		0		0–30	1.7	1.6	+4.1	+4.1	Choi *et al.* (2006)
SMS		2.6 – 4.6[3]	58–172[4]	+4.7 – + 5.6		1.6	1.6	+4.1	+4.4	
CM		4.4 – 10.7	82–397	+6.8 – + 8.5		2.0	2.2	+3.9	+4.3	
U		466	39–90	–0.6 – + 1.9		1.7	1.6	+3.9	+4.0	

[1] C — control; SMC — swine manure compost; CM — cattle manure; SMS — swine manure slurry; U — urea
[2] All values are means of 2 or 3 replicates with a standard error within ± 0.3‰
[3] Unit is g/L
[4] Yr 1–3 (no slurry was applied in year 4)

TABLE 7. N concentration and natural ^{15}N abundance of annual fertilizer amendments and total N in surface soil in long-term field experiments (crop rotations) with animal excreta, composts and synthetic N fertilizer

Annual fertilizer amendment					Soil[7]				
Type[1]	Time (yr)	Total N (g/kg)	N rate (kg/ha)	δ^{15}N (‰)	Total N (g/kg)		δ^{15}N (‰)		Reference
					Initial	Final	Initial	Final	
C	42		0		1.7	1.3 ± 0.05		+8.5[2]	Gerzabek *et al.* (2001)
AM		17.6 ± 3.0	217	+7.6[6] ± 1.4		2.2 ± 0.1		+8.7[2]	
C	91		0			1.2 ± 0.05		+4.7[3] ± 0.2	Bol *et al.* (2005)
AM			42–98			1.3 ± 0.04		+5.8[3] ± 0.2	
C	30		0		0.9	1.0	+2.6	+2.1	Nishida *et al.* (2007)
AS		212	60–192	–0.9 - –1.4[4]	1.6	1.6	+3.2	+1.4	
LMC		4.0 ± 1.6 -6.0 ± 0.9	81–127[5]	+6.4 ± 1.0 - +17.4 ± 0.7	1.0	2.6	+3.7	+6.9	

[1] C — control; AM — animal manure; AS — ammonium sulphate; LMC — livestock manure compost
[2] Values are not significantly different (*p < 0.05)
[3] The archived 1985 crop of sugarbeet (the experiment was started in 1894) had δ^{15}N values of +2.0 and +6.5‰ in the tops in control and manure treatments, respectively
[4] Values for 2002 and 2003 samples
[5] Calculated assuming the tabulated moisture content (0.703–0.811 g/g) was on a dry weight basis
[6] Six samples from individual yr in the 1980s–1990s
[7] Soil depth was 0–20 cm except for Nishida *et al.* (2007) where it was 0–15 cm

ever, Koerner *et al.* (1999) found that soil δ^{15}N signatures could be used to identify past agricultural land use where fields had reverted to forests during the past 70–100 yr. Previous garden soils with a history of manure inputs had significantly higher δ^{15}N signatures on average (+3.8‰) than ancient forests (0.0‰) or previous pastures (+1.4‰).

Soil biota

Dijkstra *et al.* (2006a) found that on average the soil microbial biomass had a consistently higher δ^{15}N value (+9.7‰) compared with the total soil N (+6.6‰) across a broad range of soil types, vegetation and climates. Dijkstra *et al.* (2006b) similarly found consistently higher δ^{15}N values of microbial N compared with total soil δ^{15}N across a cattle manure gradient extending 100 m from a reservoir in a semi-arid, high-desert grassland, and whereas the total N increased closer to the reservoir the δ^{15}N value of the total N remained relatively constant (~+10‰), while the microbial δ^{15}N increased closer to the reservoir from ~+14 to ~+18‰.

Schmidt and Ostle (1999) similarly found that soil invertebrates (earthworms) had higher δ^{15}N signatures compared with total soil N in an experiment where cattle slurry (δ^{15}N = +13.2 to +17.0‰) and NH_4NO_3 (δ^{15}N = –2.0 to +0.5‰) were individually applied to plots for three consecutive yr. Soil total N (0–10 cm) in organic- and synthetic-fertilized plots had δ^{15}N signatures of +5.9 ± 0.6‰ and +3.9 ± 0.1‰, respectively, while earthworms had δ^{15}N signatures of +6.5 ± 0.2‰ and +5.2 ± 0.3‰, respectively.

Leachates

Choi, Lee and Ro (2003) highlighted the difficulties of identifying sources of NO_3^- contamination of groundwater using δ^{15}N signatures, since the δ^{15}N value is not only a function of source but also of fractionation during formation or consumption. For example, denitrification enriches ^{15}N in nitrate, and if this process is significant it could mask predicted differences between sources such as synthetic fertilizers which are relatively more depleted in ^{15}N compared with animal excreta and composts. In a survey of wells monitored over a 3–y period within defined agricultural management systems, Choi *et al.* (2007) were able to correlate the nitrate concentrations and δ^{15}N signatures of well water with applications of compost, compost + urea fertilizer or no soil amendment.

δ^{15}N signatures have proven to be a valuable tool in identifying leakages of animal wastes stored and treated in anaerobic lagoons as well as from land application of the lagoon effluent by spray irrigation onto adjacent fields (Karr *et al.*, 2001 and Karr, Showers and Jennings, 2003; Israel *et al.*, 2005). Nitrate generated from commercial application of swine waste within a catchment was discharged to surface waters by ground water passing beneath the sprayfields and adjacent riparian buffers (Karr *et al.*, 2001). Median values of δ^{15}N of +15.4 ± 0.2‰ were measured *in situ* in the liquid total N of the waste lagoons, and in nitrate in shallow ground water beneath and adjacent to sprayfields, a stream draining sprayfields and waters up to 1.5 km downstream. Israel *et al.* (2005) pointed out that the study of Karr *et al.* (2001) was carried out on a site that had received lagoon effluent for 20 yr prior to the more stringent regulations on land application of animal waste imposed in 1993, and concluded that the riparian buffer was overwhelmed either due to the nitrate concentration in the ground water moving to the stream or to its rapid flux and shallow flow path.

Karr, Showers and Jennings (2003) further demonstrated the sensitivity of δ^{15}N monitoring where low-level export of nitrate from confined dairy farming could be detected even when stream nitrate concentrations were low and derived predominantly from natural soil sources.

δ^{15}N signatures in the soil-plant-atmosphere continuum in pastures subject to organic N inputs

Long-term (32–36 yr) measurements were made of δ^{15}N in soils and plants inside and outside enclosures in an area subject to native ungulate grazing (Frank and Evans, 1997). Across six topographically diverse sites, δ^{15}N of soil (0–20 cm) outside enclosures was 0.7‰ higher on average than inside enclosures, while plant N was 0.7‰ less on average under grazing. Soil δ^{15}N of urine and dung patches were significantly higher than control areas. Frank and Evans (1997) concluded that grazing probably led to an increase in soil δ^{15}N by promoting N losses (NH_3 volatilization, etc). In a later study, Frank,

Evans and Tracy (2004) measured $\delta^{15}N$ in soil, plants and NH_3 volatilized from simulated ungulate urine patches. $\delta^{15}N$ of acid-trapped NH_3 increased from –28‰ (day 1) to –0.3 ‰ (day 10) from urine that originally had a $\delta^{15}N$ value of +1.2‰. The isotope data showed that shoots absorbed ^{15}N-depleted NH_3 volatilized from the soil, which confirms the results obtained by Denmead *et al.* (1976) using chemical and micro-meteorological techniques.

The natural ^{15}N abundance of plants and soils in medium- to long-term experimental plots (8–50 yr) maintained under different management practices were measured in a montane grassland (Watzka, Buchgraber and Wanek, 2006). Plots differed in the types of N inputs (mineral fertilizer, cattle slurry, stable manure) and rates of application (0–200 $kg{\cdot}N{\cdot}ha^{-1}{\cdot}y^{-1}$). $\delta^{15}N$ of topsoil and plants increased with N fertilizer rate, and the $\delta^{15}N$ signatures reflected the higher values for the organic compared with the mineral inputs. N balances were calculated from N inputs (fertilizer, atmospheric deposition, biological N_2 fixation) and outputs in harvested material. Strong positive correlations were found between $\delta^{15}N$ of topsoil and N balance (range –60 to +120 $kg{\cdot}N{\cdot}ha^{-1}{\cdot}y^{-1}$). The authors concluded that the different $\delta^{15}N$ signals in topsoil were due to isotopic fractionation arising from increased N losses (mineral fertilizer induced) and to both increased N losses and preservation of the $\delta^{15}N$ input signal (organic fertilizers).

In another long-term experiment (20 yr), Krizan *et al.* (2009) measured changes in the concentration and $\delta^{15}N$ values of total soil N in a lysimeter experiment where cattle slurry ($\delta^{15}N$ = +8.9 ± 0.5‰) and calcium ammonium nitrate ($\delta^{15}N$ = –1.0 ± 0.2‰) were applied at 0 and 480 $kg{\cdot}N{\cdot}ha^{-1}{\cdot}y^{-11}$ to temperate grassland. Total N remained unchanged during the experiment and leaching losses were small. The $\delta^{15}N$ of topsoil increased on average from +1.8 ± 0.4‰ to +6.0 ± 0.4‰ and that of the plants from –1.2 ± 1.3‰ to +4.8 ± 1.2‰ with increasing N fertilizer rate, with samples from slurry plots being relatively more enriched in ^{15}N. The results suggested that part of the fertilizer $\delta^{15}N$ signal was preserved in the soil, but that isotope fractionation of up to 1.5‰ added to the $\delta^{15}N$ values in soils and plants, indicative of long-term inefficient N usage and past N management.

Yamulki *et al.* (2000) found that cattle excreta patches were an important source of atmospheric N_2O, with emissions significantly greater from urine than from dung. Flux patterns showed a marked diurnal variation with maxima in early morning or late afternoon, which were not in phase with soil temperature changes. $\delta^{15}N$ and $\delta^{18}O$ of the N_2O emitted from soil indicated that denitrification was the major loss pathway, and after a heavy rainfall the larger $\delta^{15}N$ and $\delta^{18}O$ values suggested a consumption of N_2O by reduction to N_2. In contrast, Tilsner *et al.* (2003) found no unequivocal evidence of the source of N_2O emitted in an extensively managed grassland involving an unfertilized control, a synthetic fertilizer treatment and a slurry treatment based on the ^{15}N and ^{18}O natural abundance data for emitted N_2O. They concluded that the $\delta^{15}N$ values of emitted N_2O were not only influenced by source processes but also by the microbial reduction of N_2O to N_2 and that a minimum a flux of 3.4 mmol N_2O $m^{-2}{\cdot}h^{-1}$ was required to obtain accurate isotope data.

Yamulki *et al.* (2001) showed that the temporal intra-molecular distribution of $\delta^{15}N$ and $\delta^{18}O$ in N_2O emitted from urine patches, together with the site preference values for N_2O using the isotopomer methodology, were indicative of a process shift during the measurement period. Using the same methodology, Köster *et al.* (2011) found a rapid shift from denitrification-derived N_2O to N_2O production via nitrification after three weeks following the exhaustion of labile C compounds originating from the addition of biogas fermentation residue to a grassland soil. On the other hand, Cardenas *et al.* (2007) found that the isotopomer signatures for N_2O in control and sheep slurry treatments (lucerne diet) indicated that denitrification was the main process responsible for N_2O emissions from a grassland soil. Based on the majority of the above-mentioned results, it appears that bulk $\delta^{15}N$, $\delta^{18}O$ and isotopomer signatures are promising tools for separating pathways of N_2O production in grassland soils.

TABLE 8. Range of $\delta^{15}N$ values of plant products according to production system (Inácio *et al.*, 2013)

Production system	$\delta^{15}N$ (‰)
Conventional[1]	–2.5 to +8.7
Organic[2]	+0.3 to +14.6

[1]Synthetic and organic N fertilizers permitted
[2]Synthetic N fertilizers excluded

Differentiating conventional and organic plant products using $\delta^{15}N$

Because organic and synthetic fertilizer sources often differ markedly in $\delta^{15}N$ composition, it would appear to be a promising marker to distinguish organically- and conventionally-fertilized plant products. The greater the difference between organic and synthetic fertilizer the more robust will be the differentiation. However, different crops show greater or smaller differences between $\delta^{15}N$ values of organic and conventional products, and a certain degree of overlap can occur (Table 8). For example, organic tomatoes showed greater differences in $\delta^{15}N$ values compared with conventional production (+8.1 ± 3.2‰ vs. –0.1 ± 2.1‰, respectively), whereas differences between lettuce were smaller (+7.6 ± 4.1‰ vs. +2.9 ± 4.3‰, respectively), although still statistically significant (Bateman, Keely and Woolfe, 2007). However, $\delta^{15}N$ values of organic and conventional carrots (+5.7 ± 3.5‰ vs. +4.1 ± 2.6‰) were not significantly different. Perennial crops tend to show smaller but significant differences in $\delta^{15}N$ between mode of production, such as orange fruit (+7.3 to +7.9‰ for organic vs. +5.1 to +6.1‰ for conventional) (Camin *et al.*, 2011).

Nevertheless, many production or external factors may confound product designation. e.g. (i) legume products or the use of legume cover crops on organic farms, (ii) crop species with a low N requirement, (iii) annual vs. perennial growth habit, (iv) use of organic fertilizers by conventional farmers, and (v) marketing of organic products as conventional products (Inácio *et al.*, 2013).

For animal products, $\delta^{13}C$ might be the most promising marker for mode of production in temperate regions because of its relationship to diet, i.e. differences between C4 maize grain used in intensive animal feeding operations and C3 pasture grasses and legumes available under free-range conditions. However, $\delta^{13}C$ seems unlikely to be useful in tropical regions for grazing animals due to abundant C4 pasture grasses, e.g. *Brachiaria spp.* (Inácio *et al.*, 2013).

CONCLUSIONS

The ^{15}N natural abundance of animal excreta and composts is a useful tool for following the fate of organic N sources in the soil-plant-atmosphere continuum. The alternative approach of using organic fertilizers artificially-enriched in ^{15}N is time-consuming, expensive and inefficient, with the attendant risks of non-uniform labelling and perturbation of the system under study. However, fewer studies have been conducted at the level of natural ^{15}N abundance compared with artificially-enriched materials, and δ values have generally been

used as qualitative rather than quantitative measures of N processes at the system level.

Nevertheless, recent results showing significant positive and negative linear relationships during storage of animal excreta, between the bulk δ^{15}N signature and cumulative NH_3 loss and between bulk δ^{15}N of composts and N concentration, respectively, suggest that δ^{15}N may have wider applications in estimating the efficiency of N conservation during storage or composting. The combined use of bulk δ^{15}N and δ^{18}O signatures of N_2O evolved during storage and composting, together with the isotopomer-derived site preference of N_2O, are powerful tools for identifying the processes of N_2O formation in order to enable formulation of mitigation strategies.

Finally, it has been demonstrated that δ^{15}N signatures could play a role in differentiating organic and conventional plant products provided each of the two populations for each product has been adequately described by a frequency distribution that enables a statistical analysis of a sample. The potential use of stable isotopes in differentiating conventional and organic animal products remains to be addressed. In addition, a review and analysis of the post-1998 literature on animal excreta artificially enriched in ^{15}N needs to be undertaken to complement and extend the results obtained with ^{15}N natural abundance reported here.

REFERENCES

Bateman, A.S., Kelly, S.D. & Woolfe, M. 2007. Nitrogen isotope composition of organically and conventionally grown crops. *J. Agric. Food Chem.,* 55: 2664–2670.

Bol, R., Eriksen J., Smith, P., Garnett, M.H., Coleman K. & Christensen B.T. 2005. The natural abundance of ^{13}C, ^{15}N, ^{34}S and ^{14}C in archived (1923–2000) plant and soil samples from the Askov long-term experiments on animal manure and mineral fertilizer. *Rapid Commun. Mass Spectrom.,* 19: 3216–3226.

Bol, R., Toyoda, S., Yamulki, S., Hawkins, J.M.B., Cardenas, L.M. & Yoshida, N. 2003. Dual isotope and isotopomer ratios of N_2O emitted from a temperate grassland soil after fertiliser application. *Rapid Commun. Mass Spectrom.,* 17: 2550–2556.

Camin, F., Perini, M., Bontempo, L., Fabroni, S., Faedi, W., Magnani, S., Baruzzi, G., Bonoli, M., Tabilio, M.R., Musmeci, S., Rossmann, A., Kelly, S.D. & Rapisarda, P. 2011. Potential isotopic and chemical markers for characterizing organic fruits. *Food Chem.,* 125: 1072–1082.

Cardenas, L.M., Chadwick, D., Scholefield, D., Fychan, R., Marley, C.L., Jones, R., Bol, R., Well, R. & Vallejo, A. 2007. The effect of diet manipulation on nitrous oxide and methane emissions from manure applied to incubated grassland soils. *Atmos. Environ.,* 41: 7096–7107.

Chalk, P.M. 1995. Isotope ratios. *In* A. Townshend & P. Worsfold, eds. *Encyclopedia of analytical science,* pp. 2409–2415. London, Academic Press Limited.

Chalk, P.M. 1997. *The dynamics of soil, fertilizer and biologically-fixed nitrogen in soil-plant systems.* The University of Melbourne. (D. Agr. Sc. dissertation). 618 pp.

Chalk, P.M., Magalhães, A.M.T. & Inácio, C.T. 2013. Towards an understanding of the dynamics of compost N in the soil-plant-atmosphere system using ^{15}N tracer. *Plant Soil,* 362: 373–388.

Cheng, L., Kim, E.J., Merry, R.J. & Dewhurst, R.J. 2011. Nitrogen partitioning and isotopic fractionation in dairy cows consuming diets based on a range of contrasting forages. *J. Dairy Sci.,* 94: 2031–2041.

Choi, W.J., Arshad, M.A., Chang, S.X. & Kim, T.H. 2006. Grain ^{15}N of crops applied with organic and chemical fertilizers in a four-year rotation. *Plant Soil,* 284: 165–174.

Choi, W-J., Han, G-H., Lee, S-M., Lee, G-T., Yoon, K-S., Choi, S-M. & Ro, H-M. 2007. Impact of land-use types on nitrate concentration and δ^{15}N in unconfined groundwater in rural areas of Korea. *Agric. Ecosyst. Environ.,* 120: 259–268.

Choi, W-J., Lee, S-M. & Ro, H-M. 2003. Evaluation of contamination sources of groundwater NO_3^- using nitrogen isotope data: A review. *Geosci. J.,* 7: 81–87.

Choi, W-J., Lee, S-M., Ro, H-M., Kim, K-C. & Yoo, S-H. 2002. Natural ^{15}N abundances of maize and soil amended with urea and composted pig manure. *Plant Soil,* 245: 223–232.

Clough, T.J., Ledgard, S.F., Sprosen, M.S. & Kear, M.J. 1998. Fate of ^{15}N labelled urine in four soil types. *Plant Soil,* 199: 195–203.

Denmead, O.T., Freney, J.R. & Simpson, J.R. 1976. A closed ammonia cycle within a plant canopy. *Soil Biol. Biochem.,* 8: 161–164.

Dijkstra, P., Ishizu, A., Doucett, R., Hart, S.C., Schwartz, E., Menyailo, O.V. & Hungate, B.A. 2006a. ^{13}C and ^{15}N natural abundance of the soil microbial biomass. *Soil Biol. Biochem.,* 38: 3257–3266.

Dijkstra, P., Menyailo, O.V., Doucett, R.R., Hart, S.C., Schwartz, E. & Hungate, B.A. 2006b. C and N availability affects the ^{15}N natural abundance of the soil microbial biomass across a cattle manure gradient. *Eur. J. Soil Sci.,* 57: 468–475.

Dittert, K., Georges, T. & Sattelmacher, B. 1998. Nitrogen turnover in soil after application of animal manure and slurry as studied by the stable isotope ^{15}N: A review. *J. Soil Sci. Plant Nutr.,* 161: 453–463.

Frank, D.A. & Evans, R.D. 1997. Effects of native grazers on grassland N cycling in Yellowstone National Park. *Ecol.,* 78: 2238–2248.

Frank, D.A., Evans, R.D. & Tracy, B.F. 2004. The role of ammonia volatilization in controlling the natural ^{15}N abundance of a grazed grassland. *Biogeochem.,* 68: 169–178.

Gerzabek, M.H., Haberhauer, G. & Kirchmann, H. 2001. Nitrogen distribution and ^{15}N natural abundance in particle size fractions of a long-term agricultural field experiment. *J. Plant Nutr. Soil Sci.,* 164: 475–481.

Högberg, P. 1997. Tansley Review No. 95. ^{15}N natural abundance in soil-plant systems. *New Phytol.,* 137: 179-203.

Hristov, A.N., Zaman S., Vander Pol, M., Ndegwa, P., Campbell, L. & Silva, S. 2009. Nitrogen losses from dairy manure estimated through nitrogen mass balance and chemical markers. *J. Environ. Qual.,* 38: 2438-2448.

Inácio, C.T., Chalk, P.M. & Magalhães, A.M.T. 2013. Principles and limitations of stable isotopes in differentiating organic and conventional foodstuffs: 1. Plant products. *Crit. Rev. Food Sci. Nutr.,* (in press)

Israel, D.W., Showers, W.J., Fountain, M. & Fountain, J. 2005. Nitrate movement in shallow groundwater from swine-lagoon-effluent spray fields managed under current application regulations. *J. Environ. Qual.,* 34: 1828-1842.

Junk, G. & Svec, H.J. 1958. The absolute abundance of the nitrogen isotopes in the atmosphere and compressed gas from various sources. *Geochim. Cosmochim. Acta,* 14: 234–243.

Karr, J.D., Showers, W.J., Gilliam, J.W. & Andres, A.S. 2001. Tracing nitrate transport and environmental impact from intensive swine farming using delta nitrogen-15. *J. Environ. Qual.,* 30: 1163–1175.

Karr, J.D., Showers, W.J. & Jennings, J.D. 2003. Low-level nitrate export from confined dairy farming detected in North Carolina streams using δ^{15}N. *Agric. Ecosyst. Environ.,* 95: 103–110.

Kim, Y-J., Choi, W-J., Lim, S-S., Kwak, J-H., Chang, S.X., Kim, H-Y., Yoon, K-S. & Ro, H-M. 2008. Changes in nitrogen isotopic compositions during composting of cattle feedlot manure: effects of bedding material type. *Bioresour. Technol.,* 99: 5452–5458.

Koerner, W., Dambrine, E., Dupouey, J.L. & Benoît, M. 1999. δ^{15}N of forest soil and understory vegetation reflect the former agricultural land use. *Oecologia,* 121: 421–425.

Köster, J.R., Cárdenas, L., Senbayram, M., Bol, R., Well, R., Butler, M., Mühling, K.H. & Dittert, K. 2011. Rapid shift from denitrification to nitrification in soil after biogas residue application as indicated by nitrous oxide isotopomers. *Soil Biol. Biochem.,* 43: 1671–1677.

Kriszan, M., Amelung, W., Schellberg, J., Gebbing, T. & Kühbauch, W. 2009. Long-term changes in the $\delta^{15}N$ natural abundance of plants and soil in a temperate grassland. *Plant Soil,* 325: 157–169.

Lee, C., Hristov, A.N., Cassidy, T. & Heyler K. 2011. Nitrogen isotope fractionation and origin of ammonia nitrogen volatilized from cattle manure in simulated storage. *Atmosphere,* 2: 256-270.

Lim, S-S., Lee, S-M., Lee, S-H. & Choi, W-J. 2010. Nitrogen isotope compositions of synthetic fertilizer, raw livestock manure slurry, and compost livestock manure. *Korean J. Soil Sci. Fert.,* 43: 453–457.

Lynch, D.H., Voroney, R.P. & Warman, P.R. 2006. Use of ^{13}C and ^{15}N natural abundance techniques to characterize carbon and nitrogen dynamics in composting and in compost-amended soils. *Soil Biol. Biochem.,* 38: 103–114.

Maeda, K., Toyoda, S., Shimojima, R., Osada, T., Hanajima, D., Morioka, R. & Yoshida, N. 2010. Source of nitrous oxide emissions during the cow manure composting process as revealed by isotopomer analysis of and *amoA* abundance in betaproteobacterial ammonia-oxidizing bacteria. *Appl. Environ. Microbiol.,* 76: 1555–1562.

Mariappan, S., Exner, M.E., Martin, G.E. & Spalding, R.F. 2009. Variability of anaerobic animal waste lagoon delta ^{15}N source signatures. *Environ. Forensics,* 10: 19–26.

Nicholson, R.J. & Brewer, A.J. 1997. Estimates of volumes and exposed surface areas of stored animal manures and slurries in England and Wales. *J. Agric. Eng. Res.,* 66: 239–250.

Nishida, M., Iwaya, K., Sumida, H. & Kato, N. 2007. Changes in natural ^{15}N abundance in paddy soils under different, long-term soil management regimes in the Tohoku region of Japan. *Soil Sci. Plant Nutr.,* 53: 310–317.

Robinson, D. 2001. $\delta^{15}N$ as an integrator of the nitrogen cycle. *Trends Ecol. Evolut.,* 16: 153–162.

Sasaki, H., Kitazume, O., Nonaka, J., Hikosaka, K., Otawa, K., Itoh, K., & Nakai, Y. 2006. Effect of a commercial microbiological additive on beef manure compost in the composting process. *Anim. Sci. J.,* 77: 545–548.

Schmidt, O. & Ostle, N.J. 1999. Tracing nitrogen derived from slurry in earthworms using $^{15}N/^{14}N$ stable isotope ratios at natural abundance. *Appl. Soil Ecol.,* 12: 7–13.

Selles, F. & Karamanos, R.E. 1986. Variations in natural N-15 abundance as an aid in manure- nitrogen studies. *J. Environ. Qual.,* 15: 24–30.

Sponheimer, M., Robinson, T.F., Roeder, B.L., Passey, B.H., Ayliffe, L.K., Cerling, T.E., Dearing, M.D. & Ehleringer, J.R. 2003. An experimental study of nitrogen flux in llamas: Is ^{14}N preferentially excreted? *J. Archaeol. Sci.,* 30: 1649–1655.

Steele, K.W. & Daniel, R.M. 1978. Fractionation of nitrogen isotopes by animals: a further complication to the use of variation in the natural abundance of ^{15}N for tracer studies. *J. Agric. Sci.,* 90: 7–9.

Sutka, R.L., Ostrom, N.E., Ostrom, P.H., Breznak, J.A, Gandhi, H., Pitt, A.J. & Li, F. 2006. Distinguishing nitrous oxide production from nitrification and denitrification on the basis of isotopomer abundances. *Appl. Environ. Microbiol.,* 72: 638–644.

Szpak, P., Millaire, J-F., White, C.D. & Longstaffe, F.J. 2012. Influence of seabird guano and camelid dung fertilization on the nitrogen isotopic composition of field-grown maize (*Zea mays*). *J. Archaeol. Sci.,* 39: 3721–3740.

Tilsner, J., Wrage, N., Lauf, J. & Gebauer, G. 2003. Emission of gaseous nitrogen oxides from an extensively managed grassland in NE Bavaria. Germany. II. Stable isotope natural abundance of N_2O. *Biogeochem.,* 63: 249–267.

Watzka, M., Buchgraber, K. & Wanek, W. 2006. Natural ^{15}N abundance of plants and soils under different management practices in a montane grassland. *Soil Biol. Biochem.,* 38: 1564–1576.

Wrage, N., Lauf, J., del Prado, A., Pinto, M., Pietrzak, S., Yamulki, S., Oenema, O. & Gebauer, G. 2004. Distinguishing sources of N_2O in European grasslands by stable isotope analysis. *Rapid Commun. Mass Spectrom.,* 18: 1201–1207.

Yamulki, S., Toyoda, S., Yoshida, N., Veldkamp, E., Grant, B. & Bol, R. 2001. Diurnal fluxes and the isotopomer ratios of N_2O in a temperate grassland following urine amendment. *Rapid Commun. Mass Spectrom.,* 15: 1263–1269.

Yamulki, S., Wolf, I., Bol, R., Grant, B., Brumme, R., Veldkamp, E. & Jarvis, S.C. 2000. Effect of dung and urine amendments on the isotopic content of N_2O released from grasslands. *Rapid Commun. Mass Spectrom.,* 14: 1356–1360.

Yoh, M., Akita, Y., Toyoda, S. & Yoshida, N. 2003. Nitrogen stable isotope abundance of N_2O from composting of livestock waste: Its variation and mechanics. *Geochim. Cosmochim. Acta Suppl.,* 67 Issue 18: 565.

Yun, S-I., Lim, S-S., Lee, G-S., Lee, S-M., Kim, H-Y., Ro, H-M. & Choi, W-J. 2011. Natural ^{15}N abundance of paddy rice (*Oryza sativa* L.) grown with synthetic fertilizer, livestock manure compost, and hairy vetch. *Biol. Fertil. Soils,* 47: 607–617.

Yun, S-I., & Ro, H-M. 2009. Natural ^{15}N abundance of plant and soil inorganic-N as evidence for over-fertilization with compost. *Soil Biol. Biochem.,* 41: 1541–1547.

Zhao, B., Maeda, M. & Ozaki, Y. 2002. Natural ^{15}N and ^{13}C abundance in Andisols influenced by long-term fertilization management in Japan. *Soil Sci. Plant Nutr.,* 48: 555–562.

Spatial and Temporal Variation in the Isotopic Signature of Transpired Water from a Conifer Forest Canopy

D.G. Williams[1,2,3,*] and B.E. Ewers[2,3]

ABSTRACT

Most conifer tree species have intrinsically low rates of leaf gas exchange and relatively high leaf water volumes. These traits establish low leaf-water turnover rates, which greatly extend the time required to achieve transpiration at isotopic steady state as environmental conditions change over diurnal periods. Canopy level variation in leaf physiology and microclimate contributes further uncertainty to the estimation of the isotopic composition of transpiration fluxes in forests dominated by conifers. Oxygen stable isotope ratios of water in needles of different age cohorts and from different canopy positions in subalpine fir *(Abies lasiocarpa)* were measured over a diurnal period during the growing season of 2008 in the Snowy Range of southeastern Wyoming, USA. Concurrent measurements of leaf gas exchange, canopy surface temperature, and the delta oxygen-18 ($\delta^{18}O$) and mixing ratio of water vapour within the canopy air allowed modelling of leaf water isotopic enrichment at sites of evaporation and the isotope ratio values of transpiration from different canopy positions. Leaf water achieved isotopic steady state with plant source water over only a brief period of the day in late afternoon, and $\delta^{18}O$ values of water from leaves lower in the canopy and from younger leaf cohorts were closer to those predicted from a steady-state model than those of older leaf cohorts and from higher in the canopy. The $\delta^{18}O$ value of transpired water differed by up to 10‰ from that of source water at midday in some parts of the canopy. Modelling the isotope composition of transpiration from conifer forest should take into account variation in leaf water turnover rates associated with differences in physiology and microclimate of needles of different age and from different canopy positions.

Key words: *gas exchange, oxygen stable isotope ratios, transpiration, conifer forest.*

INTRODUCTION

Estimates of direct soil evaporation and plant transpiration are required to understand productivity responses of vegetation to inputs of irrigation or precipitation. Direct soil evaporation is a 'nonproductive' water loss, and management strategies focus on minimizing this loss in favour of 'productive' water usage through transpiration. Measurements of the stable isotope ratios of hydrogen ($\delta^{2}H$) and oxygen ($\delta^{18}O$) in water are useful for tracing sources of evapotranspiration (ET) and partitioning transpiration (T) from direct soil evaporation (E) fluxes. Because E and T often have unique isotopic signatures, measurements of the isotope ratio composition in the atmospheric water vapour within the canopy boundary layer or in the residual soil water over time provide information on the sources of and processes controlling water exchange in the soil–plant–atmosphere system (Yakir and Sternberg, 2000; Williams *et al.,* 2004).

Several approaches employing isotope measurements have been developed to estimate fractions of evaporation and transpiration in ET and their flux rates. Each approach has advantages and disadvantages related to the type of information provided (E/T fractions versus E and T fluxes), instrumentation costs, level of technical training required, the spatial and temporal scales of inference, and the number of assumptions and parameters requiring validation and estimation. These approaches are broadly defined as: (i) steady-state mixing approaches, including the 'Keeling plot' method (Williams *et al.*, 2004), (ii) soil water isotope mass balance (Hsieh *et al.*, 1998), (iii) the isotope flux gradient approach (Wang and Yakir, 2000), and (iv) isotope mass balance calculations for canopy air (Lai *et al.*, 2006). The Keeling plot approach only provides information on the fractions of E and T in total ET, whereas the flux gradient and air mass balance approaches offer estimates of the flux rates of each of these components. Each approach involves varying levels of sophistication with respect to measurement and process-level understanding of isotopic fractionations that occur at the soil and leaf scale as water is released to the atmosphere and mixes with background air. Any of these approaches can be used in soil-plant-atmosphere transfer models to simulate and predict isotopic exchanges under varying conditions.

Using isotope measurements of atmospheric vapour to partition component fluxes requires accurate estimates of the isotope composition of plant-transpired water (δT). Spatial, temporal and species-level heterogeneity in δT makes this task challenging, and validation of leaf-level isotope fractionation models (Barbour, 2007) are required. But discerning how rigorous one needs to be in accounting for fractionation processes and variation within canopies is dependent on the context of the study. Variation in leaf temperature, humidity and leaf-water turnover rates contribute to the complexity of δT within individual plant canopies. For example, it is often assumed in studies of leaf water isotopic enrichment that leaf temperature is closely coupled to air temperature. Yet this assumption may be invalid, especially where radiation loads and boundary layer resistances are high (Helliker and Richter, 2008).

1 Department of Ecosystem Science and Management, University of Wyoming, Laramie, Wyoming, USA 82071
2 Department of Botany, University of Wyoming, Laramie, Wyoming, USA 82071
3 Program in Ecology, University of Wyoming, Laramie, Wyoming, USA 82071
* E-mail address of corresponding author: dgw@uwyo.edu

L.K. Heng, K. Sakadevan, G. Dercon and M.L. Nguyen (eds), Proceedings — International Symposium on Managing Soils for Food Security and Climate Change Adaptation and Mitigation. Food and Agriculture Organization of the United Nations, Rome, 2014: 349–353

This study addresses how heterogeneity of gas exchange properties and microclimate of different leaves within a single complex canopy influence the isotopic signature of transpired water. Low rates of leaf gas exchange in some conifer species cause low leaf-water turnover rates, which greatly extend the time required to achieve transpiration at isotopic steady-state as environmental conditions change over diurnal periods (Pendall, Williams and Leavitt, 2005; Lai *et al.*, 2006). Differences in stomatal conductance, transpiration and microclimate within the vertical profile of a conifer tree in a high-elevation environment with high radiation loads were investigated to understand the basis for variation in leaf water ^{18}O enrichment and its deviation from plant source water.

MATERIALS AND METHODS

The study was conducted at the Glacier Lakes Ecosystem Experiments Site (GLEES) (41° 22.0′ N, 106° 14.4′ W, 3190 m a.s.l.) in subalpine mixed conifer forest in southeastern Wyoming, United States (Musselman, 1994). The oxygen stable isotope ratio ($\delta^{18}O$) of water was measured in leaves of different ages and from different vertical canopy positions in a subalpine fir *(Abies lasiocarpa)* tree over a diurnal period during the growing season of 2008. Needles were collected every 3–4 h over a 24 h period to investigate the rapid changes in leaf-water isotopic enrichment. Concurrent measurements of leaf gas exchange, humidity and temperature allowed estimation of the isotope ratio of transpiration from the different canopy positions and investigation of the deviation of leaf water $\delta^{18}O$ values from isotopic steady state.

Leaf sampling, gas exchange and canopy temperature measurements

Needles were collected from an *A. lasiocarpa* tree growing adjacent to a tall (30 m) scaffold. The scaffold, used to support instrumentation for the GLEES Ameriflux measurements, allowed easy access to the canopy without major disturbance to the tree. Needles were sampled from 9.5, 13.7 and 17 m above ground surface on the approximately 20 m tall tree every 3–4 h (seven times in total) over 24 h beginning at 08:00 h on day-of-year 213 (July 31), 2008. Needles were collected separately from the current year's growth and from 1- and 3-year-old needle cohorts at each canopy position and time period. Approximately 30–40 needles were removed from twigs for each sample and sealed in screw-cap glass vials. Stems were collected during the mid-day period for plant source water isotope analysis. Small twigs were collected from each canopy position, separated from attached needles and placed also in screw-cap glass vials. Vials were covered with parafilm and stored in a freezer at –2°C until water extraction (described below).

Stomatal conductance and transpiration of needles in each cohort and canopy position were measured during the same seven time periods used for needle collection. Gas exchange measurements were made using a LiCor 6400 with a standard leaf cuvette and with all environmental conditions (cuvette temperature, light level, humidity) set to match ambient conditions. A hand-held infrared thermometer was used to monitor needle temperature at each canopy height.

Canopy air water vapour sampling

Atmospheric water vapour was collected at each of the three canopy positions used for gas exchange measurements and needle collection, employing an automated sample profiler that routed air from each height through low-absorption Bev-a-Line IV tubing to Pyrex glass traps (Helliker *et al.*, 2002) held at –80°C in an ethanol bath. The air stream from each position in the canopy was diverted frequently through an infrared gas analyzer (LI 840, LiCor, Inc.) for measurement of air water-vapour mixing ratio. The sampling system is thoroughly described by Yepez *et al.* (2003) and Williams *et al.* (2004). For the current study, water vapour was trapped in air at a flow rate of 300 mL/min for 30 min during each of the seven sampling periods at each of the three heights in the canopy.

Water extraction and stable isotope analysis

Water from needle and stem samples was retrieved using cryogenic vacuum distillation (Ehleringer and Osmond, 1989). Complete quantitative extraction was verified from weight measurements performed before and after cryogenic extraction and then again after oven drying. Extraction efficiency was better than 95 percent for all samples. The $\delta^{18}O$ values of stem, needle and atmospheric water samples were determined by the CO_2 equilibration technique using a Gas Bench II coupled to a Thermo Delta Plus XP Isotope Ratio Mass Spectrometer (Thermo Scientific Corporation, Bremen, Germany) at the University of Wyoming Stable Isotope Facility. Measured $\delta^{18}O$ values were linearly corrected to the V-SMOW international scale using two calibrated laboratory standards that were analysed with each batch of unknowns along with a QA/QC standard. Precision of repeated analysis of the laboratory QA/QC standard was better than 0.2‰.

Steady state leaf water isotope model

Measured $\delta^{18}O$ values of water extracted from needles were compared with values predicted by a Craig and Gordon steady-state model adapted for leaves (Farquhar and Lloyd, 1993):

$$\delta^{18}O_e = \delta^{18}O_s + \varepsilon^* + \varepsilon_k + (\delta^{18}O_v - \delta^{18}O_s - e_k)e_a{:}e_i \quad (1)$$

where $\delta^{18}O_s$ = the oxygen isotope ratio of plant source water; $\delta^{18}O_v$ = the oxygen isotope ratio of atmospheric water vapour; ε^*

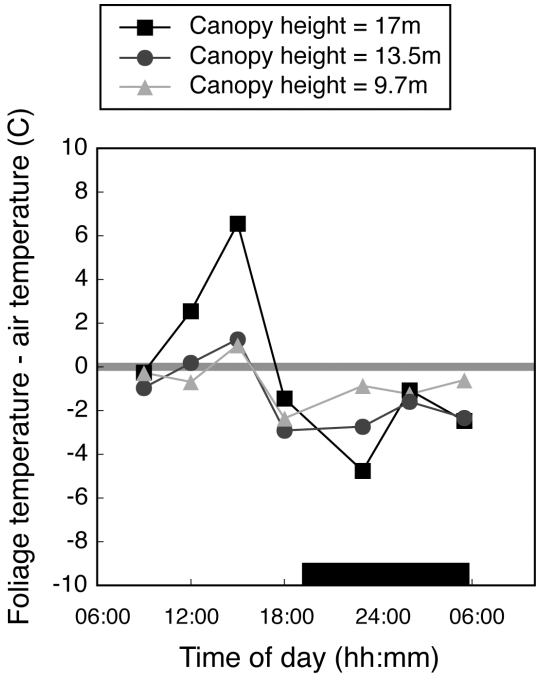

FIGURE 1. Difference between foliage (needle) temperature and surrounding air temperature in the canopy of *A. lasiocarpa*

= the temperature-dependent equilibrium fractionation factor (Bottinga and Craig, 1969); ε_k = the kinetic fractionation factor during diffusion through the stomata and boundary layer; and e_a:e_i is the ratio of ambient to intercellular vapour pressure.

The ε_k value is dependent on the proportion of diffusion resistance through the stomatal pores (r_s) and boundary layer (r_b) (Farquhar, Barbour & Henry, 1998; Cappa *et al.*, 2003) and is calculated by:

$$\varepsilon_k = (32r_s + 21r_b)/(r_s + r_b) \quad (2)$$

The $\delta^{18}O$ value of water in leaves predicted by Equation 1 is that for sites of evaporation, and not for the bulk leaf water. To estimate the $\delta^{18}O$ value of bulk leaf water at isotopic steady state ($\delta^{18}O_L$), a model was employed that accounts for the back diffusion and mixing of ^{18}O enriched water at sites of evaporation with un-enriched source water from leaf veins:

$$\delta^{18}O_L = \delta^{18}O_s + (\delta^{18}O_e - \delta^{18}O_s)(1-e^{-P})/P \quad (3)$$

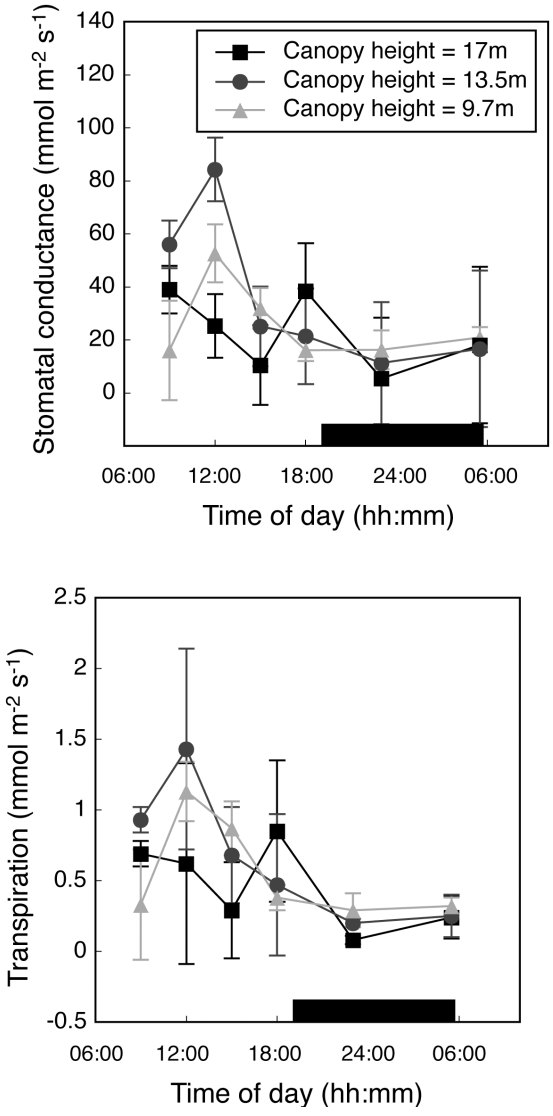

FIGURE 2. Stomatal conductance and transpiration at different canopy heights of *A. lasiocarpa* surrounding air temperature in the canopy of *A. lasiocarpa*.

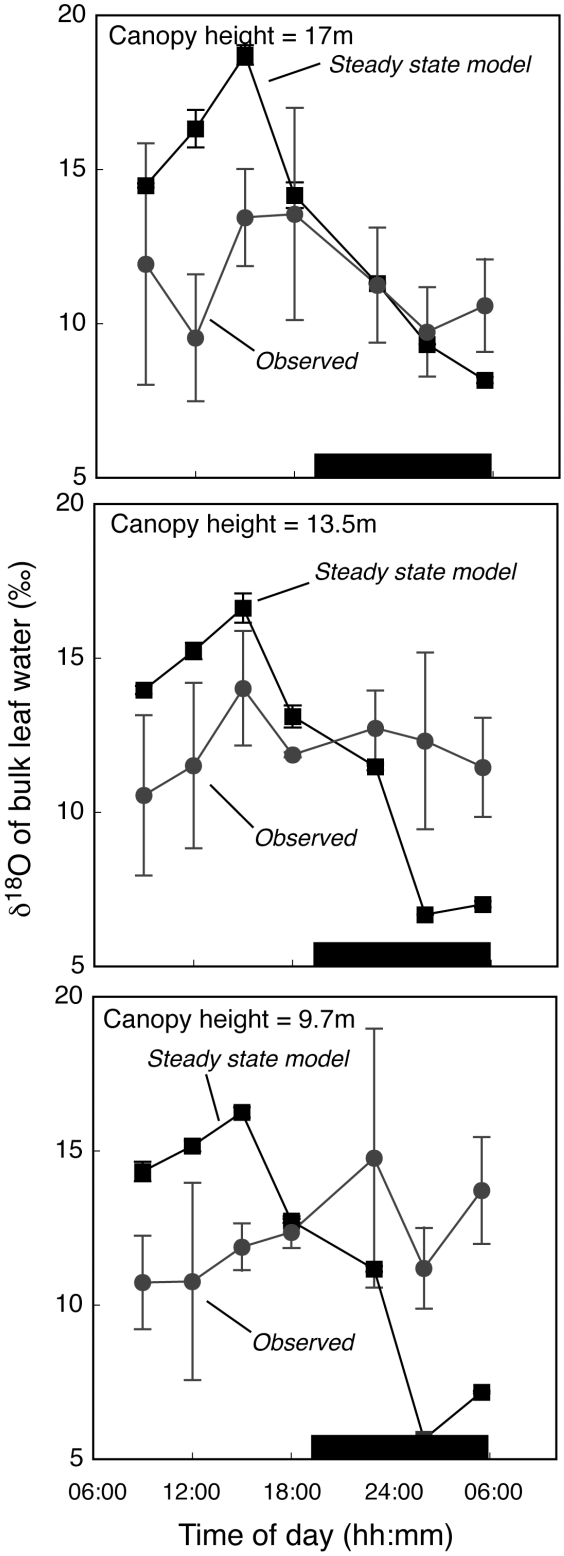

FIGURE 3. The observed and predicted $\delta^{18}O$ values of bulk leaf water at different canopy heights.

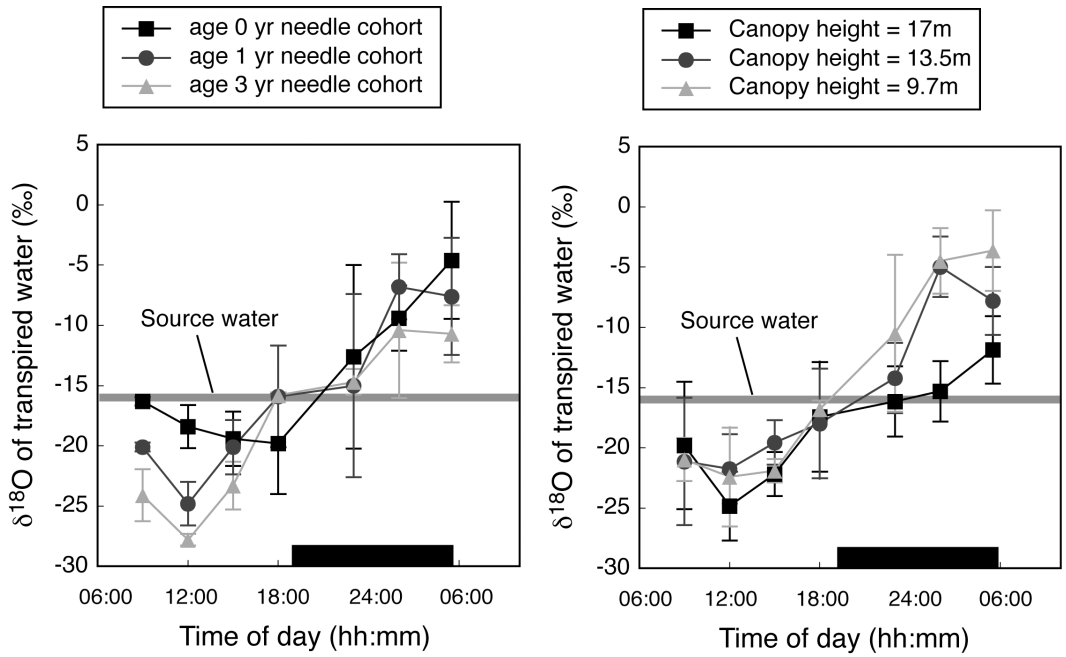

FIGURE 4. The $\delta^{18}O$ values of leaf transpired water in *A. lasiocarpa* calculated from bulk leaf $\delta^{18}O$ values.

where P is the Péclet number. P is calculated as EL/CD, where: E = transpiration rate ($mol \cdot m^{-2} \cdot s^{-1}$); L = the effective path length (taken as 0.008 m); C = the molar density of water (55.5×10^3 mol/m^3); and D = the diffusivity of $H_2{}^{18}O$ in water (2.66×10^{-9} m^2/s) (Farquhar and Lloyd, 1993).

RESULTS AND DISCUSSION

Needle temperature differed substantially from air temperature during daytime and night time periods (Figure 1). The largest difference was observed for needles in the upper canopy exposed to high radiation, where needle temperature was as much as 6.5°C higher than air temperature in mid-afternoon. Radiative cooling of the canopy during nighttime caused needle temperatures to drop below air temperature by as much as 4.5°C. Despite the high wind speeds common at this forest site, the simple assumption of close coupling of leaf and air temperature would lead to substantial error in modelling leaf water ^{18}O enrichment. For example, a 6.5°C difference in needle temperature from 15 to 21.5°C would produce a 0.6‰ difference in ε^* (Equation 1). The assumption also would introduce error in the calculation of e_a/e_i; at 15°C air temperature and 50 percent air humidity, e_a/e_i would be 0.35 assuming equal leaf and air temperature and 0.5 with a 6.5°C higher value of leaf temperature.

The hot, dry conditions in the afternoon period reduced stomatal conductance and transpiration, especially in upper parts of the tree canopy (Figure 2). Low hydraulic conductivity in the xylem of stems caused by bark beetle transmission of a fungal pathogen may have substantially limited the rates of transpiration from the upper canopy in this plant. Leaf longevity is also quite high (ca. 6–10 years) in this species and stomatal conductance and transpiration rates tend to decline as leaves age in conifers. Indeed, stomatal conductance was higher in the youngest needle cohort compared to the 1- and 3-year-old cohorts (data not shown) in the current study. Values of stomatal conductance and transpiration were used to estimate leaf water ^{18}O enrichment using Equations 1–3 for comparison against measured values. Differences in leaf gas exchange properties among the three different aged needle cohorts and at the different canopy heights were sufficient to cause substantial variations in leaf water ^{18}O enrichment within the *A. lasiocarpa* canopy that translated into variations in the $\delta^{18}O$ values of leaf-transpired water vapour.

Overall, the generally low rates of leaf-level T (and consequentially low leaf water turnover rates) in the *A. lasiocarpa* in this study did not allow $\delta^{18}O$ values of needle water to achieve steady state with environmental conditions (Figure 3). However, leaves lower in the canopy compared with those higher in the canopy were closer in their $\delta^{18}O$ values as predicted by the Craig and Gordon steady-state model.

Bulk leaf water $\delta^{18}O$ values were used to calculate leaf transpiration $\delta^{18}O$ values. These values, reported by canopy height and by leaf age cohort, were different than tree source water $\delta^{18}O$ values over much of the diurnal period (Figure 4), indicating the importance of considering isotopic non-steady state T in ET partitioning studies.

The dynamics of leaf water ^{18}O enrichment and the $\delta^{18}O$ value of transpired water in needles of subalpine fir (*A. lasiocarpa*) are poorly represented by a simple isotopic steady state model, and deviations are systematically related to canopy position and leaf age. It is concluded that modelling the isotope composition of forest T and leaf water to increase predictive understanding of ET should take into account the variation in leaf water turnover rates associated with variation in physiological properties of needles of different ages and canopy position that affect isotopic non-steady state T values. To predict short-term changes in the isotope composition of water vapour in forest canopy air (e.g. Lai *et al.*, 2006), models should account also for the potential differences between leaf and air temperature that drive equilibrium and kinetic fractionations.

ACKNOWLEDGEMENTS

We thank R.C. Musselman, W. Massman, and J. Frank for access to the GLEES Ameriflux scaffold and J. Angstmann for assistance with field work. The research was supported by a Technical Contract to D.G. Williams under the IAEA Coordinated Research Project D1.20.09.

REFERENCES

Barbour, M.M. 2007. Stable oxygen isotope composition of plant tissue: a review. *Funct. Plant Biol.*, 34: 83–94.

Bottinga, Y. & Craig, H. 1969. Oxygen isotope fractionation between CO_2 and water, and the isotopic composition of marine atmospheric CO_2. *Earth Planet. Sci. Lett.,* 5: 285–295.

Cappa, C.D., Hendricks, M.B., DePaulo, D.J. & Cohen, R.C. 2003. Isotopic fractionation of water during evaporation. *J. Geophys. Res.,* 108: 4525–4534.

Ehleringer, J.R. & Osmond, C.B. 1989. Stable Isotopes. *In* R.W. Pearcy, J.R. Ehleringer, H.A. Mooney & P.W. Rundel, eds. *Plant physiological ecology: field methods and instrumentation,* pp. 281–300. Chapman and Hall.

Farquhar, G.D. & Lloyd, J. 1993. Carbon and oxygen isotope effects in the exchange of carbon dioxide between terrestrial plants and the atmosphere. *In* J.R. Ehleringer, A.E. Hall & G.D. Farquhar, eds. *Stable isotopes and plant carbon–water relations,* pp. 47–70. San Diego, Academic Press.

Farquhar, G.D., Barbour, M.M. & Henry, B.K. 1998. Interpretation of oxygen isotope composition of leaf material. *In* H. Griffiths, ed. *Stable isotopes: Integration of biological, ecological and geochemical processes,* pp. 27–61. Oxford, BIOS Scientific Publishers.

Helliker, B.R. & Richter, S.L. 2008. Subtropical to boreal convergence of tree-leaf temperatures. *Nature,* Vol. 454: doi:10.1038/nature07031.

Helliker, B.R., Roden, J.S., Cook, C. & Ehleringer, J.R. 2002. A rapid and precise method for sampling and determining the oxygen isotope ratio of atmospheric water vapor. *Rapid Commun. Mass Spectrom.,* 16: 929–932.

Hsieh, J.C.C., Chadwick, O.A., Kelly, E.F. & Savin, S.M. 1998. Oxygen isotopic composition of soil water: Implications for partitioning evapotranspiration. *Geoderma,* 82: 269–293.

Lai, C.T., Ehleringer, J.R., Bond, B.J. & Paw, U.K.T. 2006. Contributions of evaporation, isotope non-steady-state transpiration and atmospheric mixing on the $\delta^{18}O$ of water vapour in Pacific Northwest coniferous forests. *Plant, Cell & Environ.,* 29: 77–94.

Musselman, R.C. 1994. *The Glacier Lakes ecosystem experiments site*. General Technical Report RM-249. USDA Forest Service, Rocky Mountain Forest and Range Experiment Station, Fort Collins, CO.

Pendall, E., Williams, D.G. & Leavitt, S.W. 2005. Comparison of measured and modeled variations in pinon pine leaf water isotopic enrichment across a summer moisture gradient. *Oecologia,* 145: 605–618.

Wang, X.-F. & Yakir, D. 2000. Using stable isotopes of water in evapotranspiration studies. *Hydrol. Process.,* 14: 1407–1421.

Williams, D.G., Cable, W., Hultine, K., Hoedjes, J.C.B., Yepez, E., Simonneaux, V., Er-Raki, S., Boulet, G., de Bruin, H.A.R., Chehbouni, A., Hartogensis, O.K. & Timouk, F. 2004. Components of evapotranspiration determined by stable isotope, sap flow and eddy covariance techniques. *Agric. For. Meteorol.*, 125: 241–258.

Yakir, D. & Sternberg, L.S.L. 2000. The use of stable isotopes to study ecosystem gas exchange. *Oecologia,* 123: 297–311.

Yepez, E.A., Williams, D.G., Scott, R. & Lin, G. 2003. Partitioning overstory and understory evapotranspiration in a semi-arid savanna ecosystem from the isotopic composition of water vapor. *Agric. For. Meteorol.*, 119: 53–68.

Isotope Mass Balance Method to Partition Evaporation from Soil Total Water Loss in Winter Wheat and Spring Maize Cropping Systems in North China Plain

G. Li[1,3,*], Q. Hu[2,3], X. Wang[2,3] and B. Li[1,3]

ABSTRACT

Evaporation (E) is one of main paths of soil water loss in most dryland farming systems. Since it is considered to be of no benefit to crop production, E should be minimized as much as possible. However, the partitioning of E from total water loss (TWL) via transpiration (T) and seepage (S), under field condition is not an easy task. The isotope mass balance (IMB) method is one of the few ways to do so. This study was designed to separate E from TWL in winter wheat and spring maize cropping systems in the North China Plain using the IMB method. In field experiments conducted over two years, plot surfaces were covered with plastic film, with straw mulch, left bare or left as normally in the field, and stable isotope values and amounts of soil water, rainfall, and irrigation water were measured periodically. Results showed that the proportion of E to TWL was 18 percent and 31 percent in winter wheat and spring maize, respectively in the conventional plot, 21 and 12 percent, respectively in plastic film-covered (hereafter referred to as filming) plot, and 47 and 38 percent, respectively in the bare plot. In conclusion, it was found that the IMB method is a simple way to partition average E from TWL over a growing season, and the method is sensitive enough to separate E between straw mulching, filming, conventional practice, and bare soil. The most sensitive factor in using IMB is the determination of the depth of E front within the soil. In the current experiment, isotope measurements of soil water at depths of 0–5 cm were critical to the success of IMB.

Key words: *evaporation, soil total water loss, spring maize, winter wheat, isotope mass balance, mulching.*

INTRODUCTION

Evaporation (E) is one of main paths of water loss in the winter wheat and spring maize cropping system in the North China Plain (NCP), and irrigation is managed to minimize E and seepage (S) to the deep soil layers. Assuming E represents water loss with nearly no benefit to crop production, many agronomic practices such as straw mulching and plastic filming have been used to minimize this component as much as possible. However, it is generally difficult to separate E from total water loss (TWL) under field condition. Isotope techniques may be the most reliable methods to do so. Since the pioneering work of Hsieh *et al.* (1998) to separate E and transpiration (T) using the isotope mass balance (IMB) method in natural systems and similar studies in a natural grassland system (Ferrette *et al.*, 2003) and in a manipulated closed system (Rothfuss *et al.*, 2010), there have been no reports of using the IMB method in an arable field system to separate E from TWL.

The objectives of this research were therefore to test the suitability of IMB for partitioning E from TWL in irrigated winter wheat and spring maize cropping systems in NCP, and to explore the effects of soil temperature, root water absorbing depth and depth of E on the results obtained.

MATERIALS AND METHODS

Field experiment

Four micro-plots were set up in a large area of a field with a light loam soil texture. The plots were 3 m × 3 m and located randomly within the field. The plots were set up as follows: (i) conventional practice, i.e. in the usual way to produce winter wheat or spring maize, (ii) soil left bare after sowing, and all small plants were removed from the plot just after germination, (iii) plastic filming was placed between plant rows as much as possible, and (iv) straw mulching in which maize straw was placed between plant rows as much as possible. Pictures of the field are shown in Figure 1.

Soil samples were collected by drilling soil cores at depths of 0–5, 5–10, 10–20, 20–40, 40–60 and 60–100 cm and at different times. The delta oxygen-18 ($\delta^{18}O$) and delta hydrogen-2 ($\delta^{2}H$) values of soil water were measured. Rainfall and irrigation were recorded and their $\delta^{18}O$ and $\delta^{2}H$ values were also measured.

Soil temperatures at depths of 5, 10, 15, 20 and 25 cm were measured by thermal probes and recorded using a data logger every 20 min.

Yields of winter wheat and spring maize were recorded by harvesting all plants in each plot and measuring the dry weight of grain.

1 Key Laboratory of Cropland Conservation in North China, Ministry of Agriculture
2 Department of Soil and Water Science, College of Resources and Environment
3 China Agricultural University, Beijing, 100193, China
* E-mail address of corresponding author: lgtong@cau.edu.cn

L.K. Heng, K. Sakadevan, G. Dercon and M.L. Nguyen (eds), Proceedings — International Symposium on Managing Soils for Food Security and Climate Change Adaptation and Mitigation. Food and Agriculture Organization of the United Nations, Rome, 2014: 355–359

FIGURE 1. Photos of the experimental field. Note: a, b and c represent respectively the plots of conventional cultivation, film mulching, and straw mulching in the spring maize system, and d shows the plot of film mulching in the winter wheat system.

TABLE 1. Main parameters in partitioning E from soil TWL using the IMB method

Crop	Period[1] (m/d)	Rainfall		Irrigation		Average soil T at -5 cm (°C)
		Amount (mm)	Average $\delta^{18}O$ (‰)	Amount (mm)	Average $\delta^{18}O$ (‰)	
Winter wheat	4/7 – 6/22	108	–7.33	90	–7.60	25.8
Spring maize	6/25 – 9/29	268	–7.79	0	–	22.6

1 The period for winter wheat was from tillering to harvest; for spring maize it was between elongation and harvest.

Isotope mass balance (IMB) method

The method of Hsieh *et al.* (1998) was used to calculate the ratio of E to TWL during selected periods within the whole growing seasons of the winter wheat and spring maize.

The main principle of IMB was the balance of water and its isotope during a given period.

$$x_0\delta_0 + x_r\delta_r + x_i\delta_i = x_f\delta_f + x_e\delta_e + x_{ts}\delta_{ts} \quad (1)$$

$$m_0 + m_r + m_i = m_f + m_e + m_{ts} \quad (2)$$

where m is the mass of soil water per ha within a given depth, m^3; δ is isotope value (^{18}O or ^{2}H) of water, ‰; and the subscripts 0, r, i, f, e, and ts are respectively: original state, rainfall, irrigation, final state, E, T and S, respectively.

$x_j = m_j / m_{total}$, here j = 0, r, i, f, e, and ts

$m_{total} = m_0 + m_r + m_i$

For δ_e at 20°C, the equation of Majoube (1971) was used:

$\alpha_{l\text{-}e} = (\delta_l + 1000)/(\delta_e + 1000) = 1.009563$

δ_t was assumed to be the $\delta^{18}O$ values of the weighted mixture of soil water at time 0 and of irrigation water and rainfall and:

$\delta_t = x_0\delta_0 + x_i\delta_i + x_r\delta_r$

The standard state of IMB was defined by determining the following parameters: E at a soil depth of 5 cm, average soil temperature at 5 cm depth was 19.8°C and root water absorbing depth ranging from 5 cm to 60 cm along the soil profile.

Values for the main parameters are shown in Table 1.

RESULTS

The dynamics of soil water content and the corresponding oxygen isotope values under spring maize in 2010 and winter wheat in 2012 are shown in Figures 2 and 3. For spring maize, soil water content along the upper 80 cm of the soil profile varied significantly during the whole growing season, showing that water stored in this part of the profile was influenced greatly by the water absorption capacity of maize roots, rainfall recharge and/or irrigation and E (Figure 2, a1 to d1). Thus, it was reasonable to use 80 cm as the depth of water absorption by maize roots. On the other hand, variations in isotope values of soil water ($\delta^{18}O$) caused by isotope discrimination during phase change (E), occurred only at depths above 30 cm, suggesting that E occurred mostly within this part of the soil profile (Figure 2, a2 to d2).

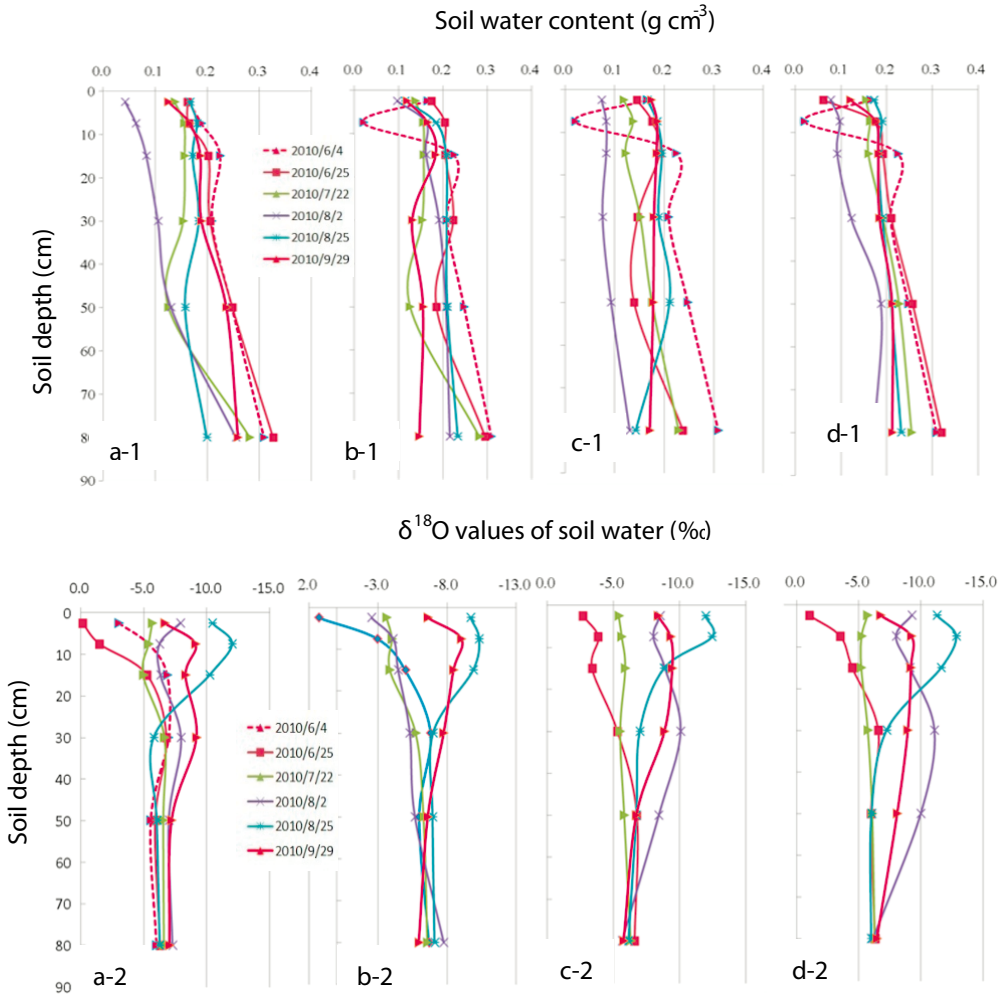

FIGURE 2. The dynamics of soil water content and the corresponding $\delta^{18}O$ values along the soil profile under spring maize. Note: a, b, c, and d represent respectively the plots of conventional cultivation, bare soil, film mulching, and straw mulching numbers 1 and 2 represent respectively the soil water content and $\delta^{18}O$ values of soil water.

TABLE 2. Depth (mm) and percent (values in brackets) of E to TWL in winter wheat and spring maize

Crop	Year	Conventional		Filming		Mulching		Bare	
		TWL	E	TWL	E	TWL	E	TWL	E
WW	2010	147	33 (22)	92	19 (21)			56	23 (41)
	2012	165	24 (15)					87	46 (53)
SM	2010	206	63 (31)	157	22 (12)	178	43 (24)	182	65 (38)

Figures in brackets are % of E to TWL; WW — winter wheat; SM — spring maize.

The depth at which the roots of spring wheat absorbed water was the same as for spring maize (about 80 cm), as shown by the great variation in soil water content along the 80 cm soil profile during the growing season (Figure 3, b). For the plot with bare soil, the soil water content decreased continuously, as no irrigation was applied to it (Figure 3, a). Again, E mostly occurred at above a soil depth of 30 cm, as reflected by the great variation of $\delta^{18}O$ values in the upper 30 cm and the relative steady values below that depth (Figure 3, c and d).

Table 2 shows the results for separating E from TWL by the IMB method and the soil water budgets at depths of 0–60 cm for winter wheat and 0–100 cm for spring maize. The IMB method enabled clear differentiation of E between the plots. For winter wheat, E was about 20 percent (range 15–22 percent) of TWL under conventional cultivation and 21 percent with filming, suggesting that filming did not reduce E significantly in winter wheat. For bare soil, E was about 50 percent of TWL (range 41–53 percent), meaning that half of water loss in bare soil was via E. On the other hand, both filming and straw mulching reduced E significantly in spring maize (by 19 percent and 7 percent, respectively).

The relatively lower E (15–22 percent) for winter wheat can be attributed to irrigation being carried out late, at the middle of May

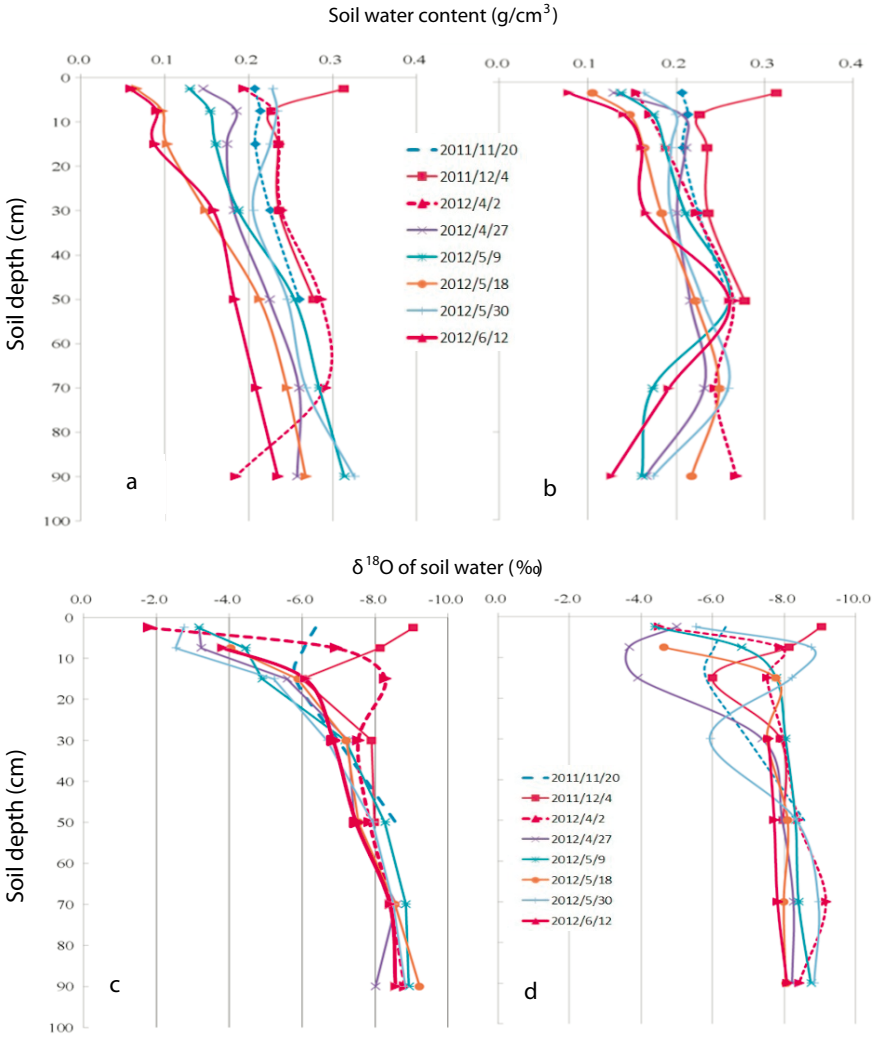

FIGURE 3. The dynamics of soil water content and corresponding $\delta^{18}O$ values along the soil profile under winter wheat. Note: a and b represent respectively the soil water contents in the plots of bare soil and conventional cultivation, and c and d represent the corresponding $\delta^{18}O$ values of soil water.

when the crop cover is nearly 100 percent. Before May, the top soil is very dry and E is inhibited.

The component of E for spring maize (31 percent) can be assumed to occur mainly during May to June when the crop cover is lower with excessive rainfall events.

DISCUSSION

In IMB, three factors affect the results of calculations, namely depth of soil E, root water absorbing depth, and soil temperature. It is difficult to determine the depth beneath soil surface at which soil water evaporates. Yet, the depth at which E takes place is critical since it determines the δ_l value of soil water to be used in the estimation of δ_e of the vapour. The present results show that with different depths of E, the ratio of E to TWL could be as much as 18 percent more or 44 percent less than the current depth of 33 mm (Table 3), indicating the importance of determining the depth to be used for calculations of E to obtain reasonable values when using the IMB method. In Table 3, a sensitivity analysis was carried out where different soil depths (0–5, 0–10 and 0–20 cm) of E were used to determine the evaporation ratio. These were then compared with that of the standard which is E occurred at soil depth of 5 cm, at a soil temperature of 19.8°C at that depth, with root water absorbing depth ranging from 5 cm to 60 cm. The aim of this exercise is to see the difference in E ratio calculated by IBM using different E depths.

Root water absorbing depth is also important in the IMB method since it determines the δ_{ts} values used in the calculations. Results obtained here show that it could vary by as much as 30 percent less than the current depth (Table 3). However, the influence of the root water absorbing depth is smaller than the depth at which E occurs.

The effect of soil temperature on E at a soil depth of 5 cm was not so significant, with only a 2–3 percent difference being recorded when the temperature changed from 20°C to 15°C, which is not likely to happen at a given location between different years.

CONCLUSIONS

IMB is a simple way to partition E from the TWL of a soil body over the whole growing season, and is especially effective for small plot field experiments. Its sensitivity is good enough to demonstrate differences in E between plot treatments of straw mulching, filming, conventional practice and bare soil.

TABLE 3. Effects of depth of E, root water absorption, and soil temperature at 5 cm depth on the evaporation ratio (%) calculated using the IMB method

State	Conventional	Filming
Standard	33	19
E occurring depth (cm)		
0–5	31 (–6%)	22.5 (+18%)
0–10	23 (–30%)	14.5 (–24%)
0–20	18.5 (–44%)	11.5 (–41%)
Root water absorption depth (cm)		
5–60	26.5 (–21%)	17.5 (–8%)
5–40	24.5 (–25%)	16.5 (–13%)
20–60	23 (–30%)	16.5 (–13%)
Soil temp. at 5cm depth (°C)		
20	24 ± 2 (S.E.)	16 ± 2 (S.E.)
15	21 ± 2 (S.E.)	14 ± 2 (S.E.)

Figures in brackets are differences between E and the corresponding current state.

The most important factor determining results using the IMB method is the depth of E within the soil. In this experiment, isotope measurement of soil water at a depth of 0–5 cm was critical to the success of the IMB technique.

ACKNOWLEDGEMENTS

The authors are grateful for the support provided in conducting this work through the FAO/IAEA Coordinated Research Project "Managing Irrigation Water to Enhance Crop Productivity under Water-Limiting Conditions using Nuclear Techniques".

REFERENCES

Ferretti, D. F., Pendall, E., Morgan, J. A., Nelson, J. A., LeCain, D. & Mosier, A. R. 2003. Partitioning evapotranspiration fluxes from a Colorado grassland using stable isotopes: Seasonal variations and ecosystem implications of elevated atmospheric CO_2. *Plant Soil,* 254: 291–303.

Hsieh, J.C.C., Chadwick, O.A., Kelly, E.F. & Savin, S.M. 1998. Oxygen isotopic composition of soil water: Quantifying evaporation and transpiration. *Geoderma,* 82: 269–293.

Majoube, M. 1971. Fractionnement en oxygene-18 et en deuterium entre l'eau et sa vapaeur. *J. Chim. Phys.,* 68: 1423–1436.

Rothfuss, Y., Biron, P., Braud, I., Canale, L., Durand, J.L., Gaudet, J.-P., Richard, P., Vauclin, M. & Bariac, T. 2010. Partitioning evapotranspiration fluxes into soil evaporation and plant transpiration using water stable isotopes under controlled conditions. *Hydrol. Process.,* 24: 3177–3194.

An Improved Vacuum Distillation Method for Extracting Soil Water for Stable Isotope Analyses

L. Mayr[1,*], M. Aigner[1] and L. Heng[2]

ABSTRACT

A simple, fast and portable vacuum distillation setup and methodology to extract water from soil and plant samples for water stable isotope analyses (oxygen-18 [^{18}O] and hydrogen-2 [^{2}H]) was developed. The methodology was tested on two soil types (a sandy loam and a silty clay loam) over different extraction times and soil moisture (near field capacity and permanent wilting point). Using an immersion cooler instead of liquid nitrogen or solid carbon dioxide (dry ice) as the cooling agent, the results showed that full recovery (extracting more than 98 percent of the total water) and reproducible isotopic ratios (± 0.08‰ for $\delta^{18}O$ and ± 0.83‰ for $\delta^{2}H$) can be reached after 30 min with a dry sandy soil and 120 min with a dry clay soil at 100°C distillation temperature. The methodology allows large number of samples to be prepared for analysis quickly and reliably.

Key words: *Vacuum distillation, soil water extraction, stable isotope analyses.*

INTRODUCTION

The need for a rapid, inexpensive technique for routine oxygen-18/oxygen-16 ($^{18}O/^{16}O$) extraction of water from plant and soil samples is increasing due to the greater demand for isotopic data in agro-ecological, soil water, evaporation and transpiration partitioning and hydrological studies (White *et al.*, 1985; Williams *et al.*, 2004; Van Pelt *et al.*, 2010; Soderberg *et al.*, 2011). The common sample extraction techniques include: azeotropic distillation with kerosene or toluene (Revesz and Woods, 1990), centrifugation (Edmunds and Bath, 1976), liquid/vapour equilibration in plastic bags (Wassenaar *et al.*, 2008), mechanical pressing (Patterson *et al.*, 1977; Jusserand, 1980) and vacuum distillation (Araguás-Araguás *et al.*, 1995; West, Patrickson and Ehleringer, 2006; Koeniger *et al.*, 2011), the last being the most commonly used method. Nevertheless, most of the conventional techniques are often laborious, time consuming and involve complicated setups with specially-made glass apparatus. In addition, liquid nitrogen or dry ice is needed to freeze and trap water vapour evaporated during extraction. However, both of these cooling agents can be difficult to acquire in many developing countries. With water isotope analyses becoming cheaper, easier and faster (e.g. through the development of modern laser isotope analyzers e.g. cavity ring down spectroscopy [CRDS]), the bottleneck in sample throughput is often the water extraction time instead of the isotopic analysis of water.

Here we describe a simple, fast and accurate vacuum distillation method using a commercial immersion cooler and a Dewar container filled with 2-propanol at –50°C, in place of the liquid nitrogen or dry ice for freezing water vapour. The method can be easily adopted at a relatively low cost and allows large number of samples to be extracted quickly for isotopic analyses.

MATERIALS AND METHODS

The studies were carried out using two different soil types: Ebendorf silty clay loam and Reisenberg sandy loam (Table 1), adjusted to two different moisture levels: close to field capacity (Ebendorf soil at 0.1 bar; Reisenberg soil at 0.3 bar) and near wilting point (Ebendorf soil at 12.5 bar; Reisenberg soil at 1 bar). In order to avoid fractionation of delta oxygen-18 ($\delta^{18}O$) and delta hydrogen-2 ($\delta^{2}H$) during the moisture adjustment, soil moisture at both levels was adjusted using a ceramic pressure plate extractor (Soil Moisture Equipment Corp., Santa Barbara, California, USA). The two bulk soils were initially air dried and sieved to 2 mm. About 500 g of each soil type was equilibrated with one litre of water of known $\delta^{18}O$ and $\delta^{2}H$ content ($\delta^{18}O$ = –9.28‰; $\delta^{2}H$ = –67.76‰). The slurry, made by stirring the soil-water suspension thoroughly, was left standing covered and light-protected for two days at room temperature (25°C). After the equilibration time the excess water was decanted and the wet soil poured into three metal rings (55 mm diameter, 40 mm height) for each soil type (three replicates) and placed on a ceramic pressure plate. Water was removed from the soil by applying the appropriate pressure until no more water was found flowing out of the pressure chamber.

After moisture adjustment, five subsamples of 3–5 g per soil type and per moisture level were taken from each of the metal rings using an auger (10 mm diameter) and weighed into tare 100 × 16 mm glass culture tubes, and a pre-weighed portion of dry glass wool was added on top of the soil to prevent small soil particles moving into the trapping tube during distillation. The tubes were immediately closed and stored in the deep freezer at –18°C.

The setup allowed these sample storage tubes (15 mL glass culture-tubes with GL18 screw caps) to be connected to the distillation unit without the need to transfer the sample to other containers. The tubes were connected to one end of a glass assembly with a water collection tube, and a cock valve with NTFE spindle on the other side (Figure 1).

A six-litre stainless steel Dewar was filled with four litres of 2-propanol and the immersion cooler (Peter Huber, TC50-NR) was submerged into the liquid. A temperature of –50°C was reached after about three hours (h). The cooling device was on during the whole distillation procedure.

1 Soil and Water Management and Crop Nutrition Laboratory, Seibersdorf, Austria
2 Soil and Water Management and Crop Nutrition Section, Vienna, Austria
* E-mail address of corresponding author: L.Mayr@iaea.org

L.K. Heng, K. Sakadevan, G. Dercon and M.L. Nguyen (eds), Proceedings — International Symposium on Managing Soils for Food Security and Climate Change Adaptation and Mitigation. Food and Agriculture Organization of the United Nations, Rome, 2014: 361–364

TABLE 1. Characteristics and moisture level of test soils

Soil type	Soil code	% sand	% silt	% clay	Applied pressure	% moisture
Ebendorf silty clay loam	C-wet	16	57	27	0.1 bar	33.3
	C-dry				12.5 bar	19.8
Reisenberg sandy loam	S-wet	65	28	7	0.3 bar	18.7
	S-dry				1.0 bar	12.6

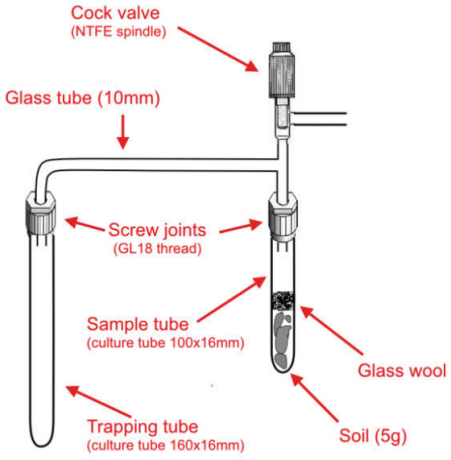

FIGURE 1. Schematic diagram of glass assembly.

FIGURE 2. An improved vacuum distillation method for extracting soil and plant water for stable isotope analyses, with heating blocks (A), Dewar filled with 2-propanol (B) and immersion cooler (C).

Prior to evacuation the sample was frozen in the Dewar connected to the immersion cooler for about three min to minimize water vapour in the gas phase and to avoid losses of water during evacuation. The assembly was attached to a vacuum pump (Edwards, E2M-15) and pumped down to a pressure of less than 1 mbar measured with a digital vacuum gauge (Vacuubrand, DVR2). The cock valve was closed to maintain the vacuum in the sample and the assembly was detached from the vacuum pump. The sample side of the unit was then put on a block heater (VWR, ANA 2BLK) set to 100°C, and the other side with the water collection tube was inserted to about one third of the total length into the cooling liquid at –50°C. Depending on the size of the block heater and the Dewar container for the immersion cooler, at least eight units can be distilled at one time. With our setup we were able to process 15 samples at once (Figure 2).

Three replicate samples per moisture level were prepared for water extraction at five different extraction times (15, 30, 60, 120 and 180 min). Fifteen samples of each soil were put on the block heater and after the corresponding extraction time three replicates each were removed, vented to air by opening and closing the stopcock valve, and left standing in a rack until the ice in the water trap had melted. Then the sample and water tubes were disconnected from the glass assembly and closed immediately with screw caps. All tubes were weighed after having reached room temperature (25°C).

Water was transferred from the trapping tubes into 2-ml autosampler glass vials (32 x 12 mm) using disposable pipettes. For water volumes of less than 0.5 ml, vials with a 0.3 ml insert were used. The samples were analysed for $\delta^{18}O$ and $\delta^{2}H$ using a cavity ring down laser spectrometer (CRDS Picarro Isotopic Water Analyzer L2130-i).

After extraction the soil dry weight was recorded and the tubes containing soil were placed on a separate block heater at 110°C and closed with silicone stoppers holding two syringe needles. One was connected to an aquarium pump blowing dry air onto the soil using a molecular sieve filter. The other needle was for release of the moist air. With this special drying procedure all remaining moisture could be removed overnight. After cooling to room temperature the soil samples were again weighed and the difference between soil weight after extraction and soil weight at "complete dryness" was determined.

MEASUREMENTS AND CALCULATIONS

The percent recovery was determined using the following equation:

$$\% \text{ water recovery} = (S_{wet}-S_{dist})/(S_{wet}-S_{dry}) \times 100$$

where S_{wet} is weight of wet soil S_{dist} is weight of soil after distillation and S_{dry} is weight of soil after oven drying (48 h at 110°C). Araguas-Araguas *et al.* (1995) suggested 98 percent recovery as the minimum for isotope analyses to obtain unfractionated water.

RESULTS AND DISCUSSION

S-wet and S-dry (sandy soil)

The results of the isotopic ($\delta^{18}O$ and $\delta^{2}H$) values for the two soil types under both wet and dry initial water levels were plotted against the extraction time (Figure 3). The isotopic value of extracted water increased with extraction time until it became essentially constant. These values were respectively 15 min for wet sandy soil and 30 min for dry sandy soil.

For Ebendorf clay soil, 30 min was required for extraction of wet soil while it took 120 min to recover 98 percent of the total water from dry soil (Figure 3; Table 2). In general, extraction of dry soil took longer to obtain unfractionated water than wet soil. The Ebendorf clay soil also took slightly longer than the Reisenberg sandy soil. Differences in soil texture and hence in pore size distribution between

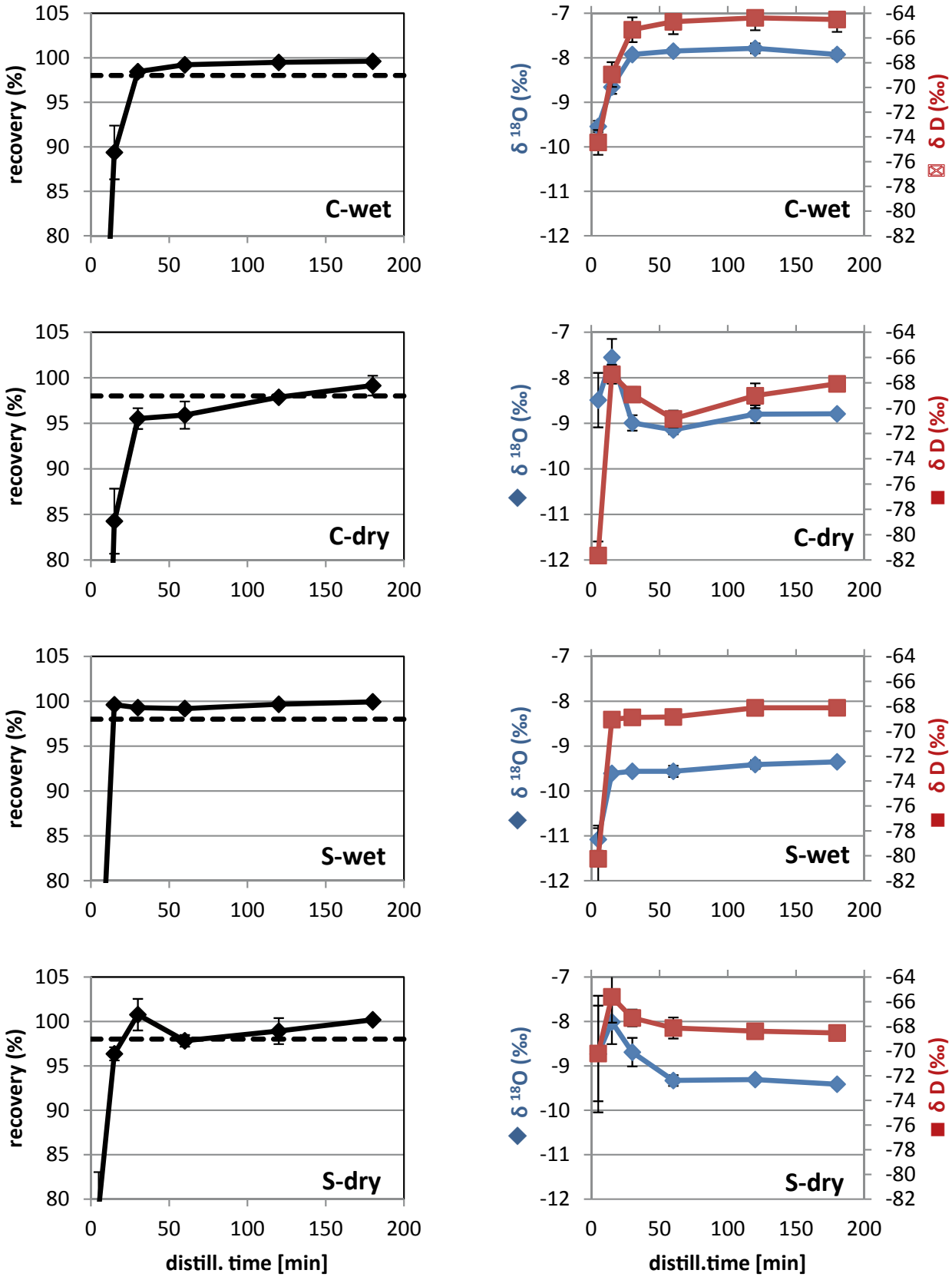

FIGURE 3. Extraction time for 98 percent recovery from Reisenberg sandy and Ebendorf clay soils under wet and dry conditions (left); corresponding $\delta^{18}O$ and $\delta^{2}H$ values under various extraction times are also shown (right).

TABLE 2. Minimum distillation time required to achieve a water recovery of > 98 percent and their corresponding $\delta^{18}O$ and $\delta^{2}H$ precisions at one standard deviation

Soil type		Time (min)	Precision (1σ SD)	
			$\delta^{18}O$ (‰)	$\delta^{2}H$ (‰)
Ebendorf clay soil	C-wet	>= 30	± 0.09	± 0.58
	C-dry	>= 120	± 0.13	± 0.83
Reisenberg sandy soil	S-wet	>= 15	± 0.11	± 0.51
	S-dry	>= 60	± 0.08	± 0.43

the soil types may influence the extraction time. West *et al.* (2006) presented water extraction times for plant and soil materials also using a vacuum distillation method. They obtained extraction times of 30 min for sandy soils and 40 min for clay soils for a 98 percent recovery of water, which is comparable with the findings from the present study.

The precision of the analytical method is shown in Table 2. Single standard deviation was calculated from all respective samples with a water recovery higher than 98 percent. Just like the findings of West, Patrickson and Ehleringer (2006), our results showed low standard deviations of extracted water for $\delta^{18}O$ and $\delta^{2}H$ in both sandy and clay soils.

CONCLUSIONS

A simple, fast, affordable and portable vacuum distillation method for extracting soil samples for isotopic analysis was developed. The extraction times were 30 min for the Reisenberg sandy soil and 120 min for the Ebendorf clay soils. The method does not require the use of liquid nitrogen or dry ice hence can be adapted easily for developing countries. The storage vials can be connected directly to minimize the transfer of sample. Other advantages of this system are the portability, the relatively low price (US$8 000 for a setup of 12 samples) and the high throughput. The fast recovery and reproducibility of the new methodology developed is valuable for quantifying the removal of water from the soil around crop roots through soil evaporation and transpiration. This information will be used to identify soil and water management practices that minimize water losses via soil evaporation.

ACKNOWLEDGEMENTS

This work was done under FAO/IAEA coordinated research project D1.20.09 on "Managing irrigation water to enhance crop productivity under water-limiting conditions: A role for isotopic techniques".

REFERENCES

Araguás-Araguás, L., Rozanski, K., Gonfiantini, R. & Louvat, D. 1995. Isotope effects accompanying vacuum extraction of soil water for stable isotope analyses. *J. Hydrol.*, 168: 159–171.

Edmunds, W.M. & Bath, A.H. 1976. Centrifuge extraction and chemical analysis of interstitial waters. *Environ. Sci. Technol.*, 10: 467–472.

Jusserand, C. 1980. Extraction de l'eau interstitielle des sédiments et des sols–comparison des valeurs de l'oxygène 18 par différentes méthodes, premiers résultats. *Catena,* 7: 87–96; doi: 10.1016/S0341-8162(80)80006-3.

Koeniger, P., Marshall, J.D., Link, T. & Mulch, A. 2011. An inexpensive, fast, and reliable method for vacuum extraction of soil and plant water for stable isotope analyses by mass spectrometry. *Rapid Commun. Mass Spectrom.*, 25: 3041–3048.

Patterson, R.J., Frape, S.K., Dykes, L.S. & Mcleod, R.A. 1977. A coring and squeezing technique for the detailed study of subsurface water chemistry. *Can. J. Earth Sci.*, 15, 162–169.

Revesz K. & Woods P. 1990. A method to extract soil water for stable isotope analysis. *J. Hydrol.*, 115: 397–406.

Soderberg, S., Good, S.P., Wang, L. & Caylor, K. 2011. Stable isotopes of water vapor in the vadose zone: A review of measurement and modeling techniques. *Vadose Zone J.*, doi:10.2136/vzj2011.0165.

Van Pelt, A., Williams, D., Mayr, L. & Sun, W. 2010. Real-time field-based water vapor isotope measurements with a CRDS analyzer: Probing cropland evapotranspiration. *In* A. Knohl, N. Buchmann, & M. Bahn, eds. *Stable isotopes and biogeochemical cycles in terrestrial ecosystems: Coupling plant and soil processes across spatial and temporal scales*, P2.14, Monte Verità, Switzerland.

Wassenaar, L.I., Hendry, M.J., Chostner, V.L. & Lis, G.P. 2008. High resolution pore water delta deuterium and oxygen-18 measurements by water (liquid)-water (vapor) equilibration laser spectroscopy. *Environ. Sci. Technol.*, 42: 9262–9267.

West, A.G., Patrickson, S.J. & Ehleringer, J.R. 2006. Water extraction times for plant and soil materials used in stable isotope analysis. *Rapid Commun. Mass Spectrom.*, 20: 1317–1321.

White, J.W.C., Cook E.R., Lawrence J.R. & Broecker, W.S. 1985. The D/H ratios of sap in trees: Implications for water sources and tree ring D/H ratios. *Geochim. Cosmochim. Acta,* 49: 237.

Williams, D.G. Cable, W., Hultine, K., Hoedjes, J.C.B., Yepez, E.A., Simonneaux, V., Er-Raki, S., Boulet, G., de Bruin, H.A.R., Chehbouni, A., Hartogensis, O.K. & Timouk, F. 2004. Evapotranspiration components determined by stable isotope, sap flow and eddy covariance techniques. *Agric. For. Meteorol.*, 125: 241–258.

Dynamics of *de Novo* Formation of Amino Sugars in Soil via CSSIA

S. Bodé[1], Z. Bai[1,2], D. Huygens[1,3], X. Zhang[2] and P. Boeckx[1,*]

ABSTRACT

Amino sugars are the building blocks of microbial cell walls and have been used widely to assess microbial residues. To have a better insight in the formation dynamics of amino sugars in soil, uniformly carbon-13 (^{13}C)-labelled wheat residue of different quality (grain, leaf and root) was amended to two soils under distinct tillage managements. The isotopic composition of individual amino sugars was measured using liquid chromatography — isotope ratio mass spectrometry (LC-IRMS). Maximum formation was reached within a few days after residue addition. Glucosamine and galactosamine followed dissimilar formation kinetics. The maxima of incorporation of residue C into the amino sugar pools ranged from 1.0 percent for galactosamine to 10.6 percent for glucosamine. Formation rate constants of residue-derived amino sugars ranged from 0.11 to 0.48/d for galactosamine and glucosamine, respectively. In general, larger amounts of amino sugars were formed at a higher rate with increasing plant residue quality. The microbial community of the no-till soil was better adapted to assimilate low quality plant residues (i.e. leaf and root). All together, the formation dynamics of microbial cell wall components was component-specific and determined by residue quality and the soil microbial community.

Key words: *amino sugar, kinetics, organic residue, tillage, carbon-13, LC-IRMS.*

INTRODUCTION

Microbial decomposition of soil organic matter (SOM) releases 60 Pg of carbon dioxide and 300 Tg of methane to the atmosphere each year. Aerobic or anaerobic microbial breakdown of soil organic matter is controlled by its recalcitrance, physicochemical protection and microbial enzyme activity, and controls the potential for terrestrial ecosystems to sequester or release carbon (C) to the atmosphere (Craine, Fierer and McLauchlan, 2010). Slight changes in the rate of SOM decomposition due to human disturbances or temperature can significantly affect the concentration of carbon dioxide or methane in the atmosphere. Predicting the sensitivity of SOM decomposition to temperature change or human disturbance is therefore critical to predicting future atmospheric greenhouse gas concentrations and feedbacks to climate warming and soil degradation.

1 Isotope Bioscience Laboratory - ISOFYS, Ghent University, Gent, Belgium
2 State Key Laboratory of Forest and Soil Ecology, Institute of Applied Ecology, Chinese Academy of Sciences, Shenyang, P. R. China
3 Institute of Agricultural Engineering and Soil Science, Faculty of Agricultural Sciences, Universidad Austral de Chile, Valdivia, Chile
* E-mail address of corresponding author: pascal.boeckx@ugent.be

One of the most significant impacts that microbial communities have on their environment is their ability to recycle essential elements that make up their cells (Glaser, Turrion and Alef, 2004). Therefore, there is considerable interest in understanding the biological mechanisms that regulate C exchanges between the land and atmosphere, including microbial metabolism (Allison, Wallenstein and Bradford, 2010). Amino sugars are useful microbial biomarkers to investigate the dynamics of microbial communities due to their prevalence in the cell walls of microorganisms, their insignificant content in plant residues and their recalcitrance after cell death (White, 1968; Amelung *et al.,* 2001; Glaser and Gross, 2005; He *et al.,* 2005; Liang and Balser, 2010). Over 90 percent of amino sugars are found in dead cells (Amelung *et al.,* 2001). Therefore, the amino sugar content is used to quantify microbial residues rather than a proxy for living microbial biomass and activity (van Groenigen *et al.,* 2010). Glucosamine in soil is mainly derived from chitins of fungal cell walls, though it also occurs in bacteria. Muramic acid originates exclusively from peptidoglycans of bacterial cell walls (Farkas, 1979; Amelung *et al.,* 2001 and 2008; He *et al.,* 2005). The origin of galactosamine is less clear and is typically considered to be non-specific, as actinomycetes, bacteria and fungi all likely contain considerable amounts of galactosamine (He *et al.*, 2005; Ding *et al.*, 2010).

Therefore, the first aim of this study was to elucidate residue-derived amino sugar formation kinetics following plant residue addition. Also evaluated was the use of residue C incorporation dynamics into the amino sugar pools as a tool to assess microbial physiology.

To these ends, a laboratory incubation experiment was carried out in which two soils with a distinct tillage management were incubated with carbon-13 using ^{13}C-labelled wheat residues of different quality (wheat grain, leaves and roots). The amino sugar formation dynamics were determined by measuring the evolution of the ^{13}C content of individual amino sugars via liquid chromatography — isotope ratio mass spectrometry (LC-IRMS).

MATERIALS AND METHODS

Soil description and incubation

Soil description

The soils for this study were collected from the field site located in Maulde, Belgium (50°37'N, 3°34'E). The climate of the site is characterized as temperate and humid marine with a 30-year mean precipitation of 780 mm per yr, and mean maximum and minimum temperatures of 13.5°C and 6.3°C, respectively. The soil is classified as a Luvisol (FAO, 2006). The field site has been used for cropping over 100 yr and was converted from conventional tillage (moldboard plowing to 30 cm and harrowing of the top 10 cm) to reduced tillage (harrowing of the top 10 cm) in 1995. In 2006, one third of the field was reconverted to conventional tillage, another third to "no-till"

L.K. Heng, K. Sakadevan, G. Dercon and M.L. Nguyen (eds), Proceedings — International Symposium on Managing Soils for Food Security and Climate Change Adaptation and Mitigation. Food and Agriculture Organization of the United Nations, Rome, 2014: 365–369

(no soil disturbance and direct seeding). Soils from both conventional (CT) and no-till (NT) fields were collected.

Incubation experiment

The uniformly ^{13}C labelled wheat (*Triticum aestivum*) had been grown with $^{13}CO_2$ (2 atom% excess) (Denef and Six, 2006). The grain, leaves and roots were collected, dried at 45°C and stored at room temperature until incubation. Residues were ground to a size <250 µm and mixed thoroughly with the soil. An application rate of 6 mg substrate C/g dry soil was used in six treatments: NG (NT with grain residue), NL (NT with leaf residue), NR (NT with root residue), CG (CT with grain residue), CL (CT with leaf residue), and CR (CT with root residue). There were three microcosm replicates for each treatment.

The incubation temperature was maintained at 24°C and the moisture content at 20 percent (w/w). Sampling was done after 0, 9, 24, and 45 hrs, and at 3, 5, 10 and 21 d by instantaneously freezing the microcosms in liquid nitrogen followed by lyophilization. The subsamples were stored at –20°C for subsequent analyses.

Amino sugar analysis

The amino sugar extraction procedure was based on the method described by Bodé, Denef and Boeckx (2009). Briefly, c.a. 0.2 g soil was hydrolyzed for eight hrs at 105°C using 10 mL 6M HCl. Thereafter, the soil suspension was filtered (GF/C 25mm, Whatman) using a reusable syringe filter device (Millipore, SWINNEX). Water and HCl were removed by evaporating under reduced pressure at 45°C, and the concentrated amino sugar sample was re-dissolved in MilliQ water. After purification by a cation exchange resin, the amino sugar solution was dried and re dissolved with 1.5 mL MilliQ water. Concentration and delta carbon-13 ($\delta^{13}C$) of amino sugar were determined by liquid chromatography-isotope ratio mass spectrometry (LC-IRMS) (Thermo Electron, Bremen, Germany).

The fraction of amino sugar C derived from the ^{13}C-labelled residues at a time point t was calculated as:

$$fAS_{R,t} = \left(\frac{a^{13}C_{AS,t} - a^{13}C_{AS,t_0}}{a^{13}C_R - a^{13}C_{SOM}} \right) \quad (1)$$

where $a^{13}C_R$ and $a^{13}C_{SOM}$ are ^{13}C fractional abundances ($^{13}C/(^{13}C + {}^{12}C)$) of the added residues and original SOM, respectively; and $a^{13}C_{AS,t}$ and $a^{13}C_{AS,t0}$ are the isotopic composition of the amino sugar of interest at time *t* and at the start of the incubation experiment, respectively.

It should be noted that the $^{13}C_{AS,t0}$ was not identical to the original isotopic composition of the soil amino sugar (AS_0) due the presence of ^{13}C-labelled amino sugars in the plant residues. Since plants do not produce amino sugars (Amelung *et al.,* 2008), this is likely explained by the presence of endophytic bacteria and fungi (Appuhn *et al.,* 2004, Reinhold-Hurek and Hurek, 2011) in the labelled plant material.

Bulk soil isotopic analysis

Sub-samples of air dried soil samples were ground by a planetary ball mill (PM400, Retsch, Germany) for total C and N, and ^{13}C and nitrogen-15 (^{15}N) analyses were by an elemental analyzer (EA) (ANCA-SL, SerCon, UK) coupled to an IRMS (20-20, SerCon, UK).

Statistical analysis

Statistical analysis was performed using SPSS 19.0. A three-way analysis of variance (ANOVA) procedure with Tukey's HSD (Honestly Significant Difference) *post hoc* test was used to analyse the effects of plant residue quality, amino sugar identity and tillage on amino sugar formation and C mineralization using a general linear model. When a significant interaction between factors was observed this interaction was investigated by repeating the statistical test for the different levels of the interacting factors individually. Unless otherwise stated a significant level of difference was set at $\alpha = 0.05$. Non-linear regression analysis was used to determine *k* and maxima in non-linear equation (2).

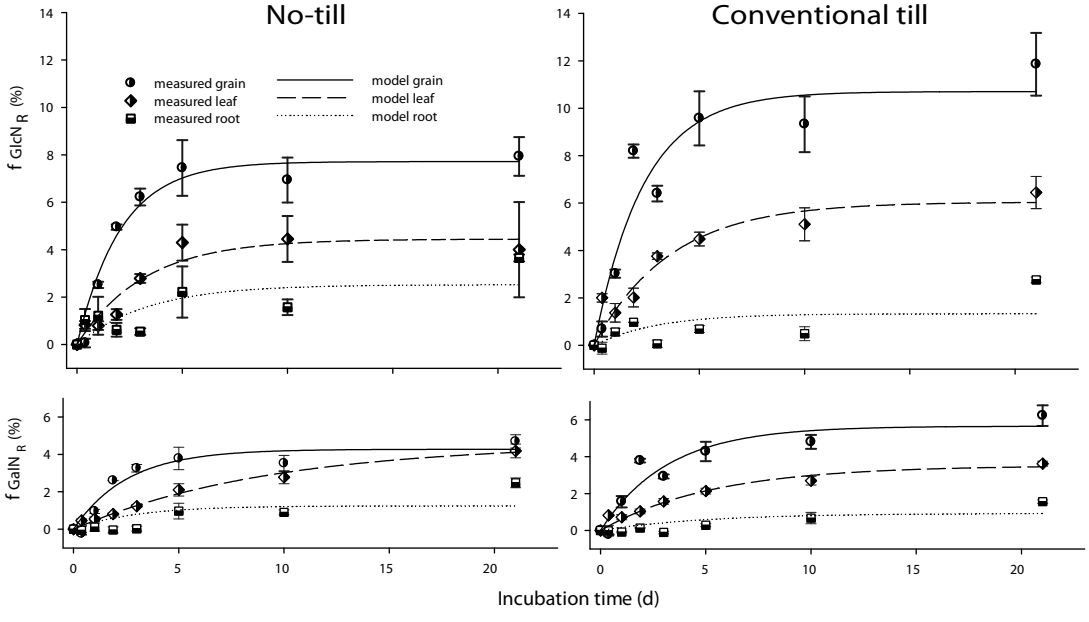

FIGURE 1. Modelled and measured contribution of residue derived C to the amino sugar pool (AS_R) as function of time. *f*$GlcN_R$ and *f*$GalN_R$ are respectively the fractions of glucosamine and galactosamine C derived from the added labelled residue. Data points are averages of three replicate experiments; error bars represent standard errors (adapted from Bai *et al.,* 2012).

TABLE 1. Parameters description for AS_R formation (adapted from Bai *et al.*, 2012)

AS	Treats	AS_0 (nmol/g dry soil)	fAS_R (%)	k (d^{-1})	R^2
GlcN	NG	3 781 ± 66	7.9 ± 0.4	0.48 ± 0.08	0.89
	NL		5.9 ± 0.6	0.20 ± 0.04	0.84
	NR		2.6 ± 0.5	0.30 ± 0.16	0.38
	CG	2 985 ± 199	10.6 ± 0.7	0.43 ± 0.08	0.86
	CL		6.0 ± 0.4	0.28 ± 0.05	0.84
	CR		1.3 ± 0.3	0.34 ± 0.24	0.35
GalN	NG	1 937 ± 102	4.5 ± 0.3	0.39 ± 0.07	0.87
	NL		4.8 ± 0.4	0.11 ± 0.02	0.93
	NR		1.6 ± 0.4	0.25 ± 0.17	0.46
	CG	1 742 ± 110	6.5 ± 0.4	0.42 ± 0.07	0.87
	CL		4.0 ± 0.2	0.22 ± 0.03	0.92
	CR		1.0 ± 0.3	0.20 ± 0.11	0.58

RESULTS

Incorporation of residue carbon in amino sugar pools

The isotopic ^{13}C composition of individual amino sugars increased exponentially during the first day of incubation, indicating a fast incorporation of the residue C into the amino sugar pools (Figure 1).

A first order kinetic model was fitted to the formation dynamics of residue-derived glucosamine and galactosamine (Figure 1) using the following equation:

$$fAS_R = fAS_{R,Max} \cdot (1 - e^{-k \cdot t}) \quad (2)$$

where $fAS_{R,Max}$ is maximum of the exponential incorporation of residue C into amino sugar pool; fAS_R is amount of residue derived amino sugar at time t; and k is the formation rate constant of the exponential formation of residue derived amino sugars.

The k-values of glucosamine and galactosamine ranged from 0.48 to 0.20/d and from 0.11 to 0.42/d, respectively (Table 1). Unfortunately, the correction for 'entophytic' (labelled) muramic acid induced a high uncertainty on the residue derived muramic acid formation, making these data unusable.

Statistical analysis of the formation kinetic parameters

Using a multi way ANOVA (Table 2), the effect of amino sugar type, residue quality and tillage history of the soil on parameters describing the dynamics of residue derived amino sugar formation ($fAS_{R,Max}$, k (Equation 1) and on $fAS_{R,Max}$ relative to the original amino sugar concentration) were investigated.

DISCUSSION

This study quantified newly formed amino sugars during peak microbial activity following plant residue addition. Noticeably, soil microorganisms prefer to feed on fresh organic residues rather than on endogenous SOM during exponential microbial activity following residue addition (Amelung *et al.,* 2008).

The incorporation of residue C into the amino sugar pool reached a maximum within ca. one week after which the residue derived amino sugars formation reached a steady state (Table 1, Figure 1). Liang *et al.* (2007) reported that amino sugar content in black soil

TABLE 2. Effect of plant residue quality (Rq), amino sugar type (AS_i) and tillage history of the soil samples (Till) on the maxima of the residue C incorporation in the amino sugar pool ($fAS_{R,Max}$) and production rate constant (k).

		$fAS_{R,Max}$	k
AS_i	rank	GlcN > GalN	GlcN > GalN
	F-value	(178) ***	(6.36)*
Rq	rank	G > L> R	G > L = R
	F-value	(355)***	(10.5)***
Till	rank	NT = CT	CT = NT
	F-value	(2.52)	(0.006)
AS_ixRq	F-value	(36.9)***	(0.006)
	AS_i on Rq	GlcN (213)***, GalN(155)***	N.A.
	Rq on AS_i	G(135)***, L(42.8)***, R(11.1) **	
Rqxtill	F-value	(5.69)*	(0.238)
	Rq on Till	G (35.9)***[a], L(2.10), R (19.3)**	N.A.
	Till on Rq	NT (123)***, CT(242)***	
AS_i xTill	F-value	32.3***	(1.24)
	AS_i on Till	GlcN (5.52)*, GalN(0.562)	N.A.
	Till on AS_i	NT (74.2)***, CT(104)***	
Rq x AS_i x Till	F-value	(3.56)	(0.133)

The levels of the factors tested are ranked in decreasing magnitude of the specific variables ($p < 0.05$) followed by the F-values (between brackets) of the factor effect, obtained from a multi way ANOVA. The F-value of the interaction of factors is followed by the F-value of one interacting factor for each individual level of the other interacting factor and an indication of the significance of the difference between the levels of the other interacting factor (adapted from Bai et al., 2012).

N.A. — not applicable; G = grain, L = leaf, and R = root; CT = conventional till and NT = no-till

Differences between factor levels were tested using Tukey's HSD ($p < 0.05$) post hoc test. *** — $p < 0.001$, ** = $p < 0.01$, * = $p < 0.05$

[a] The ranking is different from the total effect (i.e. CT > NT)

reached a maximum within three weeks upon incubation with maize residue, thereby increasing the original amino sugar content by one third. Decock *et al.* (2009) also revealed maximum ^{13}C incorporation into glucosamine and galactosamine within one week after incubation with ^{13}C-labelled wheat residues.

Glucosamine, galactosamine and muramic acid formation dynamics

As muramic acid originates exclusively from bacterial cell walls, while glucosamine and galactosamine are present in both bacterial as fungal residues (Amelung *et al.,* 2001 and 2008; Glaser and Gross, 2005; Engelking, Flessa and Joergensen, 2007), muramic acid is the preferred biomarker to differentiate bacterial and fungal activity for incorporation of residue-derived C. Unfortunately, due to the higher uncertainty concerning the muramic acid measurements and the high ^{13}C muramic acid contamination of the plant residues the formation dynamics of muramic acid could not be determined.

The $fAS_{R,Max}$ ranged from 1.3 percent 11 percent for glucosamine while for galactosamine the range was from 0.8 percent to 5.7 percent. A similar trend was also observed in other studies (Glaser and Gross, 2005; Engelking, Flessa and Joergensen, 2007; He *et al.,* 2011).

Bacteria and fungi both produce glucosamine and galactosamine (Amelung *et al.,* 2001 and 2008; Glaser and Gross, 2005). However, the strong amino sugar type effect on $fAS_{R,Max}$ and on k indicates that these amino sugars are formed through dissimilar processes. Engelking, Flessa and Joergensen (2007) reviewed the available literature on amino sugar concentrations in cultured bacteria and fungi, which revealed that the galactosamine/glucosamine ratio appeared to be on average almost three times higher in fungi compared with bacteria, making residue-derived galactosamine a 'more' fungal marker than glucosamine when considering microbial activity. The higher formation rate constant of glucosamine compared with galactosamine therefore most likely indicates that bacteria play a more important role for early stage incorporation of residue-derived C, i.e. "fast energy channel" (Rousk and Baath, 2007). The slower formation of galactosamine corroborates with the slower turnover of fungi compared with bacteria; for which fungi are involved in the slow energy channel through the soil food web (Rousk and Baath, 2007).

Effect of residue quality

The high C:N ratio and high lignin content (unpublished data) of root indicates its low quality while grain had the highest quality. This difference resulted in different $fAS_{R,Max}$ values between residues: grain > leaf > root ($p < 0.001$). The interaction between residue quality and amino sugar type revealed that the difference between the $fAS_{R,Max}$ for glucosamine and galactosamine was much more pronounced for grain than for leaf and root. Considering the higher fungal origin of galactosamine, this interaction indicates (at least during peak microbial activity) that fungi are less dependent on the quality of the residue than bacteria for *de novo* amino sugar formation. This is in accordance with expectations since it is generally believed that bacteria especially rely on easily available C compounds while the fungal community is better adapted to colonize more recalcitrant sources (Myers *et al.*, 2001; Waldrop and Firestone, 2004).

Effect of site tillage history

In general, tillage had no significant effect on $fAS_{R,Max}$ or k. However, the interaction between tillage history and residue quality (Table 2) indicated that the conventionally tilled soil was better adapted to incorporate residue C of the highest quality (grain), while the no-till soil was better adapted to incorporate residue C of the lowest quality (root). This may be explained by the microbial community differences typically found in no-till soil. Fungi, showing a great ability to decompose more recalcitrant substrates (Acosta-Martinez *et al.,* 2003; Ding *et al*., 2010; Werth and Kuzyakov, 2010), are typically more abundant in the no-till soils (Fu *et al.,* 2000; Thiet, Frey and Six, 2006; White and Rice, 2009).

Field measurements and laboratory incubations both showed that the relative change in galactosamine was significantly smaller than for glucosamine (Table 2), indicating that the more conservative response of galactosamine upon shift in tillage was (at least partially) due to a lower formation of residue derived galactosamine compared with glucosamine after receiving increased residue input in the no-till treatment.

CONCLUSIONS

A first order kinetic model could describe residue-derived amino sugar formation, which reached a maximum and steady state a few days after residue addition. During peak microbial activity *de novo* residue derived amino sugar formation was surprisingly fast, and production rate constants for glucosamine (0.20–0.48 d) were faster than those for galactosamine (0.11–0.39 d).

The faster incorporation of residue C into glucosamine underpins the role of bacteria as a "fast energy channel" as described by Rousk and Bååth (2007). In addition, the *de novo* amino sugar formation relative to the original amino sugar pool was higher for glucosamine than for galactosamine; however, this difference declined strongly with decreasing residue quality, confirming the better adaptation of fungal communities to colonize more recalcitrant C sources. Finally, the influence of tillage history on *de novo* amino sugar formation indicated a better adaptation of soil microbial community to incorporate C originating from more recalcitrant plant residues in the no-till treatment compared with conventional tillage.

ACKNOWLEDGEMENTS

This paper represents a contribution to the FAO/IAEA Coordinated Research Project D1.20.11 under IAEA technical contract No 15752. We thank Katja Van Nieuland and Jan Vermeulen for ^{13}C analysis of bulk soil and CO_2. We would like to acknowledge Karolien Denef and Joan Six for providing the labelled plant material. Dries Huygens is a postdoctoral fellow of the Fund for Scientific Research - Flanders (FWO) and holds a Marie Curie International Outgoing Fellowship from the European Commission. Zhen Bai's scientific mission was financed by the National Natural Science Foundation of China and the "Departement Onderwijs en Vorming" of the Flemish Government.

REFERENCES

Acosta-Martinez, V., Zobeck, T.M., Gill, T.E. & Kennedy, A.C. 2003. Enzyme activities and microbial community structure in semiarid agricultural soils. *Biol. Fert. Soils*, 38: 216–227.

Allison, S.D., Wallenstein, M.D. & Bradford, M.A. 2010. Soil-carbon response to warming dependent on microbial physiology. *Nat. Geosci.*, 3: 336–340.

Amelung, W., Brodowski, S., Sandhage-Hofmann, A. & Bol, R. 2008. Combining biomarker with stable isotope analyses for assessing the transformation and turnover of soil organic matter. *Adv. Agron.*, 100: 155–250.

Amelung, W., Miltner, A., Zhang, X. & Zech, W. 2001. Fate of microbial residues during litter decomposition as affected by minerals. *Soil Sci.*, 166: 598–606.

Appuhn, A., Joergensen, R.G., Raubuch, M., Scheller, E. & Wilke, B. 2004. The automated determination of glucosamine, galactosamine, muramic acid, and mannosamine in soil and root hydrolysates by HPLC. *J. Plant Nutr. Soil Sc.,* 167: 17–21.

Bai, Z., Bodé, S., Huygens, D., Zhang, X. & Boeckx, P. 2012. Kinetics of amino sugar formation from organic residues of different quality. *Soil Biol. Biochem.*, 10.1016/j.soilbio.2012.08.006.

Bodé, S., Denef, K. & Boeckx, P. 2009. Development and evaluation of a high-performance liquid chromatography/isotope ratio mass spectrometry methodology for $\delta^{13}C$ analyses of amino sugars in soil. *Rapid Commun. Mass Spec.*, 23: 2519–2526.

Craine, J.M., Fierer, N. & McLauchlan, K.K. 2010. Widespread coupling between the rate and temperature sensitivity of organic matter decay. *Nat. Geosci.*, 3: 854–857.

Decock, C., Denef, K., Bode, S., Six, J. & Boeckx, P. 2009. Critical assessment of the applicability of gas chromatography-combustion-isotope ratio mass spectrometry to determine amino sugar dynamics in soil. *Rapid Commun. Mass Spec.*, 23: 1201–1211.

Denef, K. & Six, J 2006. Contributions of incorporated residue and living roots to aggregate-associated andmicrobial carbon in two soils with different claymineralogy. *Eur. J. Soil Sci.*, 57: 774–786.

Ding, X.L., Zhang, X.D., He, H.B. & Xie, H.T. 2010. Dynamics of soil amino sugar pools during decomposition processes of corn residues as affected by inorganic N addition. *J. Soil Sediment.,* 10: 758–766.

Engelking, B., Flessa, H. & Joergensen, R.G. 2007. Shifts in amino sugar and ergosterol contents after addition of sucrose and cellulose to soil. *Soil Biol. Biochem.,* 39: 2111–2118.

FAO. 2006. *World reference base for soil resources*. Report 013, p. 86. Rome.

Farkas, V. 1979. Biosynthesis of cell-walls of fungi. *Microbiol. Rev.*, 43: 117–144.

Fu, S.L., Coleman, D.C., Schartz, R., Potter, R., Hendrix, P.F. & Crossley, D.A. 2000. C-14 distribution in soil organisms and respiration after the decomposition of crop residue in conventional tillage and no-till agroecosystems at Georgia Piedimont. *Soil Till. Res.*, 57: 31–41.

Glaser, B. & Gross, S. 2005. Compound-specific delta C-13 analysis of individual amino sugars – a tool to quantify timing and amount of soil microbial residue stabilization. R*apid Commun. Mass Sp.*, 19: 1409–1416.

Glaser, B., Turrion, M.B. & Alef, K. 2004. Amino sugars and muramic acid - biomarkers for soil microbial community structure analysis. *Soil Biol. Biochem.*, 36: 399–407.

He, H.B., Xie, H.T., Zhang, X.D., Wang, Y.H. & Wu, Y.Y. 2005. A gas chromatographic/mass spectrometric method for tracing the microbial conversion of glucose into amino sugars in soil. *Rapid Commun. Mass Spec.,* 19: 1993–1998.

He, H.B., Zhang, W., Zhang, X.D., Xie, H.T. & Zhuang, J. 2011. Temporal responses of soil microorganisms to substrate addition as indicated by amino sugar differentiation. *Soil Biol. Biochem.,* 43: 1155–1161.

Liang, C., Zhang, X.D., Rubert, K.F. & Balser, T.C. 2007. Effect of plant materials on microbial transformation of amino sugars in three soil microcosms. *Biol. Fert. Soils,* 43: 631–639.

Myers, R.T., Zak, D.R., White, D.C. & Peacock, A. 2001. Landscape-level patterns of microbial community composition and substrate use in upland forest ecosystems. *Soil Sci. Soc. Am. J.,* 65: 359–367.

Reinhold-Hurek, B. & Hurek, T. 2011. Living inside plants: Bacterial endophytes. *Curr. Opin. Plant Biol.*, 14: 435–443.

Rousk, J. & Baath, E. 2007. Fungal and bacterial growth in soil with plant materials of different C/N ratios. *FEMS Microbiol. Ecol.*, 62: 258–267.

Thiet, R.K., Frey, S.D. & Six, J. 2006. Do growth yield efficiencies differ between soil microbial communities differing in fungal: bacterial ratios? Reality check and methodological issues. *Soil Biol. Biochem.*, 38: 837–844.

van Groenigen, K.J., Bloem, J., Baath, E., Boeckx, P., Rousk, J., Bode, S., Forristal, D. & Jones, M.B. 2010. Abundance, production and stabilization of microbial biomass under conventional and reduced tillage. *Soil Biol. Biochem.,* 42: 48-55.

Waldrop, M.P. & Firestone, M.K. 2004. Microbial community utilization of recalcitrant and simple carbon compounds: impact of oak-woodland plant communities. *Oecologia,* 138: 275–284.

Werth, M. & Kuzyakov, Y. 2010. ^{13}C fractionation at the root-microorganisms-soil interface: A review and outlook for partitioning studies. *Soil Biol. Biochem.*, 42: 1372–1384.

White, P.A. & Rice, C.W. 2009. Tillage effects on microbial and carbon dynamics during plant residue decomposition. *Soil Sci. Soc. Am. J.,* 73: 138–145.

White, R.J. 1968. Control of amino sugar metabolism in *Escherichia coli* and isolation of mutants unable to degrade amino sugars. *Biochem. J.*, 106: 847–858.

Suess Effect on Biomarkers Used to Determine Sediment Provenance from Land Use Changes

M. Gibbs[1,*], A. Swales[1] and G. Olsen[1]

ABSTRACT

A compound-specific stable isotope (CSSI) technique developed to positively identify the source of soil by landuse provides a tool to determine the provenance of sediment from watershed erosion. The CSSI technique uses the carbon-13 (^{13}C) isotopic signatures of plant-derived fatty acid biomarkers in the source soils and a mixing model to deconstruct the sediment isotopic signatures into contributing source soils by land use. While the CSSI technique provides qualitative information on where the sediment is coming from, for quantitation it requires erosion rate information from the fallout radionuclide (FRN) techniques. Together, the CSSI and FRN techniques can identify landuse practices that are exacerbating soil erosion i.e. hot spots. These tools can provide the information that allow managers to target the resources available to mitigate soil erosion. The data can also be used to map the dispersion of contemporary terrigenous sediments through an estuary and to identify land use changes through time from sediment cores. However, when the CSSI technique is used to look back in time using contemporary source libraries, the ^{13}C isotopic signatures of the biomarkers need to be corrected for the Suess effect, i.e. the isotopic depletion of the $\delta^{13}C$ signature of atmospheric carbon dioxide (CO_2) due to the admixing of isotopically depleted CO_2 from the burning of fossil fuels.

Key words: *compound-specific stable isotope, fallout radionuclides, fatty acid biomarkers, soil erosion, Suess effect.*

INTRODUCTION

Management of natural and agricultural resources in agro-ecosystems for conservation of soil and sustainable food production requires an understanding of the landuse practices exacerbating soil losses and where the 'hot spots' of erosion occur within the watershed. Information on sources is a key requirement for targeting sediment control measures (Walling, Collins and Stroud, 2008). A compound-specific stable isotope (CSSI) technique has been developed to determine the provenance by land use of soil contributing to contemporary sediment at any location in a sediment deposition zone (Gibbs, 2008). For source identification the technique uses a 'reference library' of contemporary soil bulk carbon stable isotopic ($\delta^{13}C$) data and compound specific $\delta^{13}C$ values of fatty acid biomarkers from a range of landuse types. Although only recently developed in New Zealand (Gibbs, 2008), the CSSI technique has been successfully tested in several countries including Australia, England, and Austria (Hancock and Revill, 2011; Blake *et al.*, 2012; Gibbs and Mabit, 2012), providing new information into sources and causes of erosion that could not be obtained with conventional geochemical catchment modelling techniques (Hancock and Revill, 2011).

The limitation of the CSSI technique is that it provides qualitative data on the source proportions and requires additional information on mass transport from other techniques to become quantitative. In contrast, geochemistry techniques using soil mineralogy (Foster and Lees, 2000) and fallout radionuclide (FRN) techniques using beryllium-7 (^{7}Be), caesium-137 (^{137}Cs) and lead-210 (^{210}Pb) (Walling and He, 1999; Walling, He and Blake, 1999; Wilson, Matisoff and Whiting, 2007) provide information on recent erosion but cannot positively identify the sources of the sediment within the watershed (Walling and Collins, 2008; Walling, Collins and Stroud, 2008). In combination with the CSSI technique, these techniques have the potential to provide quantitative information on soil erosion sources to enable identification of hot spots of erosion in the landscape, and which may be used to make informed decisions on the design and implementation of mitigation measures to reduce soil erosion.

Originally the CSSI technique was developed to identify contemporary sources of soil erosion by deconstructing the source soil proportional contributions in contemporary sediments (Figure 1). These data indicated that one landuse was contributing substantially more soil to the downstream environment than would be expected from the area occupied by that landuse i.e. a hot spot. On-site investigation of the landuse (production forestry) located the hot spot and identified the landuse practice (clearfell harvesting across a stream) exacerbating the erosion. With this knowledge it was possible to develop mitigation measures to reduce the erosion and protect the downstream ecosystem.

The CSSI technique has also been used to determine the sources of terrigenous soil contributing to sediment in the Bay of Islands, New Zealand, and to evaluate erosion due to changes in landuse over time (Gibbs and Olsen, 2010). This application used the present day catchment soil library of CSSI values to deconstruct the soil sources from the past contributing to depth-defined subsections from a 140 cm long core (RAN S-9) from the Veronica Channel in the Bay of Islands. Each subsection in the upper 70 cm of the core was dated using FRN techniques with ^{210}Pb providing an estimate of sediment accumulation rates. The CSSI data were aligned with the ^{210}Pb data to give relative contributions of the main landuse soil sources at different times (shadow graphs, Figure 2), and these sources of erosion were related to historical events using historical data records (Figure 2).

During this phase of the study, it was found that there were errors in the CSSI interpretations with the CSSI data indicating the presence of pasture grasses had been introduced to New Zealand before the arrival of the European settlers (Figure 2). The CSSI errors were attributed to the Suess effect (Keeling, 1979), which results in

1 National Institute of Water and Atmospheric Research (NIWA), PO Box 11-115, Hamilton 3251, New Zealand
* E-mail address of corresponding author: Max.Gibbs@niwa.co.nz

L.K. Heng, K. Sakadevan, G. Dercon and M.L. Nguyen (eds), Proceedings — International Symposium on Managing Soils for Food Security and Climate Change Adaptation and Mitigation. Food and Agriculture Organization of the United Nations, Rome, 2014: 371–375

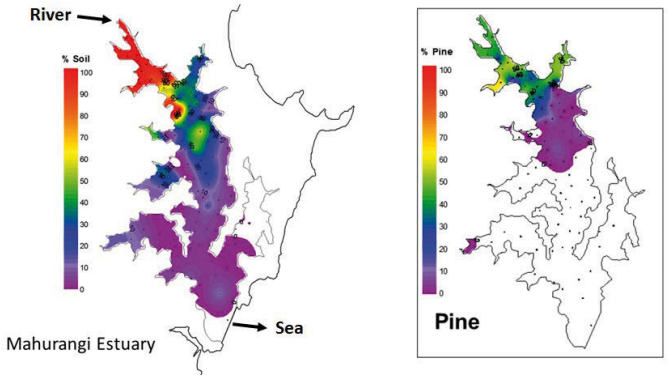

FIGURE 1. Left: Spatial distribution of terrigenous soil in the Mahurangi Estuary relative to the river inflow and the outflow to the sea. Right: the spatial distribution of the sediment component derived from pine forest. The land area occupied by pine forest in the watershed was 12 percent but the proportion of soil from pine forest in the river delta was up to 60 percent. (Contour plots produced using Surfer32 by Golden Software)

a change in the isotopic abundance of $\delta^{13}C$ in atmospheric CO_2 over time, and require correction (Verburg, 2007).

This paper defines the isotopic corrections needed to allow the CSSI technique to be used to determine changes in landuse erosion sources over time and applies these corrections to examine the spatial and temporal changes in sediment erosion by landuse in the Bay of Islands based on data from two sediment cores over a period of up to 2 500 years before present (BP).

METHODS

Study site

The Bay of Islands (Lat: –35.23°S; Long: 174.10°E) is a large coastal inlet on the east coast of the upper North Island of New Zealand (Figure 3). The area is historically important to New Zealand as it is the landing place of the discoverer, James Cook in 1796, and the signing place of the Treaty of Waitangi in 1840, the founding document for New Zealand. The bay receives the discharge from five watersheds around the bay via the Waikare, Kawakawa, Waitangi, Kerikeri and Te Punga Rivers (Figure 3). Based on hydrological modelling of these river inflows (Pritchard *et al.*, 2010), the Kawakawa, Waitangi and Kerikeri rivers are the main sources of sediment to the bay.

A 140-cm long sediment core was collected from the Veronica Channel (RAN S-9) and another shorter core (20 cm) was collected from the middle of the bay (KAH S-20) at a depth of 30 m (Figure 3). Both cores were split lengthwise to extract a 1-cm thick longitudinal slab which was X-rayed to assess layering of different density particles at different depths in the cores. The X-ray images also located shell fragments at different depths in the long core and these were removed for carbon-14 (^{14}C) dating.

Analytical

Depth-related horizontal sections 1 cm thick were taken from the remainder of the core. These were dried in an air fan oven at 50°C, then ground to a fine powder (< 100 µm mesh). An aliquot (2 g) from each dried sample was acidified with 1 M hydrochloric acid (HCl) to remove inorganic carbonates as follows.

The sediment was placed in a 50 mL plastic centrifuge tube and 2 mL of HCl was added. When effervescence stopped, a further drop of HCl was added to see whether all carbonate had been removed. This step was repeated until no further effervescence occurred.

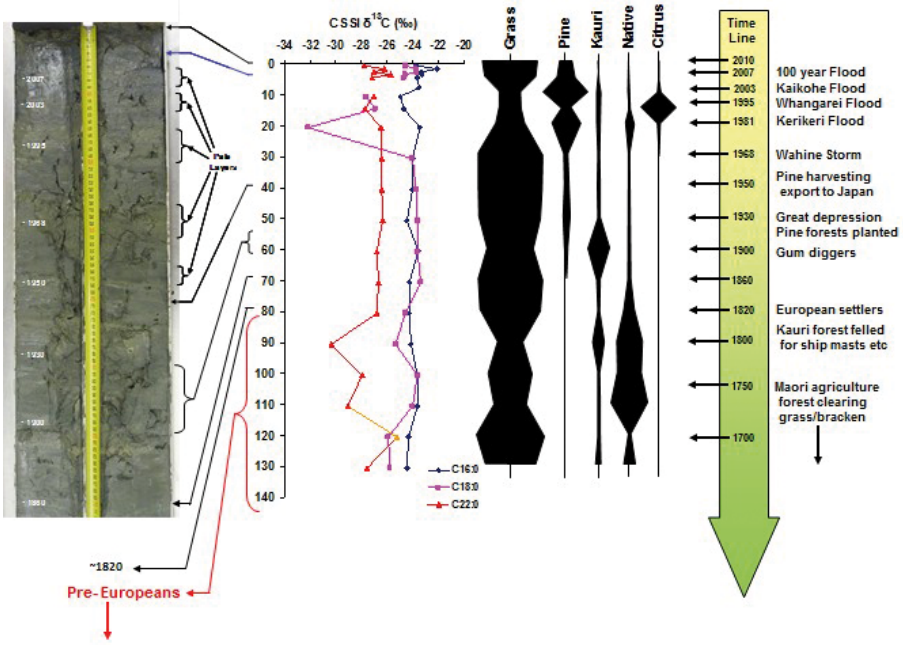

FIGURE 2. Alignment of the CSSI values for C16:0, C18.0 and C22.0 fatty acids with section depths in the top 70 cm of the sediment core RAN S-9, allowed the deconstruction of the sediment at each depth into proportional contributions by landuse at that time. The shadow graphs sum to 100 percent across the five landuse types. The timeline was constructed from historical data. (Redrawn from Gibbs and Olsen, 2010).

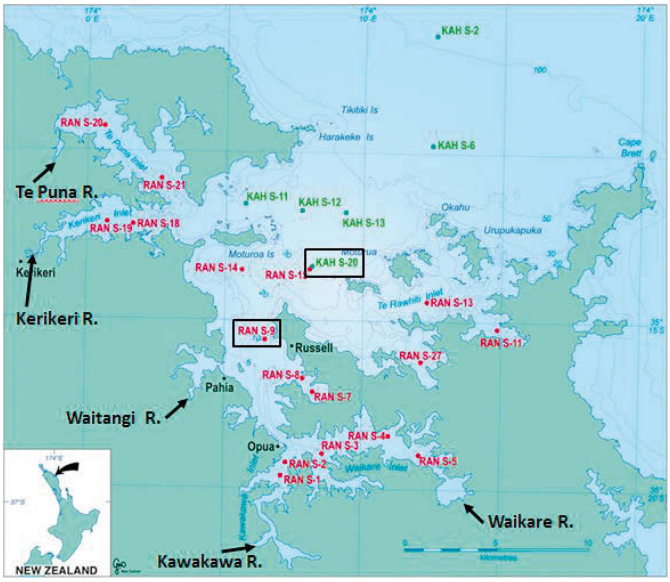

FIGURE 3. Site map of the Bay of Islands, New Zealand showing the five river inflows and the location of the two sediment cores (square boxes) used in this study. Red and green codes in the bay are sediment core locations from two visits (from Swales *et al.*, 2010).

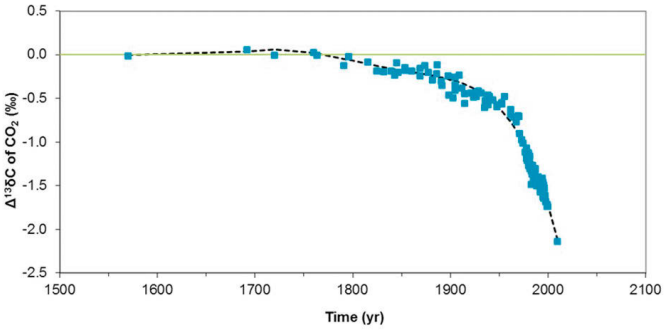

FIGURE 4. Time-series plot of the change (Δ) in $\delta^{13}C$ abundance of atmospheric CO_2 that has occurred since pre-industrial times (AD 1700), the zero line in this graph. The broken line is a 6th order polynomial curve fitted through the data. (Redrawn using data from Verburg, 2007 and papers therein)

The acid mixture in the centrifuge tube was diluted to 50 mL with distilled water before centrifuging at 3000 rpm for 10 min. The supernatant liquid was discarded and the sediment was rinsed with 10 mL of distilled water and centrifuged. The rinse water was discarded and the acidified sediment was dried at 50°C, and then reground to a fine powder before being analysed for bulk $\delta^{13}C$ and organic carbon (C) on a continuous flow, isotope ratio mass spectrometer (CF-IRMS) (Thermofinnigan Delta Plus).

The extraction and preparation of soil fatty acids used in the CSSI technique is described in detail in Gibbs (2008 and 2010). In brief, a 20 g aliquot from each dried sediment sample was extracted twice in hot (100°C) dichloromethane solvent (DCM) at high pressure (2000 psi) in an automated solvent extractor (Dionex ASE 200). After drying, the fatty acids were converted to their non-polar fatty acid methyl esters (FAME) by methylation using 5 percent BF_3 in methanol at 70°C for 20 min. The $\delta^{13}C$ isotopic signature of each FAME from each sediment section was determined by gas chromatography–combustion–isotope ratio mass spectroscopy (GC-C-IRMS).

Deconstruction of sediment into source soils

Contemporary sediment samples

The isotopic proportions of each landuse source soil contributing to a surficial sediment sample were determined using reference library samples in the mixing model "IsoSource" (Phillips and Gregg, 2003). These isotopic proportions were converted to soil proportions using the C content of the source soils in the sediment (Gibbs, 2008). Individual river delta samples were used to define landuse sources from each of the five river watersheds.

Historical sediment samples

To determine the landuse source soils contributing to the sediment sections at different depths (ages) in the sediment cores using present day reference library data, the age of the sediment section must be determined to allow the CSSI values to be corrected for the Suess effect. Dating was achieved using FRNs with excess ^{210}Pb providing date estimations for up to 150 year BP. This timeline was extended back more than 2 500 year BP to around 640 BC using ^{14}C dates from the shell fragments in the core.

Suess effect

The Suess effect refers to the isotopic depletion of atmospheric CO_2 due to the admixing of isotopically depleted (18‰) CO_2 from the burning of fossil fuels, i.e. coal. Since the beginning of the industrial revolution in the 1700s, the $\delta^{13}C$ value of atmospheric CO_2 has decreased by around 2.2‰ with the rate of that depletion increasing in recent years (Figure 4).

Since plants use atmospheric CO_2 as a major C source, the $\delta^{13}C$ values of biomarkers in present day reference plants will be up to 2.2‰ more depleted than those of the same biomarkers from the past. As the Suess effect only began around AD 1700 (Figure 4), all CSSI values from the core sections before that time were made more isotopically depleted by 2.2‰, i.e. they were corrected by –2.2‰. The CSSI values from the core sections between AD 1700 and present day were corrected by the isotopic depletion value. This value was calculated from the 6th order polynomial equation from Verburg (2007), and adding the absolute $\delta^{13}C$ value (8.55‰) of present day CO_2 (year 2012) as an offset to obtain the change (Δ) in the $\delta^{13}C$ isotopic value for the year (Y) of the core section. Between 1700 and present the CSSI values from the core were made more isotopically depleted by the correction value:

$$\text{Correction value} = 8.55 + 7.7738118 \times 10^{-16} \times Y^6 - 1.2222044 \times 10^{-11} \times Y^5 + 7.1612441 \times 10^{-8} \times Y^4 - 2.1017147 \times Y^3 + 3.3316112 \times 10^{-1} \times Y^2 - 273.715025 \times Y + 91703.261$$

Note that the polynomial coefficients in this equation have been rounded to seven decimal places. More precise coefficients to 14 decimal places can be obtained from the author of Verburg (2007).

RESULTS AND DISCUSSION

Erosion due to changes in landuse over time can be referenced to present day erosion. Contemporary sediment from soil erosion in the watershed will tend to deposit in the river delta before some is redistributed into the bay (e.g. Figure 1). Consequently, surficial sediments from the river deltas provide the present day erosion data. For changes in landuse effects on erosion, samples from different depths in sediment cores will reflect the soil sources associated with erosion events at the time that sediment layer was deposited.

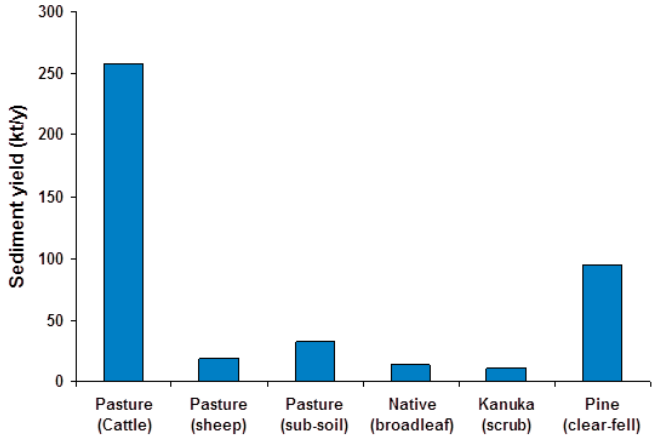

FIGURE 5. Estimated annual sediment yields (kilo tonnes, kt/yr) of sediment to the Bay of Islands from the six main soil sources identified by the CSSI technique (Gibbs and Olsen, 2010) and quantified using the flow and sediment load information from Pritchard *et al.* (2010). The pasture (cattle) includes both dry stock and dairy (redrawn from Gibbs and Olsen, 2010).

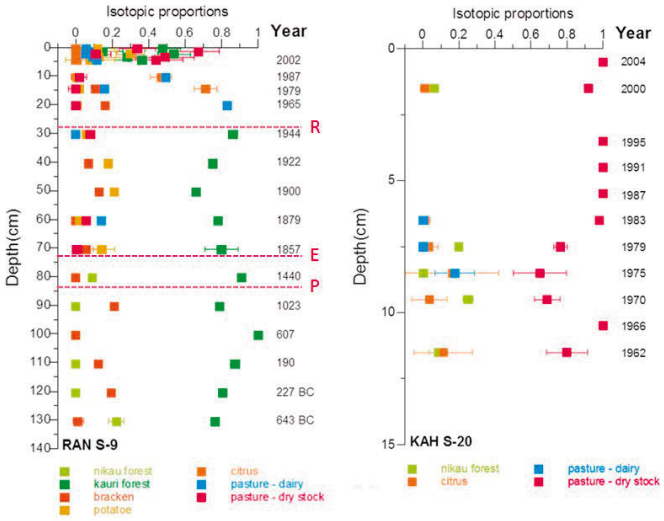

FIGURE 6. Proportional contributions of terrigenous soil in sediment cores RAN S-9 and KAH S-20 based on CSSI values corrected for the Suess effect. The markers for each landuse include the standard deviation as the error term although in most samples the error bars are within the marker point. The X-axis is in isotopic proportion with a range of 0 to 1 representing 0 percent to 100 percent. The "Year" column represents the timeline date for the depth down the core (cm). On the core RAN S-9 graph, the red broken lines represent special historical events: P — the arrival of the Polynesians around 1300 AD; E — European settlement in 1814 AD; R — returned servicemen land allocation after World War 2 in 1945.

River delta sites

Surficial sediments collected from each of the five river deltas in the Bay of Islands were deconstructed using the mixing model to obtain the present day source proportions of terrigenous soil by landuse (Gibbs and Olsen, 2010). Flow and sediment load information from Pritchard *et al*. (2010) were used to convert these estimates to total sediment yield by land use, discharging into the Bay of Island on an annual basis (Figure 5).

These results show that most of the annual sediment load comes from pasture used for beef and dairy farming (258 kt/yr) and pine forest that has been clear-felled (95 kt/yr). Other pasture landuse sources combined contribute about 50 kt/year, while native forest and kanuka scrubland contribute a total of 24 kt/yr. Overall, more than 70 percent of the present day soil deposited in the Bay of Islands came from pasture sources.

Sediment cores

The sediment core from the Veronica Channel (RAN S-9) was taken within the zone of influence of sediment inputs from the Waikare, Kawakawa and Waitangi Rivers, and a 20 cm core from a depth of 30 m in the open bay (KAH S-20) was taken within the zone of sediment accumulation for the whole bay. For core RAN S-9, the ^{210}Pb and ^{14}C data provided a historical timeline extending back 2500 years BP and for core KAH S-20, ^{210}Pb provide a timeline back to 1962 (Figure 6). After applying the correction for the Suess effect to the CSSI values from the depth-related sections from these sediment cores, it was found that the major sources of sediment before 1944 were kauri forest, nikau forest and bracken (Figure 6).

Core RAN S-9 shows that the major sources of land erosion before humans arrived in New Zealand are consistent with what is known of the region. The land was covered with native forest with broadleaf forest on the flatter land, kauri forest on the drier hillsides and nikau forest in the wetter valleys and alongside rivers. Bracken is a coarse fern which rapidly colonizes bare ground such as would be left after a landslide. With this region of New Zealand being subjected to heavy rainfall and tropical storms, it is likely that the kauri signature represents landslide events exposing subsoils to erosion and the bracken signature represents further erosion of those slip faces after the bracken had become established. The nikau forest signature is likely to reflect erosion in the valleys associated with heavy rainfall events. Broadleaf forest on relatively flat land would protect the soil from direct impact of rainfall and only minimal erosion would occur and was not detected above a threshold of 1 percent.

The arrival of the Polynesians around AD 1300 saw little change in this erosion pattern and it was not until the arrival of the European settlers in 1814 that other landuse sources of soil erosion could be detected i.e. the presence of European grasses and potatoes. A dairy signature was also detected but the potato signature was more consistent. Presumably this was because land had to be cultivated to grow potatoes exposing bare soil to erosion by the locally heavy rainfall.

The continuing presence of the kauri forest signature is likely to have been associated with the clearing of the hilly land exposing historical subsoil horizons to erosion and the draining of swamps where forest sediments had accumulated. After 1945, the kauri signature stopped. This is attributed to the allocation of land for farming to servicemen returning from World War 2. That land was cleared and planted in pasture grasses eliminating much of the subsoil erosion. The occasional presence of strong dairy signatures between 1960 and the present day are likely to correspond with the erosion of soil during flood events.

A citrus signature is consistent with the establishment kiwi fruit orchards in the Bay of Islands in the late 1960s and 1970s. Large areas of citrus orchard were removed leaving bare ground, which would carry the citrus CSSI signature, while the kiwifruit plants became established.

In core KAH S-20, the major terrigenous soil source components were from pasture associated with dry stock (beef), dairy nikau for-

est and citrus (Figure 6). Although the citrus signature was detected in the late 1960s to 1970s, the CSSI signatures suggest that most of the soil erosion from the Bay of Island watershed was from pasture used for dry stock farming. This observation is consistent with the contemporary sediment assessment from the river deltas (Figure 5) and indicates that the landuse practice causing this erosion has persisted over a period of at least 50 yr.

CONCLUSIONS

While there are similarities between the interpretation of the landuse sources of sediment with (Figure 6) and without (Figure 2) the Suess effect correction, the use of the correction has allowed identification of the causes of major soil erosion in the distant past and the effect of more recent landuse changes on erosion patterns. The use of the corrected CSSI values correctly identified the transition period between citrus and kiwifruit orchards around 1970, which was missed using the uncorrected CSSI values. The uncorrected CSSI values indicated a high proportion of sediment from production forestry harvest. Soil from this landuse was a minimal component of the total soil load identified when using the corrected CSSI values, consistent with best management practices to prevent soil entering permanent waterways during forest harvest. Using the Suess effect correction, both sediment cores showed evidence of a recent (last ~50 yr) increase in the amount of soil being eroded from pasture used for dry stock beef was much larger than previously estimated without the correction. This proportional source contribution is consistent with the proportion of the estimated annual mass load of sediment from this landuse being discharged into the Bay of Islands, as determined from the analysis of contemporary sediments from the river deltas. These results confirm the need to apply a correction to the CSSI values for the Suess effect when examining sediment source changes over time using the CSSI technique.

REFERENCES

Blake, W.H., Ficken, K., Taylor, P., Russell, M. & Walling, D.E. 2012. Tracing crop-specific sediment sources in agricultural catchments. *Geomorph.,* 139–140: 322–329.

Foster, I.D.L. & Lees, J.A. 2000. Tracers in geomorphology: theory and applications in tracing fine particulate sediments, *In* I.D.L. Foster, ed. *Tracers in geomorphology,* pp. 1–20. New York, Wiley.

Gibbs, M. 2008. Identifying source soils in contemporary estuarine sediments: A new compound-specific isotope method. *Estuaries & Coasts*, 31: 344–359.

Gibbs, M. 2010. *Protocols on the use of compound-specific stable isotopes to identify and apportion soil sources from land use*. NIWA report HAM2010-129 to Joint FAO/IAEA Division of Nuclear Techniques in Food and Agriculture. 97pp.

Gibbs, M. & Olsen, G. 2010. *Determining sediment sources and dispersion in the Bay of Islands. Bay of Islands OS20/20 Survey report. Chapter 5.* NIWA client report WLG2010-38 for Land Information New Zealand. 30 pp. (www.os2020.org.nz).

Gibbs, M. & Mabit, L. 2012. Test of compound-specific stable isotope (CSSI) technique to investigate sediment provenance in a small Austrian watershed. *Soils Newsletter*, 34 (2): 29.

Hancock, G. & Revill, A. 2011. *Land-use and erosion source discrimination of soil and carbon sources to the Logan and Albert rivers using compound specific isotope analysis.* CSIRO Land and Water Science Report 2/11. Canberra, CSIRO. 28 pp.

Keeling, C.D. 1979. The Suess effect: ^{13}Carbon–^{14}Carbon interrelations. *Environ. Internat.,* 2: 229–300.

Phillips, D.L. & Gregg, J.W. 2003. Source partitioning using stable isotopes: Coping with too many sources. *Oecologia*, 136: 261–269. (The mixing model software is available free at www.epa.gov/wed/pages/models/stableIsotopes/isotopes.htm).

Pritchard, M., Reeve, G., Swales, A., Hart, C. & Hancock, N. 2010. *Bay of Islands OS20/20 Survey report. Chapter 6: TRANS – Sediment Transport Model*. NIWA client report WLG2010-38 for Land Information New Zealand. (www.os2020.org.nz).

Swales, A., Ovenden, R., Wadhwa, S. & Rendle, D. 2010. Recent sedimentation rates (over the last 100–150 years), *Bay of Islands OS20/20 Survey report. Chapter 4.* NIWA client report WLG2010-38 for Land Information New Zealand. (www.os2020.org.nz).

Verburg, P. 2007. The need to correct for the Suess effect in the application of δ^{13}C in sediment of autotrophic Lake Tanganyika, as a productivity proxy in the Anthropocene. *J. Paleolimn*., 37: 591–602.

Walling, D.E. & Collins, A.L. 2008. The catchment sediment budget as a management tool. *Environ. Sci. & Policy*, 11: 136–143.

Walling, D.E., Collins, A.L. & Stroud R.W. 2008. Tracing suspended sediment and particulate phosphorus sources in catchments. *J. Hydrol.*, 350: 274–289.

Walling, D. & He, Q. 1999. Using fallout lead-210 measurements to estimate soil erosion on cultivated land. *Soil Sci. Soc. Am. J.,* 63: 1404–1412.

Walling, D., He, Q. & Blake, W. 1999. Use of ^{7}Be and ^{137}Cs measurements to document short- and medium-term rates of water-induced soil erosion on agricultural land. *Water Resour. Res.*, 35: 3865–3874.

Wilson, C.G., Matisoff, G. & Whiting, P.J. 2007. The use of ^{7}Be and ^{210}Pbxs to differentiate fine suspended sediment sources in South Slough, Oregon. *Estuaries & Coasts* 30: 348–358.

Microbial Assimilation of Atmospheric CO_2 to Synthesize Organic Matter in Soils

T. Ge[1], X.J. Chen[1], H.Z. Yuan[1], S. Nie[1], H.A. Xiao[1], C.L. Tong[1], J.S. Wu[1,*] and P. Brookes[2]

ABSTRACT

There are no reports on the activity and quantitative capacity of microbial atmospheric carbon dioxide (CO_2) assimilation in terrestrial ecosystems, although such CO_2 assimilative microorganisms are numerous and widespread. Both non-phototrophic and phototrophic microbial CO_2 assimilations were investigated in two sets of microcosms of eight selected soils in a closed, continuously carbon-14 (^{14}C)-labelled CO_2 atmosphere chamber. A significant amount of ^{14}C-labelled CO_2 was incorporated into the microbial biomass, accounting for between 0.12 percent and 0.59 percent of the soil organic carbon (average 37.8 ± 19.4 mg/kg after 80 d, CV = 51.3 percent, n = 8) in the set exposed to artificial light (about 500 mmol·photons·m^{-2}·s^{-1} parabolic aluminized reflector light [PAR]), whereas none was detected in the set in the dark condition. Hence, soil phototrophic CO_2 assimilation represents a significant part of microbial activity which cannot be ignored since it is estimated to have an annual organic C assimilative capacity of 4.9–37.5 g·C/m.

Key words: *microbial assimilation, atmospheric CO_2, soil microorganisms, ^{14}C continuous labelling.*

INTRODUCTION

The atmospheric concentration of carbon dioxide (CO_2) has increased from 280 parts per million by volume (ppmv) in 1750 to 367 ppmv in 1999 and is currently increasing at the rate of 1.5 ppmv per year, primarily due to the large consumption of fossil fuels since the industrial revolution (IPCC, 2007). Terrestrial ecosystems were recognized as a major sink of global CO_2 emissions. This leads to a wide interest in carbon (C) cycling in terrestrial ecosystems and its potential to mitigate rising atmospheric CO_2 concentrations (Lal, 2004; Hill *et al.*, 2006). Autotrophic microorganisms which have the ability to assimilate atmospheric CO_2 biologically are commonly present in aquatic ecosystems (Stanley *et al.*, 2003; Savage *et al.*, 2010). Cannon *et al.* (2001) showed that the cyanobacteria and chemoautotrophs in oceans are responsible for about 40 percent of CO_2 removed from the atmosphere annually. Such microorganisms are also widespread in terrestrial ecosystems, and significant atmospheric CO_2 fixation by microorganisms has been observed in certain soil microenvironments such as in the vicinity of legume nodules (Dong and Layzell, 2001) or other niches with high hydrogen (H_2) production (Stein *et al.*, 2005). Miltner *et al.* (2004) observed a constant CO_2 fixation in soil under dark conditions. Besides the above mentioned special microenvironments, there is a critical gap in our knowledge of the microbial atmospheric CO_2 assimilation potential in soils and their contribution to global C balance. Therefore, our aim was to clarify the activity and capacity of soil microbial assimilation of atmospheric CO_2 for the better understanding of C cycling processes.

MATERIALS AND METHODS

Eight soils including four paddy soils under permanently flooded rice cultivation (referred to as P1, P2, P3 and P4), one paddy soil under flooded/drought rotation (P5), and three upland soils under vegetable (V1) or cereal cultivation (U1 and U2) were selected as representatives of the dominant types of cropping soils in the sub-tropical region of China (Table 1). The sites of the soils had a mean annual temperature about 16.8°C and an annual rainfall of about 1 400 mm. Soil cores were collected from the upper layer (Ap, 0 cm) and coarse plant residues removed. Site information and soil properties are shown in Table 1.

Prior to use, soils P1, P2, P3 and P4 were adjusted to about 100 percent of field water holding capacity (FWHC), and the others to 45 percent of FWHC with sterilized water. Two sets of microcosms of the soils with four replicates were prepared by weighing 1.0 kg fresh soil (on an oven-dried basis) in a plastic container (10 cm diameter and 22 cm height). One set, used as the control, was covered with 0.7 cm thick dark plastic foam to ban light but allow air flux through. The microcosms of the other set were perforated clear plastic sheets to eliminate duckweed growth. All soil microcosms were placed in growth chambers (China Patent No. ZL2006100197402). During the incubation period (80 d), artificial light (about 500 mmol ·photons·m^{-2}·s^{-1} parabolic aluminized reflector light [PAR]) was provided between 8:00 am and 8:00 pm each day. Temperature was set at 28–32°C in the illuminating period and 22°C in the dark period, and constant relative humidity at 80–90 percent. The ^{14}C-labelled CO_2 was generated from a ^{14}C-labelled Na_2CO_3 solution (Irvine CA, USA) containing 1.6×10^4 mg·C/mL with a radioactivity of 1.01×10^6 decays per min (DPM), by reaction with HCl (2 M) in a plastic beaker placed inside the chamber. The CO_2 concentration was controlled at 270–350 mL/L by regularly adjusting with ^{14}C-Na_2CO_3. The paddy soil pots were maintained in a continuously flooded condition, and upland soil pots kept at a moisture level

1 Key Laboratory of Agro-ecological Processes in Subtropical Region, Institute of Subtropical Agriculture, Chinese Academy of Sciences, Hunan 410125, P. R. China
2 Department of Sustainable Soils and Grassland Systems, Rothamsted Research, Harpenden, Herts. AL5 2JQ United Kingdom
* E-mail address of corresponding author: jswu@isa.ac.cn; gtd@isa.ac.cn

L.K. Heng, K. Sakadevan, G. Dercon and M.L. Nguyen (eds), Proceedings — International Symposium on Managing Soils for Food Security and Climate Change Adaptation and Mitigation. Food and Agriculture Organization of the United Nations, Rome, 2014: 377–380

TABLE 1. Characteristics of the paddy and upland soils used in this study

Soils	Cultivation systems	Soil type	Clay content (%)	CEC (c·mol/kg)	pH	SOC (g/kg)	Total N	MBC (mg/kg)
P1	Double rice	Ultisol	35	10.6	6.0	25.7	2.0	865
P2	Double rice	Fluvisol	25	6.2	5.2	15.9	1.6	1223
P3	Double rice	Fluvisol	11	7.2	4.7	14.8	1.6	638
P4	Double rice	Ultisol	12	12.2	5.1	17.9	1.7	879
P5	Rice-oil seed rotation	Ultisol	28	8.8	5.6	6.34	1.0	182
V1	Vegetable	Fluvisol	34	11.9	6.0	16.9	1.9	373
U1	Maize	Ultisol	42	10.3	4.6	9.07	1.2	152
U2	Maize-wheat	Ultisol	44	11.5	5.2	5.63	0.8	178

Note: SOC and CEC indicate soil organic carbon and cation exchange capacity, respectively.

of 45 percent of FWHC by the addition of distilled water throughout the incubation.

After labelling, samples were taken from each of the soil microcosms for analyses of ^{14}C-labelled microbial biomass C and organic C assimilated from ^{14}C-labelled CO_2. The ^{14}C-labelled soil organic C (^{14}C-SOC) was measured according to Wu and O'Donnell (1997). The total amount of extractable microbial C (MBC) was determined by the difference between K_2SO_4-extractable C in fumigated and non-fumigated soil using k factor 0.45 (Wu *et al.*, 1990). ^{14}C-organic C in the extractant was determined by liquid scintillation counting as described above. Soil organic C and total N were determined by dry combustion using an elemental analyzer (Vario MAX C/N, Elementar, Germany). Soil pH was determined in 1:2.5 (w:v) soil to H_2O ratio extracts. Soil clay content was determined using the pipette method (Müller and Höper, 2004). Cation exchange capacity (CEC) was measured using titration (Rhoades, 1982). Data were analysed with SPSS 10.5 (SPSS Inc., Chicago, IL, USA) using one-way ANOVA procedures and linear regression by the Pearson correlation method.

RESULTS AND DISCUSSION

The radioactivity in soils sampled from all of the covered microcosms was scarcely detectable, and no organic C assimilation occurred in any of the eight soils, whereas large quantities of ^{14}C-SOC were determined in the soil microcosms exposed to light for 12 h per day (Figure 1A).

The significant positive relationship ($r = 0.945$, $p = 0.0004$) between the amounts of ^{14}C-SOC and ^{14}C-MBC (Figure 2) revealed directly that the phototrophic CO_2 assimilation is a microbially-mediated process. To the best of our knowledge, this has been demonstrated for the first time. However, Miltner *et al*. (2004) found a significant transfer of ^{13}C-labelled CO_2 into soil organic matter (1.3 μmol C/g soil after 61 days) in the dark. In a ^{14}C-labelled CO_2 experiment, these authors also discovered that a great deal of ^{14}C-labelled CO_2 was fixed, corresponding to 0.05 percent of the total organic C in soils after six weeks' incubation; they suggested that this non-phototrophic CO_2 fixation process was driven mainly by aerobic heterotrophic microorganisms (Miltner *et al.*, 2005). The difference between the present and earlier findings may be explained by the extremely high (319 mg/g) SOC content in the soils and the addition of readily available substrates (such as acetic acid) used in the earlier study, both of which would stimulate the growth of aerobic heterotrophic microorganisms. Thus, the significant non-phototrophic atmospheric CO_2 assimilation observed by Miltner *et al*. (2004 and 2005) is not surprising. Obviously, based on the significant ^{14}C-CO_2 assimilated in the illuminated soils, it can be speculated that phototrophic CO_2 assimilation is the dominant microbial CO_2 assimilation process and that this was possibly and mainly driven by autotrophic microorganisms (including photo- and chemo- autotrophic microbes) instead of heterotrophic microorganisms, although further work is required to highlight the relationship between the autotrophic microbial activity and soil CO_2 assimilative rate.

The amount of ^{14}C-SOC (range 8.44–64.61 mg/kg, Figure 1A) accounted for between 0.12 percent and 0.59 percent of SOC (Figure 1C). Through further calculation (the global soil (0–1 m) organic C stock is 2 300 Pg, of which about 30 percent is present in the 0–20 cm soil layer), the capacity of soil microorganisms to synthesize atmospheric CO_2 in a period of only 80 days is equivalent globally to 0.83–4.07 Pg C. This clearly shows that autotrophic CO_2 assimilation at the topsoil potentially made a significant contribution to the C cycle. Carney *et al.* (2007) considered that C emission and absorption in the terrestrial ecosystem in response to global atmospheric change do not balance. Thus, the quantity of CO_2 emission is always larger than that from CO_2 uptake. If correct, there is a 'missing C sink' of about 2–3 Pg·C/yr at the global scale (Karim, Veizer and Barth, 2008). In this study, the calculated rate of organic C assimilation was 1.12–8.57 mg C/m per hour (12-h light exposure). It is estimated that the annual rate of microbial synthesis of organic C is 4.9–37.5 g·Cm^2, or 0.068–0.53 Pg globally, assuming a total terrestrial area of 140 000 000 km^2. It may therefore be presumed that part of the "missing C sink" is C sequestrated by soil organisms. This work provides a new research direction for attempting to account for "new and missing C sinks" in terrestrial ecosystems, although the driving forces for the observed high amounts of CO_2 assimilated at the soil surface are not clear, and require further study.

The amounts of ^{14}C-MBC ranged from 1.55 to 10.36 mg/kg (Figure 1B), and about 16.04 percent (CV = 22.6, n = 8) of assimilated ^{14}C was recovered as MBC after 80 d (data not shown). Rapid incorporation of C produced into MBC proved that "new" C derived from recent assimilates was readily utilized by microorganisms in paddy and upland soils. The ^{14}C in MBC may have had three fates: a fraction released as CO_2 through respiration, another fraction transformed to structural components of microorganisms and a third entering the SOC as microbial. However, this study provided little information about the accumulation of the "new" SOC derived from assimilation at the soil interface.

Additionally, large variations in microbial CO_2 assimilative rate were also observed across the soils tested in the present study, yet the mechanism was not clear since soil types, management practices and environmental conditions could influence the activity and popu-

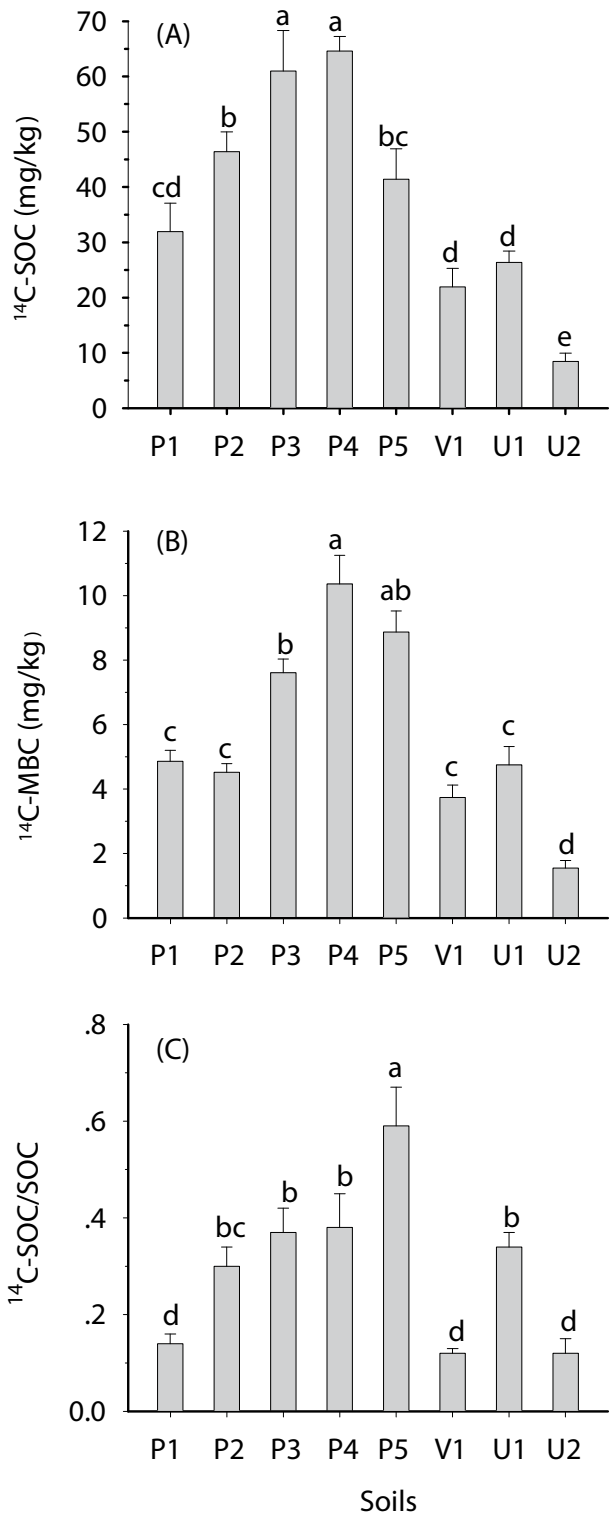

FIGURE 1. The amounts of ^{14}C-labelled CO_2 incorporated into soil organic carbon (^{14}C-SOC, A), microbial biomass (^{14}C-MBC, B) and the ratio of ^{14}C-SOC to SOC (C) in soil exposed continuously to ^{14}C-labelled CO_2 atmosphere and artificial light for 80 d. Bars indicate the standard error of the mean (n = 4). Different lowercase letters indicate significant differences among the soils at $p < 0.05$

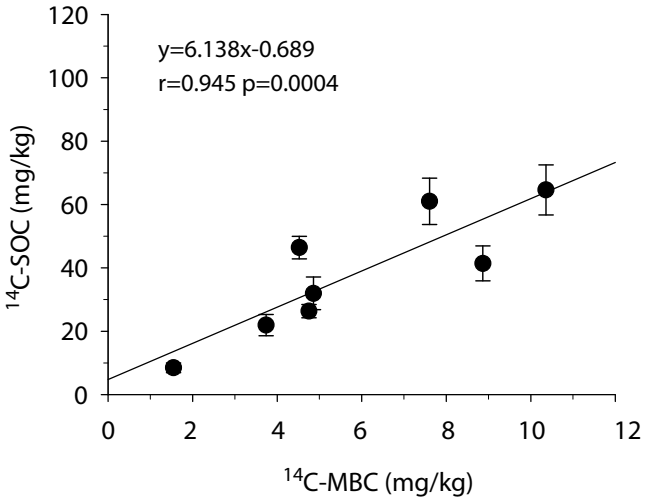

FIGURE 2. Relationship between ^{14}C-MBC and ^{14}C-SOC from eight contrasting soils during 80 d ^{14}C continuous labelling by incubation of soils under artificial light conditions. Bars represent the standard errors. For data on ^{14}C-SOC and ^{14}C-MBC, see Figure 1.

lation of microorganism associated with the C cycling process. Given the influence of climate change, further studies on the functional ecological implications of the abundance and composition of soil C assimilative microorganisms and their adaptation to local habitats and external interferences are warranted to clarify this microbial driving process.

ACKNOWLEDGEMENTS

This study was supported financially by the "Strategic Priority Research Program – Climate Change: Carbon Budget and Related Issues" of the Chinese Academy of Sciences (grant XDA05050505), the National Natural Science Foundation of China (grants 41271279 and 41090283), the Knowledge Innovation Program of the Chinese Academy of Sciences (grant ISACX-LYQY-QN-1103), and the CAS/SAFEA International Partnership Program for Creative Research Teams (grants KZCX2-YW-T07 and 20100491005-8).

REFERENCES

Cannon, G.C., Bradburne, C.E., Aldrich, H.C., Baker, S.H., Heinhorst, S. & Shively, J.M. 2001. Microcompartments in prokaryotes: carboxysomes and related polyhedra. *Appl. Environ. Microbiol.*, 67: 5351–5361.

Carney, K.M., Hungate, B.A., Drake, B.G. & Megonigal, J.P. 2007. Altered soil microbial community at elevated CO_2 leads to loss of soil carbon. *Proc. Natl. Acad. Sci. USA,* 104: 4990–4995.

Dong, Z. & Layzell, D.B. 2001. H_2 oxidation, O_2 uptake and CO_2 fixation in hydrogen treated soils. *Plant Soil*, 229: 1–12.

Hill, P.W., Jones, D.L., Marshall, C. & Farrar, J.F. 2006. Temporal and spatial dynamics of soil solution C and N concentrations during *Lolium perenne* L. sward establishment and the effects of elevated CO_2 and N additions. *Soil. Biol. Biochem.*, 38: 1290–1297.

IPCC. 2007 Climate change 2007. *Climate change impacts, adaptation and vulnerability*. Working Group II, Geneva, Switzerland. IPCC.

Karim, A., Veizer, J. & Barth, J. 2008. Net ecosystem production in the great lakes basin and its implications for the North American

missing carbon sink: A hydrologic and stable isotope approach. *Glob. Planet. Change,* 61: 15–27.

Lal, R. 2004. Offsetting China's CO_2 emissions by soil carbon sequestration. *Clim. Change,* 65: 263–275.

Miltner, A., Richnow, H.H., Kopinke, F.D. & Kästner, M.K. 2004. Assimilation of CO_2 by soil microorganisms and transformation into soil organic matter. *Org. Geochem.*, 35: 1015–1024.

Miltner, A., Kopinke, F.D., Kindler, R., Selesi, D., Hartmann, A. & Kästner, M.K. 2005. Non-phototrophic CO_2 fixation by soil microorganisms. *Plant Soil,* 269: 193–203.

Müller, T. & Höper, H. 2004. Soil organic matter turnover as a function of the soil clay content: Consequences for model applications. *Soil. Biol. Biochem.,* 36: 877–888.

Rhoades, J.D. 1982. Cation exchangeable capacity *In* A.L. Pace, R.H. Miller & D.R. Keeney, eds. *Methods of soil analysis: Part 2-chemical and microbiological properties, 2nd Edition,* pp. 149–165. Madison, American Society of Agronomy, Soil Science Society of America.

Savage, D.F., Afonso, B., Chen, A.H. & Silver. P.A. 2010. Spatially ordered dynamics of the bacterial carbon fixation machinery. *Science,* 327: 1258–1262.

Stanley, E.H., Johnson, M.D. & Ward, A.K. 2003. Evaluating the influence of macrophytes on algal and bacterial production in multiple habitats of a freshwater wetland. *Limnol. Oceanogr.,* 48: 1101–1111.

Stein, S., Selesi, D., Schilling, R., Pattis, I., Schmid, M. & Hartmann, A. 2005. Microbial activity and bacterial composition of H_2-treated soils with net CO_2 fixation. *Soil. Biol. Biochem.,* 37: 1938–1945.

Wu, J., Joergensen, R.G., Pommerening, B., Chaussod, R. & Brookes, P.C. 1990. Measurement of soil microbial biomass C by fumigation-extraction: An automated procedure. *Soil. Biol. Biochem.,* 22: 1167–1169.

Wu, J. & O'Donnell A.G. 1997. Procedure for the simultaneous analysis of total and radioactive carbon in soil and plant materials. *Soil. Biol. Biochem.,* 29: 199–202.

Cosmic-ray Soil Moisture Probe: A New Technology to Manage African Dryland Ecosystems

T.E. Franz[1,*], M. Zreda[1] and E.G. King[2]

ABSTRACT

An estimated 200 million rural smallholders practice livestock-based or mixed livestock-crop-based agriculture in sub-Saharan Africa, where levels of poverty and food insecurity are among the highest in the world. Demographic, environmental, and climate changes have led to diminishing supply of resources that is crippling dryland productivity and increasing people's vulnerability. There is a need for research to develop, monitor, and evaluate strategies to cope with diminishing resource availability and build resilient ecosystems. Reliable, long-term measurements of soil moisture are critically needed for addressing productivity and food security in African drylands. We propose that measurements of effective infiltration, plant available water and deep drainage are sufficient metrics to understand dryland ecosystem health and to assess and evaluate restoration strategies. In this work, we evaluate the advantages and disadvantages of two different measurement methods, the cosmic-ray neutron method (as implemented in the COsmic-ray Soil Moisture Observing System (COSMOS) and eddy covariance techniques, for long-term measurements of African dryland water balance. We compare estimates of ecosystem level daily evapotranspiration between the two methods over a six-month period at a site in central Kenya, and found the cosmic-ray method to be more appropriate. The eddy covariance data are smoother than the cosmic-ray measurements. However, the cosmic-ray neutron probe method provides additional information on the key variable, area-average soil moisture, allowing us to partition rainwater into infiltration, runoff, evapotranspiration, and deep drainage. In addition, cosmic-ray neutron probes are easier to operate and maintain, more robust and less expensive than eddy covariance towers, making them more appropriate for long-term deployments.

Key words: *soil moisture, evapotranspiration, cosmic-ray neutron probe, agropastoralism, Africa, drylands.*

INTRODUCTION

Sixty percent of sub-Saharan Africa is pastoral or agropastoral land (Reynolds *et al.,* 2007). These arid, semi-arid and subhumid regions are grassland to desert ecosystems and home to an estimated 200 million rural smallholders practising livestock-based or mixed livestock-crop-based agriculture (Thornton *et al*., 2002; Robinson *et al.,* 2011). These regions have some of the highest levels of poverty and food insecurity in the world (Thornton *et al*., 2002; Thomas and Twyman 2005), and they are exceptionally vulnerable to climate change. While projections of changes to mean annual precipitation vary from region to region, models agree that across all African drylands, rainfall will become less predictable, with shorter growing seasons (Thornton *et al.*, 2006), and more frequent and more severe droughts (Sheffield and Wood, 2008). This is the setting for one of Africa's greatest agricultural development challenges — dryland productivity and food security.

Of these pastoral/agropastoral areas approximately two-thirds are drylands, where annual potential evapotranspiration exceeds rainfall by 200 percent or more, and traditional smallholder agriculture relies substantially or wholly on extensive livestock husbandry (Notenbaert *et al*., 2009). This resilient production system has evolved and persisted for millennia, and represents a highly adaptive relationship between human livelihoods and the environmental stresses that typify dryland environments. Tropical drylands experience not just low amounts of rainfall, but high rainfall variability both in space and time. Systems of mobile, flexible livestock herding over extensive ranges allow smallholders to buffer themselves against the variable environmental conditions at any single location, and to access key natural resources that are distributed non unevenly across large spatial scales (Niamir-Fuller, 1998). Smallholder livestock production in drylands is not an isolated socioeconomic system, but influences the national economies of all African nations with drylands. It is a critical source of protein, nutrition, and commerce for both rural and urban populations. For example, in Kenya, livestock contributed 50 percent to the national agricultural gross domestic production in 2004, and the proportional contribution continues to increase (Hesse and MacGregor, 2006).

However the resource base for livestock production is shrinking due to four compounding effects:

(i) Population growth: there are more lives depending on each ha (Notenbaert *et al*., 2009).

(ii) Land conversion: usually to cropping, which leaves fewer ha available (Herrero *et al*., 2009), and may increase dependence on groundwater supplies to meet the increased evapotranspiration demand.

1 Hydrology and Water Resources, University of Arizona, 1133 E James E Rogers Way Rm 122, Tucson, AZ 85721, USA

2 Odum School of Ecology, University of Georgia, 140 E. Green St., Athens, GA 30602, USA

* E-mail address of corresponding author: tfranz@email.arizona.edu

L.K. Heng, K. Sakadevan, G. Dercon and M.L. Nguyen (eds), Proceedings — International Symposium on Managing Soils for Food Security and Climate Change Adaptation and Mitigation. Food and Agriculture Organization of the United Nations, Rome, 2014: 381–386

(iii) Legacy of land degradation: today the same ha produces less forage (Dregne, 2002).
(iv) Increasingly unpredictable climate: this results in fewer productive ha per year, and is expected to reduce viable pastoral areas by 20 percent in 40 years (Thornton *et al.,* 2006; Falkenmark and Rockstrom, 2008).

It is the diminishing supply of resources for livestock-based agriculture that is crippling the system's productivity and increasing people's vulnerability (Thornton *et al.*, 2006; Andersson, Brogaard and Olsson, 2011). Research is needed to proactively develop, monitor, and evaluate strategies to cope with this 'diminishing resource syndrome' in drylands.

Mitigation of the diminishing resource has typically fallen into two strategies: (i) do business as usual but search for more efficient and productive methods, or (ii) change to a new system. The first strategy falls in the sphere of range management. While managing livestock is an important issue, restoring the ecological functioning and productivity of the landscape is going to be an essential component to curtail the diminishing resource syndrome. However with increasing populations on limited lands, in many areas the demand for food is unlikely to be met by livestock management alone. The second strategy is one that many pastoralists all over Africa are now resorting to: trying to grow crops where traditionally they have only raised livestock. Depending on the context, this could increase vulnerability and food insecurity rather than reduce it. There is a need to understand these systems to find out where each of the two coping strategies or combination of the two strategies is most appropriate.

Dryland productivity is driven predominantly by landscape water balance, or the partitioning of incoming rainfall into different pathways in the ecosystem (runoff, groundwater recharge, evaporation, or transpiration). The more water that infiltrates the soil and is taken up by plants and transpired, the more plant productivity a landscape can yield. The more rainfall that is lost to runoff or evaporation directly from the soil, the smaller the proportion of soil moisture for plant growth. And importantly, the productivity of a landscape feeds back to affect the water balance in subsequent rainfall events (Ludwig *et al.,* 2005). Thus, as dryland vegetation degrades, the capacity of the landscape to capture and convert rainfall into productive growth also declines (Kefi *et al.,* 2007).

Directly improving plant water use efficiency could be a target for enhancing productivity, but in landscapes where degradation has impaired water balance, the system is still inexorably dependent on ecohydrological constraints on the supply of water available to plants. Addressing this abiotic component of the system is necessary to reinstate water–soil–vegetation feedbacks, so the system can once again sustain productivity (King and Whisenant, 2009). Increasing supply-side dynamics of water availability is the basis of the current 'Blue Revolution' in agricultural research. Here water conservation practices deliver 'more crop per drop', by enhancing water use efficiency, or the amount of productivity gained per unit of water consumed. The FAO promotes conservation agriculture with three principles: minimal soil disturbance, permanent soil cover and crop rotations (http://www.fao.org/ag/ca/; accessed on 1 August 2012). This approach has been shown to be successful in Tanzanian drylands (Owenya *et al.,* 2012).

This concept can also be applied to rangelands. Instead of targeting water use efficiency at the scale of single crop plants or agricultural fields, the approach is aimed at the scale of land tracts of a perennial ecosystem (several ha). However, at this scale additional complication is introduced, namely, spatiotemporal heterogeneity of resources. Two hallmark traits of drylands are its patchy structure and the variable, pulse-like arrival of the key limiting resource, water. Their interactions hold the key to understanding and restoring ecosystem function (Ryan, Ludwig and McAlpine, 2007; King *et al.*, 2012).

Historically, the measurement of soil water dynamics at this field scale has been notoriously difficult given the inherent limitations of direct and indirect sampling methods (Robinson *et al.*, 2008). An alternative measurement technique that uses eddy covariance towers (Stull, 1988) provides information on the water, energy, and carbon balances of ecosystems, integrated over the tower's "footprint" area, with a diameter of approximately 30 times the tower height. For example, Fluxnet is a global network of more than 400 eddy covariance towers that has operated since the 1980's (Baldocchi *et al.*, 2001), but with fewer than 20 stations in Africa, the continent is under-represented. However, flux towers provide little or no information about plant available water at the footprint scale, thus limiting our ability to fully understand the soil–atmosphere coupling (Seneviratne *et al.*, 2010) or partitioning of the water into its individual components.

The recent advent of the cosmic-ray neutron probe (Zreda *et al.,* 2008) has opened the door for measurements of near surface soil moisture at the landscape scale (Franz *et al.,* 2012). Here, the cosmic-ray moisture probe (Zreda *et al.,* 2008) is used to derive key variable needed for monitoring of agropastoral systems. We first summarize the cosmic-ray neutron probe method and COsmic-ray Soil Moisture Observing System (COSMOS) (Zreda *et al.*, 2012). Next, estimates of daily soil water flux derived from cosmic-ray neutron measurements are compared with a collocated eddy covariance tower in a central Kenyan dryland. Finally, some key points for consideration are identified for the establishment of a cosmic-ray neutron probe monitoring network in African drylands to address the critical issues of productivity and food security.

MATERIALS AND METHODS

Cosmic-ray neutron probe method

The inverse relationship between soil moisture and the intensity of cosmic-ray fast neutrons above the surface has been known for several decades (Hendrick and Edge, 1966). The removal of neutrons is dominated by neutron collisions with hydrogen atoms. Hydrogen has an extraordinarily high neutron stopping power due to a combination of its high neutron scattering cross-section and the high fractional energy loss per collision and low atomic mass (Zreda *et al.,* 2008 and 2012). Hydrogen's stopping power is an order of magnitude greater than any other element, making hydrogen the dominant factor in controlling neutron intensity (Zreda *et al.,* 2012).

Using a moderated neutron detector placed above the surface (Figure 1), Zreda *et al.* (2008) found that differences in the relative count rate of fast neutrons (~10–100 eV) in air above land surface are related to the average amount of soil water present. Desilets *et al.* (2010) found the following calibration function between soil moisture, (m^3/m), and fast neutron counts:

$$\theta(N) = \frac{0.0808}{(N/N_0) - 0.372} - 0.115 \quad (1)$$

where N is the neutron counting rate normalized to a reference atmospheric pressure and solar activity level (Zreda *et al.*, 2012), N_0 is the counting rate over dry soil under the same reference conditions, and the three coefficients were determined using a neutron particle transport code, MCNPx (Pelowitz, 2005) for pure silica sand (SiO_2). The calibration parameter N_0 can be estimated at the probe site using volumetric soil moisture around the footprint (c.f. Zreda *et al*., 2012).

Because the sensor gives an average neutron count over a circle with a radius of ~335 m (Zreda *et al.,* 2008), and the sensitivity

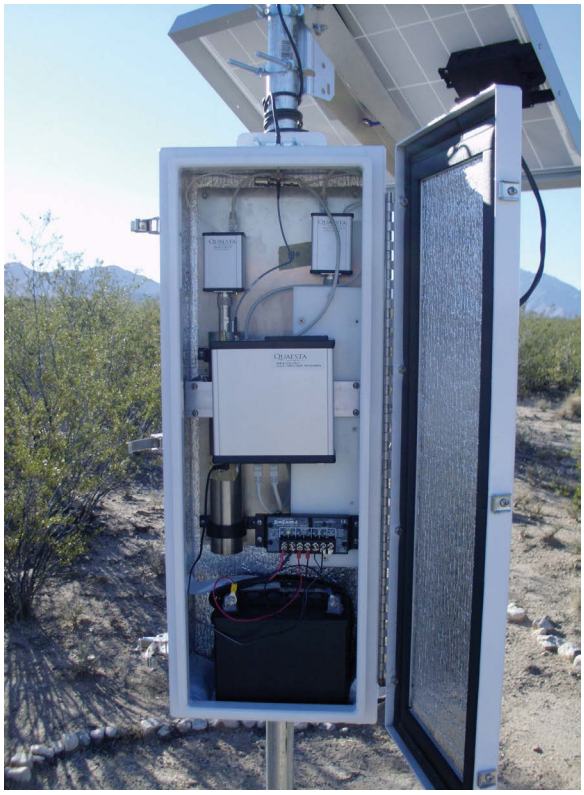

FIGURE 1. A cosmic-ray neutron probe (CRS 1000, Hydroinnova LLC, Albuquerque, NM, USA) installed at the Santa Rita Experimental Range site, located in southern Arizona, USA.

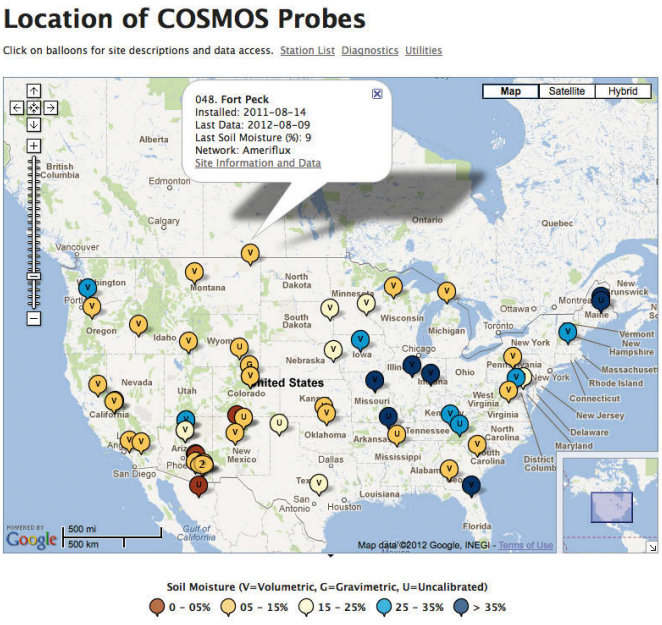

FIGURE 2. Location and status of COSMOS probes in the continental USA on 9 August 2012 (http://cosmos.hwr.arizona.edu/Probes/probemap.php). Raw and processed data from individual sites are publicly available in real time.

decreases with the distance from the probe, soil sampling at 18 locations (every 60° and at radii of 25, 75 and 200 m) gives a representative estimate of the mean water content over the footprint. Fast neutrons mix rapidly above the surface (velocities >10 km/s (Glasstone and Edlund, 1952), indicating that horizontal soil moisture heterogeneity likely plays a minor role in the average footprint neutron count. In contrast to the horizontal footprint that is independent of soil moisture content, the vertical depth of measurement of the sensor does vary with soil water content ranging between ~10 cm and 70 cm for wet and dry conditions, respectively (Zreda *et al.,* 2008). With a single or repeated calibrations at a site, Franz *et al.* (2012) found that sampling every 5 cm to a depth of 30 cm is adequate to accurately describe the average soil water content in the profile and thus estimate N_0 with an average RMSE of < 0.02 m^3/m^3.

COsmic-ray Soil Moisture Observing System

The COsmic-ray Soil Moisture Observing System (COSMOS) is a new national network in the continental USA designed for improving hydro-meteorological forecasting (Zreda *et al.* 2012, data available at http://cosmos.hwr.arizona.edu/) by providing real-time estimates of soil moisture (Figure 2). Beginning in 2009, 50 cosmic-ray neutron probes were deployed to provide hourly estimates of soil moisture. The cosmic-ray neutron probes have been designed to be rugged, energy-efficient and independently powered using solar cells, and they are equipped with a satellite data modem for reliable transmission of data from any place on the globe. A data success rate of over 90 percent has been achieved from the COSMOS probes in the continental USA and from affiliated probes in five other continents.

As part of the COSMOS project, all data are collected, processed, and checked for basic quality assurance and quality control in real-time, and then posted on the COSMOS web site. Currently, the measured neutron intensities are corrected for variations in geomagnetic latitude and local atmospheric pressure changes (Zreda *et al.,* 2012). In the near future, new corrections will be added to account for variations in lattice water, atmospheric water vapour and vegetation. Additional details about the cosmic-ray neutron probe method and the COSMOS project are in Zreda *et al.* (2012) and online (http://cosmos.hwr.arizona.edu/).

Instrumentation for water balance measurements in central Kenya

Beginning in September 2011, a cosmic-ray neutron probe was installed at a study site, referred to herein as Mpala North, in central Kenya, where a 20 m tall eddy covariance tower has been operating since 2009 (Caylor, unpublished data). The site is in the upper Ewaso Ngiro river basin of the central Kenyan highlands (36°54'E, 0°20'N). It is characterized as semi-arid woodland or shrubland, receiving 450–500 mm/yr of rainfall, typically arriving in two rainy seasons, April–May and November–December (Franz, Caylor and Nordbotten, 2010). The vegetation has 10–25 percent woody canopy cover, dominated by mixed *Acacia* species. The herbaceous layer has perennial and annual grasses, as well as a diversity of forbs and succulents, with 1–10 m bare patches with no perennial grass and sparse annual vegetation (Figure 3). Under current land use practices, average standing biomass is typically estimated to be 450–700 kg/ha (CNRIT, 2011).

The site is located on the Mpala Research Centre Conservancy (MRCC), a 20 000 ha ranch that has been used for commercial cattle production for the last century, and since 1998 has been managed as a wildlife and research conservancy while maintaining a moderate cattle herd (one tropical livestock unit (TLU) per 10 ha). Wildlife is abundant: elephant, giraffe, zebra, buffalo, impala, dik-dik, baboons, hyenas are common. The site is within three km of the Ewaso Ngiro River, which serves as the boundary between MRCC and communally-owned lands utilized and inhabited by Laikipia Maasai pastoral-

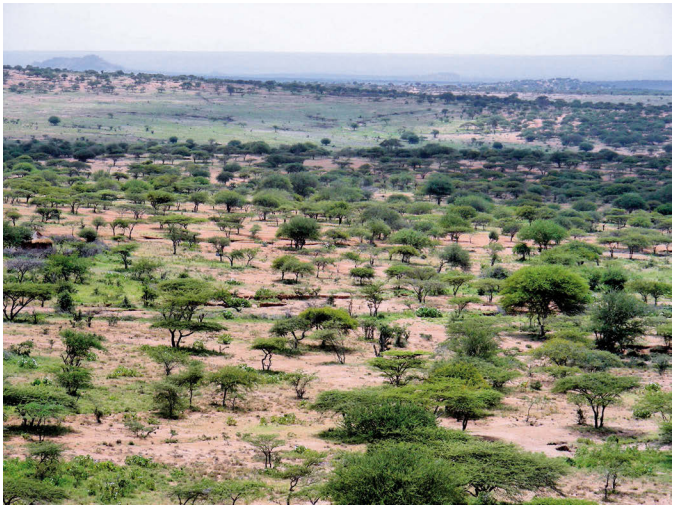

FIGURE 3. Vegetation composition and cover in central Kenya.

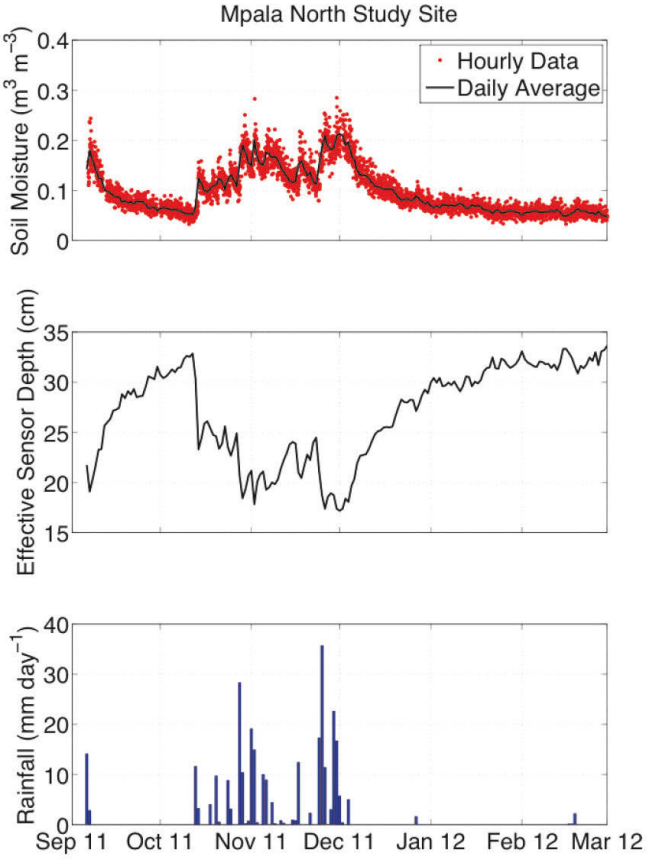

FIGURE 4. Daily soil moisture, effective sensor depth, and rainfall from the Mpala North study site in central Kenya.

ists. The communal areas have similar physiognomy and rainfall to the MRCC site, higher livestock stocking rates (one TLU per three ha), reduced wildlife densities, and decreased herbaceous vegetation cover (5–50 percent less, varying with year and season (King, unpublished data). While land use is predominantly for livestock production, a limited number of community members began small-scale maize cropping along the river in 2011. In future work, the Mpala North site and adjacent community lands will be studied to compare landscape scale water balance and ecosystem function between the land use systems.

RESULTS

The daily time series of neutron-derived soil moisture, effective sensor depth, and rainfall from the study site (Figure 4) show the response of soil moisture to rain events. Using the time series of soil moisture data, the daily flux of water into and out of the control volume were computed (Figure 5). The positive values indicate infiltration of rainwater into the soil and negative values indicate losses of water to evapotranspiration (ET) and vertical leakage (L). Small positive anomalies in the dataset not correlated to rain events are due to uncertainty in either the neutron count statistics or rainfall record. To compare different measurement techniques, the daily ET values derived from the cosmic-ray neutron probe and the daily average latent energy from the eddy covariance tower are considered (Figure 6). Despite the differences in the measurement techniques and horizontal and vertical scales of measurements, the two time series agree reasonably well over the six-month study period. Because the cosmic-ray derived ET also contains L, the values are higher than those derived from eddy covariance, which only estimate ET. Using additional information about the soil and vegetation, a soil water balance model can be used to separate the ET and L components from the integrated signal, for example using methods described in Rodriguez-Iturbe and Porporato (2004).

DISCUSSION

Comparison of the daily water fluxes indicates a general agreement between the methods, but eddy covariance derived values are smoother than those derived from the cosmic-ray neutron measurements. Given the different information obtained from each instrument, the complimentary measurements from eddy covariance and cosmic-ray instruments are preferable to understand how these ecosystems function. However, limited research budgets and unfavour-

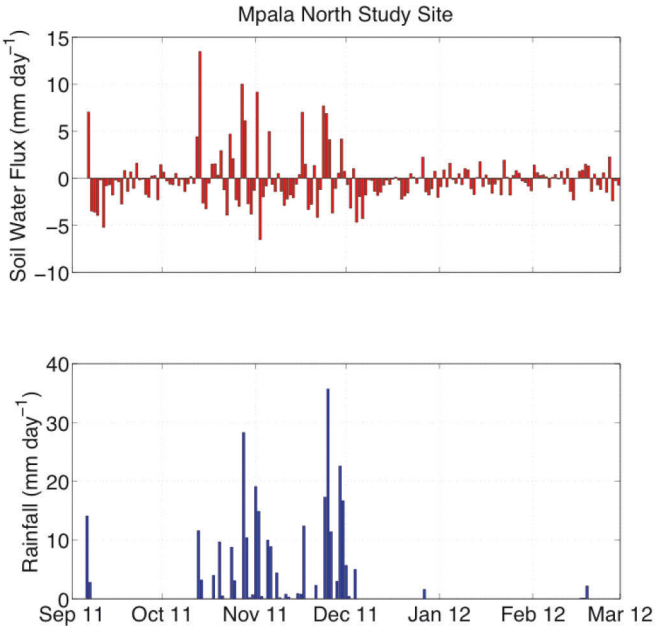

FIGURE 5. Estimates of daily soil water flux into and out of the control volume derived from the soil moisture time series.

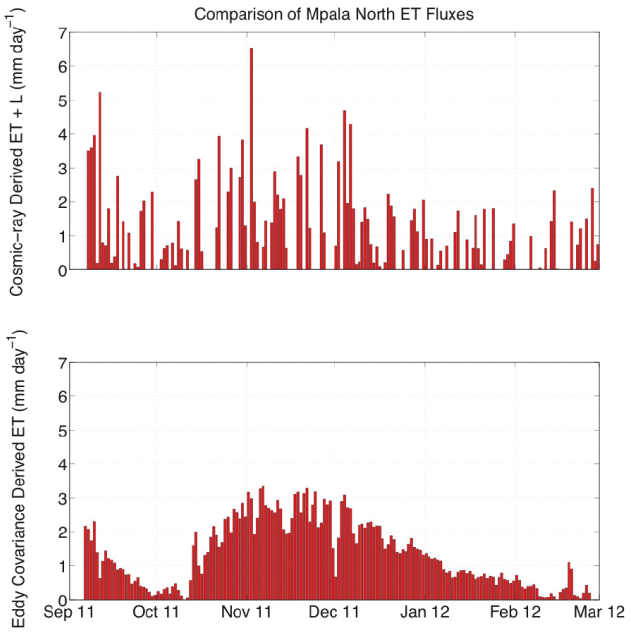

FIGURE 6. Comparison of landscape scale fluxes derived from the co-located cosmic-ray neutron probe and eddy covariance tower.

able site characteristics often restrict the total possible investment, and only one of the two instruments may be feasible. Three key differences between the measurement methods make the cosmic-ray neutron probes more suitable for monitoring and assessing the long-term ecosystem health and function of African drylands.

First, as described in the introduction, the key factor governing these dryland ecosystems is the partitioning of rainfall into run-off, infiltration, evapotranspiration, and deep drainage. Whereas the eddy covariance method provides measurements of the water, energy and carbon balances, they do not provide information on the soil water — the key variable. Knowing soil water is crucial because in order to estimate the various water fluxes in and out of the soil column, parameters and boundary conditions are needed that describe the physics of unsaturated water flow through porous media (Dingman, 2002). Point sensors are often used to measure soil moisture, but their small support volumes (~10 cm^3) result in measurements that are not representative of the footprint scale (~1 km^2) because of small-scale heterogeneities within the footprint (Robinson *et al.,* 2008). Thus, comparisons between land surface fluxes from eddy covariance towers and soil moisture dynamics based on point measurements may be unreliable. Because cosmic-ray neutrons provide area-average soil moisture (Franz *et al.,* 2012; Zreda *et al.,* 2012), effective (area-average) parameters could be derived for controlling the flow of water through porous media and thus partition rainfall into infiltration, runoff, evapotranspiration, and deep drainage at the landscape scale. For rangelands, the amount of rainfall infiltrating into the soil is the key metric to find out how the ecosystem is functioning under different land uses or to evaluate effective restoration strategies (King *et al.*, 2012). In addition, estimates of available water will be one critical piece to decide what vegetation is best suited to a particular ecosystem. Moreover, the water demand of various crops can be calculated for certain climates and compared to the estimate of available water in that ecosystem. In that regard, the amount of extra water needed from surface or ground water sources can be estimated, providing crucial information to stakeholders about the feasibility and environmental impact of the proposed land use change.

Second, from operational and maintenance standpoints the cosmic-ray neutron probes are easier to install, calibrate, and less expensive to purchase and maintain than eddy covariance towers. The cosmic-ray sensor contains a gas-filled tube, high voltage power source, data logger, 40 Ahr battery, 60 W solar panel, and satellite modem. This is simple when compared with the dozens of instruments required for an eddy covariance tower. In terms of maintenance, the major concerns are keeping the cosmic-ray probe battery charged and relative humidity inside the instrument box low. In terms of calibration, and as with most instruments, repeated calibrations are preferred and will ensure the highest quality of data, but a single calibration is adequate because of the long-term stability of the N_0 parameter (Franz *et al.*, 2012). In contrast, eddy covariance towers require yearly calibrations of the individual instruments and a full-time technician to maintain performance. Eddy covariance towers operate best with AC power but can be supported with several solar panels and battery banks. In terms of data, the cosmic-ray probe was designed to send a minimal amount data (ambient pressure, temperature, humidity, voltage, neutron count), or approximately 10 bytes of raw data, per transmission (usually every hour). Eddy covariance towers make measurements many times per sec in order to quantify the departures from the mean and accurately estimate the half-hourly averages. In addition, eddy covariance data require a significant amount of post-processing time and skilled personnel for high quality datasets (Stull, 1988).

Third, the costs of the two instruments are different. Principal investment of eddy covariance tower equipment is approximately US$100 000 with additional costs for maintenance, data transfer, data processing, and skilled onsite personnel. In contrast, cosmic-ray neutron probes cost approximately US$20 000 and require substantially less maintenance, data transmission cost and processing, and do not require permanent personnel on site.

CONCLUSIONS

Measurements of effective infiltration, plant available water, and deep drainage are sufficient metrics to understand ecosystem health and function in African drylands. This information is critical for stakeholders who wish to increase productivity and food security in their ecosystems. In addition, these data will provide useful landscape water metrics to assess and evaluate different land use and restoration strategies in drylands. Given the advantages and disadvantages of each measurement method described above, we find the cosmic-ray neutron method is more appropriate than the eddy covariance technique for environmental monitoring in African drylands. Most importantly, the cosmic-ray neutron probe method provides information on the area-average soil moisture — the key variable — allowing partitioning rainwater into infiltration, runoff, evapotranspiration, and deep drainage. Cosmic-ray neutron probes were designed to be robust, have low power consumption, low maintenance and high data reliability making them superior for long-term deployment in remote ecosystems. It is suggested that reliable long-term measurements of soil moisture constitute the critical information needed for addressing productivity and food security in African drylands.

ACKNOWLEDGEMENTS

This research and the COSMOS project were supported by the US National Science Foundation grant AGS-0838491. We would like to thank Kelly Caylor, Keir Soderberg, and Molly O'Connor of Princeton University for supplying processed flux-tower data for this work.

REFERENCES

Andersson, E., Brogaard, S. & Olsson, L. 2011. The political ecology of land degradation. *Ann. Rev. Environ. & Resour.*, 36: 295–319.

Baldocchi, D., Falge, E., Gu, L.H., Olson, R., Hollinger, D., Running, S., Anthoni, P., Bernhofer, C., Davis, K., Evans, R., Fuentes, J., Goldstein, A., Katul, G., Law, B., Lee, X.H., Malhi, Y., Meyers, T., Munger, W.W., Oechel, W., Pilegaard, K.T.P.U.K., Schmid, H. P., Valentini, R., Verma, S., Vesala, T., Wilson, K. & Wofsy, S. 2001. FLUXNET: A new tool to study the temporal and spatial variability of ecosystem-scale carbon dioxide, water vapor, and energy flux densities. *Bull. Am. Meteorol. Soc.*, 82: 2415–2434.

CNRIT (Center for Natural Resource Information Technology). 2011. African Early Livestock Warning System: East Africa, Kenya - Laikipia: KE-LA-MPA-01, KE-LA-MPA-03. Texas A & M University, CNRIT. (http://glews.tamu.edu/eastafrica; accessed online, November 2011).

Dingman, L.S. 2002. *Physical hydrology: Second Edition*. Upper Saddle River, Prentice-Hall Inc. 646 pp.

Dregne, H.E. 2002. Land degradation in the drylands. *Arid Land Res. & Manage.*, 16: 99–132.

Falkenmark, M. & Rockstrom, J. 2008. Building resilience to drought in desertification-prone savannas in sub-Saharan Africa: The water perspective. *Nat. Resour. Forum,* 32: 93–102.

Franz, T.E., Caylor, K.K., Nordbotten, J.M. Rodriguez-Iturbe, R.I. & Celia, M.A. 2010. An ecohydrological approach to predicting regional woody species distribution patterns in dryland ecosystems. *Adv. Water Resour.,* 33: 215–230.

Franz, T.E., Zreda, M., Ferre, P.A., Rosolem, R., Zweck, C., Stillman, S., Zeng, X. & Shuttleworth. W.J. 2012. Measurement depth of the cosmic-ray soil moisture probe affected by hydrogen from various sources. *Water Resour. Res.,* 48: W08515, doi:10.1029/2012WR011871.

Glasstone, S. & Edlund, M.C. 1952. *The elements of nuclear reactor theory*. New York, Van Nostrand.

Hendrick, L.D. & Edge, R.D. 1966. Cosmic-ray neutrons near earth. *Phys. Rev.,* 145: 1023–1025.

Herrero, M., Thornton, P.K., Gerber, P. & Reid, R.S. 2009. Livestock, livelihoods and the environment: understanding the trade-offs. *Curr. Opin. Environ. Sust.,* 1: 111–120.

Hesse, C. & MacGregor, J. 2006. *Pastoralism: Drylands' invisible asset?* IIED Issue Paper No 142. London, International Institute for Environment and Development.

Kefi, S., Rietkerk, M., Alados, C. L., Pueyo, Y., Papanastasis, V.P., ElAich, A. & de Ruiter, P.C. 2007. Spatial vegetation patterns and imminent desertification in Mediterranean arid ecosystems. *Nature,* 449: 213–215.

King, E.G., Franz, T.E. & Caylor, K.K. 2012. Ecohydrological interactions in a degraded two-phase mosaic dryland: implications for regime shifts, resilience, and restoration. *Ecohydrology,* 5: 733–745.

King, E.G. & Whisenant, S.G. 2009. Thresholds in ecological and linked social-ecological systems: application to restoration. *In* R.J. Hobbs and K.N. Suding, eds. *New models for ecosystem dynamics and restoration,* pp. 63–77. Washington, DC, Island Press. 366 pp.

Ludwig, J.A., Wilcox, B.P., Breshears, D.D., Tongway, D.J. & Imeson, A.C. 2005. Vegetation patches and runoff-erosion as interacting ecohydrological processes in semiarid landscapes. *Ecol.,* 86: 288–297.

Niamir-Fuller, M. 1998. The resilience of pastoral herding in Sahelian Africa. *In* F. Berkes & C. Folke, eds. *Linking social and ecological systems: Management practices and social mechanisms for building resilience,* pp. 250–284. New York, Cambridge University Press. 476 pp.

Notenbaert, A., Herrero, M., Kruska, R.L., You, L., Wood, S., Thornton, P.E. & Omolo, A. 2009. *Classifying livestock production systems for targeting agricultural research and development in a rapidly changing world*. ILRI Discussion Paper 19. Nairobi, ILRI.

Owenya, M., Mariki W., Stewart A., Friedrich T., Kienzle J., Kassam A., Shetto R. & Mkomwa S. 2012. Conservation agriculture and sustainable crop intensification in Karatu district, Tanzania. *Integr. Crop Manage.,* 15. FAO Publ., Rome, Italy.

Pelowitz, D.B. ed. 2005. *MCNPX user's manual, version 5, Rep. LA-CP-05-0369.* Los Alamos, Los Alamos National Laboratory.

Reynolds, J.F., Stafford Smith, D.M., Lambin, E.F., Turner, B.L., Mortimore, M., Batterbury, S.P.J., Downing, T.E., Dowlatabadi, H., Fernandez, R.J., Herrick, J.E., Huber-Sannwald, E., Jiang, H., Leemans, R., Lynam, T., Maestre, F.T., Ayarza, M. & Walker. B. 2007. Global desertification: Building a science for dryland development. *Science,* 316: 847–851.

Robinson, D.A., Campbell, C.S., Hopmans, J.W., Hornbuckle, B.K., Jones, S.B., Knight, R., Ogden, F., Selker, J. & Wendroth, O. 2008. Soil moisture measurement for ecological and hydrological watershed-scale observatories: A review. *Vadose Zone J.,* 7: 358–389.

Rodriguez-Iturbe, I. & Porporato, A. 2004. *Ecohydrology of water-controlled ecosystems*. New York, Cambridge University Press. 442 pp.

Robinson, T., Thornton, P.E., Franceschini, G., Kruska, R.L., Chlozza, F., Notenbaert, A., Cecchi, G., Herrero, M., Epprecht, M., Fritz, S., You, L., Conchedda, G. & See, L. 2011. *Global livestock production systems*. Rome and Nairobi, FAO and ILRI.

Ryan, J.G., Ludwig, J.A. & McAlpine, C.A. 2007. Complex adaptive landscapes (CAL): A conceptual framework of multi-functional, non-linear ecohydrological feedback systems. *Ecol. Complex.,* 4: 113–127.

Seneviratne, S.I., Corti, T., Davin, E.L., Hirschi, M., Jaeger, E.B., Lehner, I., Orlowsky, B. & Teuling A.J. 2010. Investigating soil moisture-climate interactions in a changing climate: A review. *Earth-Sci. Rev.,* 99: 125–161.

Sheffield, J. & Wood, E.F. 2008. Projected changes in drought occurrence under future global warming from multi-model, multi-scenario, IPCC AR4 simulations. *Clim. Dynam.,* 31:79–105.

Stull, R.B. 1988. *An introduction to boundary layer meteorology*. Heidelberg, Springer. 670pp.

Thomas, D.S.G. & Twyman, C. 2005. Equity and justice in climate change adaptation amongst natural-resource-dependent societies. *Global Environ. Change* 15: 115–124.

Thornton, P.K., Jones, P.G., Owiyo, T., Kruska, R.L., Herrero, M., Kristjanson, P., Notenbaert, A., Bekele, N. & Omolo, A. 2006. *Mapping climate vulnerability and poverty in Africa.* Nairobi, ILRI.

Thornton, P.K., Kruska, R.L., Henninger, N., Kristjanson, P.M., Reid, R.S., Atieno, F., Odero, A. & Ndegwa, T. 2002. *Mapping poverty and livestock in the developing world*. Nairobi, ILRI.

Zreda, M., Desilets, D., Ferre, T.P.A. & Scott, R.L. 2008. Measuring soil moisture content non-invasively at intermediate spatial scale using cosmic-ray neutrons. *Geophys. Res. Lett.,* 35: 5. doi: 10.1029/2008GL035655.

Zreda, M., Shuttleworth, W.J., Xeng, X., Zweck, C., Desilets, D., Franz, T.E., Rosolem, R. & Ferre. P.A. 2012. COSMOS: The COsmic-ray soil moisture observing system. *Hydrol. & Earth Syst. Sci.,* 16: 4079–4099.

Large Area Soil Moisture Measurement Using Cosmic Rays Neutrons: The Australian CosmOz Network

C.J. Smith[1,*], A. Hawdon[2], R. Keen[2] and J. Wallace[2]

ABSTRACT

Field measurement of soil moisture is undertaken traditionally using point based measurement techniques such as neutron probes or time domain reflectrometry (TDR). Recently, a new technique has been developed that can be used to derive soil moisture at larger spatial scales by measuring neutrons that are generated by cosmic rays within the air and soil, and emitted back into the atmosphere. A study by Hendrick and Edge (1966) in the mid 1960s showed that the intensity of the fast neutrons above the ground varied with soil moisture content. The intensity of the neutron is mainly moderated by hydrogen ions located in the water and soil, and the density is inversely correlated with soil moisture. To soil scientists and hydrologists, this has opened up the possibility of measuring surface soil moisture automatically over an area of ~40 ha to a depth of ~0.5 m. The technique has the potential to fill the gap between point scale measurements (neutron probe or TDR) and soil moisture estimated using earth observation techniques (remote sensing). In Australia, 11 probes have been deployed across a range of agro-ecological zones to demonstrate the potential for larger scale soil moisture monitoring.

Key words: *soil water, cosmic rays neutrons, cosmOz, neutrons.*

INTRODUCTION

Ground-based soil moisture (θ_s) measurements have been used in a wide variety of applications including agriculture, hydrology, meteorology and in the calibration of satellites that can sense surface moisture remotely. Although highly valuable, most ground-based measurements of θ_s are made at a "point" (<1 dm^2) scale. The methods used vary from core samples (gravimetric or volumetric), TDR or capacitance probes or neutron probes. These measurements are at the point scale and it is therefore often difficult to obtain a sufficient number of θ_s values to capture the heterogeneity present in many landscapes. Quantifying the spatial variability in θ_s presents significant challenges and may preclude meaningful determination of temporal changes in soil water content.

Recently, Zreda *et al*. (2008) developed a technique to derive soil moisture estimates by measuring neutrons produced by cosmic rays. The method is based on the early observation by Hendrick and Edge (1966) showing the intensity of fast neutrons (energy 10 eV – 1000 eV) above the land surface was related inversely to the soil water content. Hydrologists and soil scientists have rediscovered this finding with the development of the cosmic rays technique. It opens up the possibility of measuring surface soil moisture automatically over an area of ~40 ha (Zreda *et al*., 2012). In summary, the sensor works by counting "fast" neutrons that are generated by cosmic rays as they pass through the Earth's atmosphere. At the land surface these neutrons are moderated by water molecules, and their count rate is predominantly a function of the water content of the soil.

METHOD

Details of the cosmic ray probe are given by Zreda *et al*. (2008, 2012) and Desilets, Zreda and Ferré, (2010). The theory behind the technique for measuring average soil moisture is given in Zreda *et al.* (2012). By placing the neutron detector above the ground surface, average soil water measurements can be made over horizontal footprint of hectares (ha), and to a soil depth of decimetres (dm). Figure 1a shows the typical installation of the sensor in Australia where the sensor is mounted above the soil surface. The mean free path of the fast neutrons is around 100 m, and therefore the sensor can detect neutrons from several hundred m away (Zreda *et al.*, 2008; Desilets, Zreda and Ferré, 2010). The depth to which the sensor can detect θ_s is dependent on the soil water content and is ~10 cm in wet soil and up to ~50 cm in dry soil (Franz *et al*., 2012a).

In 2010, CSIRO was the first organization in Australia to order 11 commercially available custom-designed cosmic ray soil moisture probes (CRS-1000, Hydroinnova, Albuquerque, NM, US). Together with university collaborators, these 11 sensors were deployed to form the CosmOz network (http://cosmos.hwr.arizona.edu /Probes/australia.php). It serves as a prototype Australian network of CRS-1000 probes designed to support sensor evaluation, research and the development of new sensor applications. The current network of 11 probes is deployed across the country in a range of soil types, vegetation cover and climates (Figure 1b).

RESULTS AND DISCUSSION

Experience to date has shown that the CRS-1000 probe needs to be calibrated for the local soil type to obtain accurate absolute (volume percent) values of θ_s. As the probe measures θ_s over such a large area, this is done by taking a large number (72) of gravimetric soil samples at distances up to 200 m from the probe (Franz *et al*., 2013). Once this calibration has been carried out, daily θ_s changes can be detected with an accuracy of ~0.02 percent. An example of the soil

1 CSIRO Land and Water, Christian Laboratory, Black Mountain, Canberra, ACT, Australia

2 CSIRO Land and Water, Australian Tropical Science and Innovation Precinct, James Cook University, Townsville, 4811, Queensland, Australia

* E-mail address of corresponding author: chris.j.smith @csiro.au

L.K. Heng, K. Sakadevan, G. Dercon and M.L. Nguyen (eds), Proceedings — International Symposium on Managing Soils for Food Security and Climate Change Adaptation and Mitigation. Food and Agriculture Organization of the United Nations, Rome, 2014: 387–390

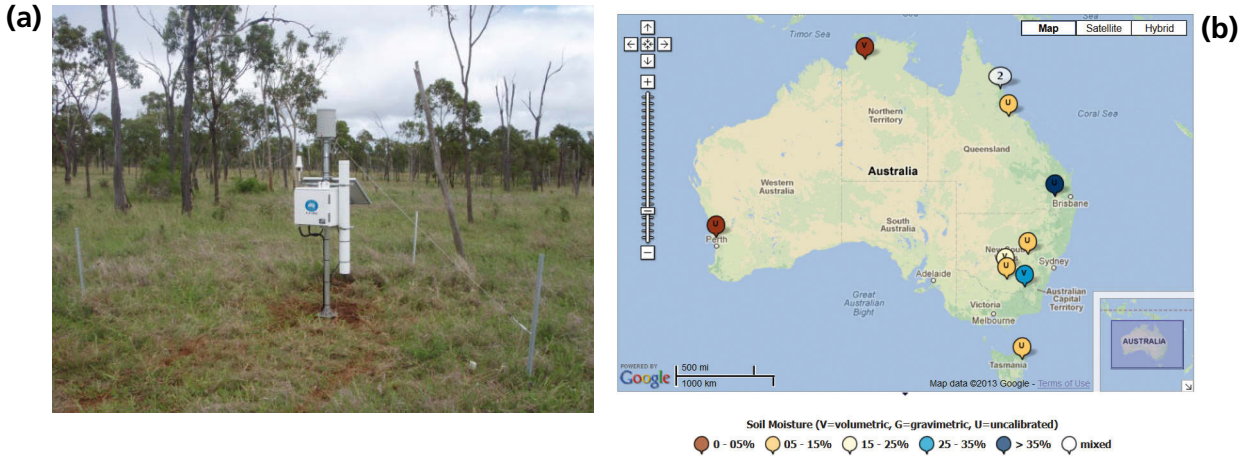

FIGURE 1. (a) A CRS-1 000 sensor installation on a grazed savannah hillslope in the dry tropics (Weany Creek, north Queensland). Picture (b) shows the locations of the current CosmOz network sites across Australia (http://cosmos.hwr.arizona.edu/Probes/australia.php).

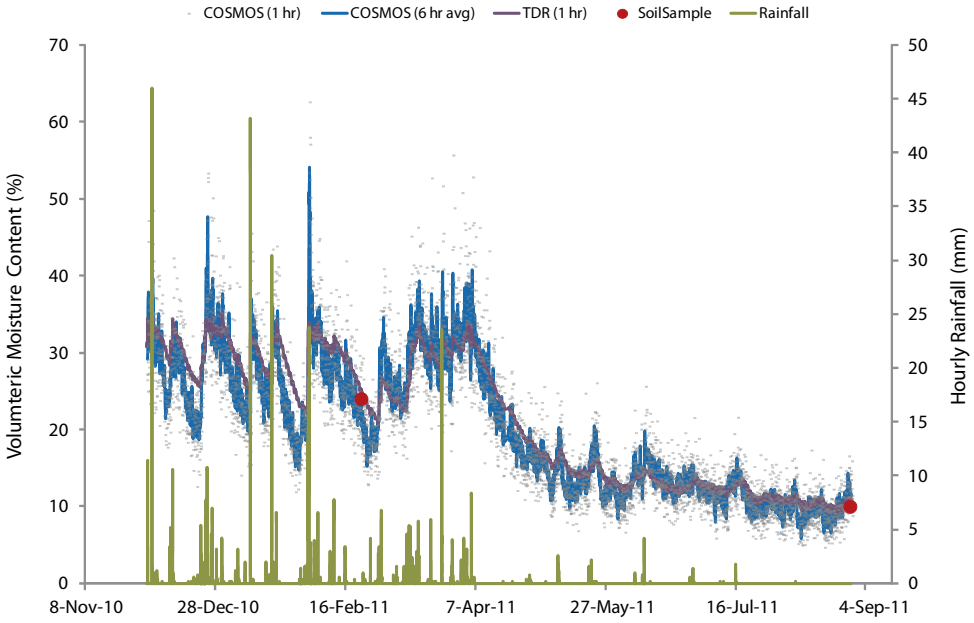

Figure 2. An example of the time series of θ_s (blue) recorded by the CosmOz probe at Weany Creek (northern Queensland). Also shown is the value of θ_s recorded using TDR probes (purple line) and rainfall (green). Two gravimetric sampling points (red) are also shown.

moisture data recorded by the CRS-1000 probe at a dry tropical site is shown in Figure 2. Over the wet season (December to April) frequent rain events raise the soil moisture content to near saturation (~40 percent) and these wetting events are followed by a period of soil drying (Figure 2). From April onwards there is little further rain and the CRS-1000 probe shows how the site dries progressively over the following months, dropping to ~10 percent by September. Figure 2 also shows the surface (0–30 cm) moisture content recorded by three conventional time-domain reflectometry (TDR) soil moisture probes. Although this is the average of only three point measurements, there is strong temporal coincidence between the TDR and CRS-1 000 time series. The CRS-1 000 soil moisture estimation equation was calibrated to the gravimetric calibration measurements made in February 2011 (Figure 2), but the second gravimetric sample in September provides an independent check of the CRS-1000 estimates.

There is significantly more variation in the soil moisture measured with the CRS-1000 probe as evidenced by the scatter in points and variation in the blue line. Less variation in water content is visible in the TDR data, because it is measuring over different depths in the soil. This is more obvious at the irrigated site (Figure 3), where there is a sharp increase in soil moisture in the surface 0.05 m shown in the TDR trace. This amplitude of the increase in θ_s is dampened in the CRS-1000 trace, showing that it is measuring the average water content over a different depth (volume) of soil, shown by the higher water content being measured with the TDR traces. These results are consistent with those reported in the literature (Franz *et al.*, 2012b).

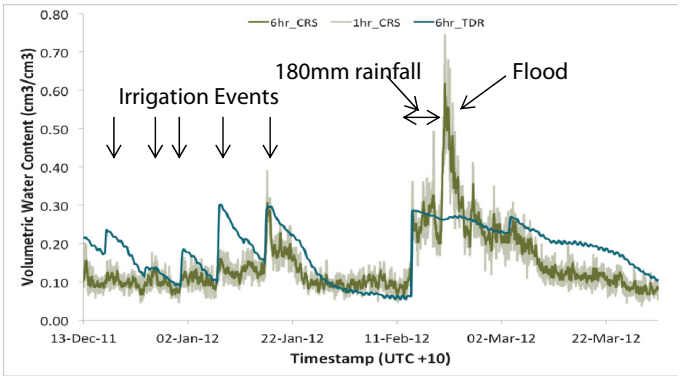

FIGURE 3. Time series of θ_s (green line) recorded by the CosmOz probe from an irrigated soil at Griffith. Also shown is the θs recorded using TDR probes (blue line).

The cosmic ray method for determining soil moisture content has some limitations. One limitation is the detection of hydrogen (H) atoms in other forms beside the soil water. For example, H can be found in the plants growing on the soil, in gypsiferous soils associated with the hydration of the calcium sulphate ($CaSO_42H_2O$) and the clay minerals that make up the soil (Schulze, 2002). Similarly, surface and/or flood water is measured as evidenced by the large increase in volumetric water content following 180 mm of rain at Griffith (Figure 3). If the hydrogen content is constant, as would be the case for clay minerals, its effect can be accounted for in the calibration and therefore largely becomes irrelevant. As with the neutron probe, if the calibration is done on pore and lattice water, the effect of the lattice water is handled in the calibration of the probe. However, the presence of lattice water must reduce the depth of measurement, and the effect will be most obvious in dry soil. If the hydrogen concentration varies with time as in the case with vegetation, it will become an unknown that may need to be determined to accurately quantify soil moisture content.

The depth of measurement depends on the water content and the amount of lattice water. Hydrogen in soil water or lattice water reduces the intensity of neutrons and the depth of measurement in the soil. That is, average soil water is measured to a greater depth in dry soils and to shallower depth in water or flooded soil. Recently, Franz *et al.* (2012a) presented the following equation to correct for soil lattice water:

$$z^* = \frac{5.8}{\rho_{bd}\tau + \theta + 0.0829}$$

where z^* is effective depth of the CRS probe (cm); ρ_{bd} is soil dry bulk density (g/cm^3); τ is weight fraction of lattice water in the mineral grains and bound water defined as the amount of water released at 1 000°C preceded by drying at 105°C (g water per g dry minerals, herein known as lattice water); and θ is volumetric pore water content (m^3/m^3). This effect is constant for any given soil and thus can be handled in the calibration.

Desilets and Zreda (2013) reported that the footprint of the CRS-1000 probe is inversely proportional to air density, and related linearly to the height of the sensor above the ground, up to a height of 125 m. There is no further impact as the height is increased. Soil moisture content has a small impact on the foot print, whereas atmospheric humidity has significant impact; reducing the foot print by 40 m for every 0.01 kg/kg increase in specific humidity. When quantifying θ_s, the effect of changes in atmospheric pressure (Rivera Villarreyes, Baroni and Oswald, 2011), incoming cosmic ray intensity (Zreda *et al.*, 2012) and atmospheric water vapour (Franz *et al.*, 2012a; Zreda *et al.*, 2012; Rosolem *et al.*, 2013) on neutron counts needs to be accounted for. Other corrections are outlined by Zreda *et al.* (2012).

The probe measures average soil moisture across a large spatial area and consequently, the site needs to be relatively uniform. Complex sites that have many different land uses would present a problem because the average water content of the different systems would be measured. Rivera Villarreyes, Baroni and Oswald, (2013) data highlights this effect as they found the calibration of the CRS-1000 probe to vary during the growing season of sunflower and winter rye. Although the neutron density was corrected for humidity, pressure, and lattice water, the CRS-1000 probe determined that the soil water content varied throughout the growing season. This probably reflects the change in the plant biomass that affects the determination of soil moisture content. The biomass of annual crops were found to change dramatically throughout the growing season and the relative water content in the above-ground vegetation ranged from 98 percent in young plant material (tillering) to 40 percent in mature plants (Teulat *et al.*, 1997). Although the relative water content was high at tillering, the mass of water (expressed on an area basis) in the biomass was low at the early stages of growth and increased significantly until maximum biomass was achieved, and then declined during maturation. For example, if there is a cereal biomass of 10 tons (t) per ha (dry weight), then it is likely to contain 15 t ha of water in the above-ground fresh material. For the purpose of comparison, a soil that has a 0.2 volumetric water content contains 200 t of water per ha in the surface 0.1 m. Thus water in the crop vegetation represents about 7 percent of the amount in the top 0.1 m of soil. Based on current knowledge and predictive capability of crop biomass using models such as the Agricultural Production Systems Simulator (APSIM), it should be possible to develop an algorithm that will correct for water in the biomass.

Because the CRS-1000 probe measures soil moisture content to different depths depending on the wetness of the soil, accurate estimates are difficult to obtain in shrink-swell soils (for example, Vertisol soils; Figure 4). When the soil is wet, the surface increases and at the same time, depth of measurement with the CRS-1000 probe would be reduced. When the soil is dry, the soil retracts (shrinks), the surface contracts and the depth of measurement with the CRS-1000 probe would increase. Although not tested, this could be solved by combining measurements with the CRS-1000 probe and the neutron probe, and using a water balance model coupled with model data fusion to integrate to a depth where there is zero change (Ringrose-Voase *et al.*, 2003).

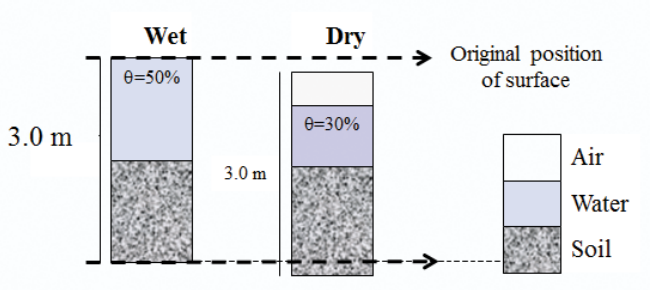

FIGURE 4. Conceptual diagram of the change in the soil surface of a Vertisol under wet and dry conditions.

Early results from the CosmOz network suggest that the CRS-1000 probe is capable of measuring near-surface soil moisture content in a range of soils and climates. The probe's large area sample creates potential uses for applications such as agricultural moisture availability monitoring and catchment scale rainfall-runoff forecasting in environments where antecedent soil moisture influences runoff generation. It may also have potential applications in weather modelling as well as short-term stream flow forecasting, where direct assimilation of ground measured soil moisture can improve forecasting. The larger scale of observation also means that the observations have applications in evaluating landscape-scale mean soil moisture estimates, for example those derived from models or from satellite remote sensing observations.

CONCLUSIONS

Results from the CosmOz network and published literature, confirm that the probes are capable of measuring near-surface soil moisture content in a large scale and in a range of soils and climates. They have the potential for use in: (i) agriculture, (ii) catchment-scale rainfall run off forecasting in environments where antecedent soil moisture influences runoff generation — however, this needs to be further tested to establish whether there are significant improvements in the predictions over the established methods, (iii) water balance assessments, and (iv) validation of soil water content obtained through remote sensing.

The large scale of observation also means that the observations have application in evaluating landscape-scale mean soil moisture estimates. The potential for data/model fusion (i.e. soil water balance coupled with vegetation and land-surface modelling) is exciting although there are some factors that need to be considered when using the probe. A key requirement is the selection of the site so that it matches the foot print of the probe (600 m). This needs to be of uniform land use and relatively uniform soils, as the probe measures average water content over this larger area. Calibration of the probe needs careful attention to include the effect of water stored in the vegetation and soil lattice water. The depth of measurement changes with water content. A cosmic ray probe has significant potential to quantify the average water content across a large area, but this needs to be validated with further research covering a range of soil types, including shrink-swell soil, differing hydrological regimes and different land-uses. Water in vegetation, especially for growing crops, needs to be quantified, and methods to correct for this effect are being developed.

REFERENCES

Desilets, D., Zreda, M. & Ferré, T.P.A. 2010. Nature's neutron probe: Land surface hydrology at an elusive scale with cosmic rays. Water Resour. Res., 46: W11505, doi:10.1029/2009WR008726, 2010.

Desilets, D. & Zreda M. 2013. Footprint diameter for a cosmic-ray soil moisture probe: Theory and monte carlo simulations. Water Resour. Res., DOI: 10.1002/wrcr.20187.

Franz, T.E., Zreda, M., Ferre, T.P.A., Rosolem, R., Zweck, C., Stillman, S., Zeng, X. & Shuttleworth, W.J. 2012a. Measurement depth of the cosmic ray soil moisture probe affected by hydrogen from various sources. Water Resour. Res., 48: W08515, doi:10.1029/2012WR011871.

Franz, T.E., Zreda, M., Rosolem, R. & Ferre, P.A. 2012b. Field validation of cosmic-ray soil moisture sensor using a distributed sensor network. Vadose Zone J., 11: doi:10.2136/vzj2012.0046.

Franz, T.E, Zreda, M., Rosolem, R. & Ferre, T.P.A. 2013. A universal calibration function for determination of soil moisture with cosmic-ray neutrons. Hydrol. Earth Syst. Sci., 17: 453–460.

Hendrick, L.D. & Edge, R.D. 1966. Cosmic-ray neutrons near earth. Phys. Rev., 145: 1023.

Rivera Villarreyes C.A., Baroni G. & Oswald S.E. 2011. Integral quantification of seasonal soil moisture changes in farmland by cosmic-ray neutrons. Hydrol. Earth Syst. Sci., 15: 3843–3859.

Rivera Villarreyes C.A., Baroni G. & Oswald S.E. 2013. Calibration approaches of cosmic-ray neutron sensing for soil moisture measurement in cropped fields. Hydrol. Earth Syst. Sci. Discuss., 10: 4237–4274. DOI: 10.5194/hessd-10-4237-2013

Ringrose-Voase A.J., Young R.R., Paydar Z., Huth N.I., Bernardi A.L., Cresswell H.P., Keating B.A., Scott J.F., Stauffacher M., Banks R.G., Holland J.F., Johnston R.M., Green T.W., Gregory L.J., Daniells I., Farquharson R., Drinkwater R.J., Heidenreich S. & Donaldson S. 2003. Deep drainage under different land uses in the Liverpool Plains catchment. Report 3, Agricultural Resource Management Report Series. NSW Agriculture.

Rosolem, R., Shuttleworth, W.J.; Zreda, M., Franz, T.E., Zeng, X. & Kurc, S. 2013. The effect of atmospheric water vapor on neutron count in the cosmic-ray soil moisture observing system. J. Hydrometeorol., (in review).

Schulze, D.G. 2002. An introduction to soil mineralogy. *In* J.B. Dixon & D.G. Schulze, eds. *Soil mineralogy with environmental applications,* pp. 1–37. Book Series No. 7. Madison, WI, Soil Science Society of America.

Teulat, B., Monneveux, P., Wery, J., Borries, C., Souyris, I., Charrier, A. & This, D., 1997. Relationships between relative water content and growth parameters under water stress in barley: A QTL study. New Phytol., 137: 99–107.

Zreda, M., Desilets, D., Ferre, T.P.A. & Scott, R.L. 2008. Measuring soil moisture content non-invasively at intermediate spatial scale using cosmic-ray neutrons. Geophys. Res. Lett., 35: L21402, doi:10.1029/2008GL035655.

Zreda, M, Shuttleworth, W.J., Zeng, X., Zweck, C., Desilets, D., Franz, T., Rosolem, R. & Ferre, T.P.A. 2012. COSMOS: The COsmic-ray Soil Moisture Observing System. Hydrol. Earth Syst. Sci. Discuss., 9: 4505–4551.

Assessing Essential and Toxic Elements in Rabbit Manure and Rock Phosphate Fertilizers Using Nuclear Techniques: A Contribution to Managing Nutrient Resources for Improved Small-Stock/Crop Integration

A.C. Avelar [1,2,*], W.M. Ferreira[1] and M.A.B.C. Menezes[2]

ABSTRACT

Industrial phosphate fertilizers are currently the major source of phosphorus for agricultural activities. Many authors maintain that the addition of organic amendments such as manure can ameliorate disturbed soils by improving some characteristics including the available phosphorus (P) in the soil. Furthermore, these products may provide macro elements such as nitrogen (N) and calcium, essential microelements and toxic contaminants. This study deals with uranium content in rabbit manure and six most common phosphates applied in Brazil. Results are compared with values from four other phosphates mined around the world. The nuclear analytical method applied was the delayed neutron technique (DNT) which is a highly precise, affordable, fast (short turnaround) instrumental technique. Three phosphates had uranium content above 145 µg/g, while rabbit manure, a high N, P and potassium (K) organic amendment contains only 2.7 µg/g of uranium. Additionally, neutron activation analysis, a sensitive multi-elemental nuclear analytical technique was used to identify essential and toxic elements in the rabbit manure and a rock phosphate, one of most inexpensive and popular fertilizers available in the Brazilian market. Results for arsenic, barium, bromine, cobalt, chromium, fluorine, iron, sodium, thallium, zinc and K are presented in order to help decision-making concerning strategies for fertilizer-soil-crop management that are both agronomically and environmentally viable. High contents of some toxic elements demonstrate the need to evaluate deposition of contaminants released by fertilizers on farmland, the wider environment and the entire food chain.

Key words: *rock phosphate, rabbit manure, delayed neutron technique, neutron activation, uranium, zinc, arsenic.*

INTRODUCTION

The UN Food and Agriculture Organization (FAO, 2006) recognizes that small farmers play a critical role in improving food security in the 21st century. If well managed, peri-urban and rural small-scale horticulture and small stock rearing and marketing could provide fresh food commodities and nutrients for a significant section of low-income populations, as well as offering a means of self-employment and income generation.

Tropical soils, a feature of some Brazilian farmland, are one impediment to realizing the full potential of small-scale farming, since they usually possess limited phosphorus (P) reserves and have a high absorbing capacity, properties that are not suitable for horticulture. Indeed, P deficiency in crops is an important constraint to plant and animal yields, especially in the hot and humid tropics where soils are predominantly acidic and often extremely P deficient with high P fixation capacities (FAO/IAEA, 2004).

The addition of organic fertilizers such as manure which is available on-farm and cost-free, can ameliorate soil deficiencies by improving their chemical and physical properties as long as the manure is high in nitrogen (N), P and potassium (K) and thereby improves fertility, increases biomass production, and enhances carbon storage in the soil (Shrestha and Lal, 2006).

Rabbit manure itself is a high quality fertilizer, in terms of N, P and K contents (FAO, 2011a and b).

Mineral phosphate fertilizers are currently the major source of P in agriculture (FAO/IAEA, 2004) Phosphates are defined as compounds which contain phosphorus-oxygen (P–O) linkages. The P–O bond has a length of 1.62 Å with bond angles of 130° at the oxygen atoms and 102° at the P atoms in the pentoxide P_2O_5, the most important oxide of P produced commercially (Sauchelli, 1965; Raschshi and Finch, 2000).

Phosphates are found naturally in rocks that form vast deposits of minerals in the strata of the earth but few phosphate sites are mined around the world. About 90 percent of world production is used to manufacture fertilizers, with the remainder being used to manufacture animal feeds, detergents and chemicals (FAO/IAEA, 2004).

Nowadays, sedimentary ore deposits provide about from 80 to 90 percent of world phosphate production (FAO/IAEA, 2004). However, igneous deposits make up 80 percent of Brazil's national reserves, the major deposits being located in the following federal states: Bahia, Ceará, Goiás, Minas Gerais, Pará, Paraíba, Pernambuco,

1 DZOO Department of Animal Sciences, Veterinary School, Universidade Federal de Minas Gerais (UFMG), Avenida Antonio Carlos, 6627 Campus UFMG, Pampulha, Belo Horizonte, Brazil
2 Nuclear Technology Development Centre, Brazilian Nuclear Energy Commission, Rua Mario Werneck, s/n, Predio 1, Campus UFMG, Pampulha, Belo Horizonte, Brazil
* E-mail address of corresponding author: avelara@ufmg.br

L.K. Heng, K. Sakadevan, G. Dercon and M.L. Nguyen (eds), Proceedings — International Symposium on Managing Soils for Food Security and Climate Change Adaptation and Mitigation. Food and Agriculture Organization of the United Nations, Rome, 2014: 391–311

Santa Catarina, Rio Grande do Norte e São Paulo. Most, however, are concentrated in the states of Minas Gerais, Goiás and São Paulo (DNPM, 2010).

In 2009, the Brazilian domestic market produced about of 5 434 022 tonnes (t) of concentrated phosphate rock, production being used for fertilizers (89 percent), animal feed (seven percent), soil amendments (one percent) and the remainder for a variety of other purposes (DNPM, 2010). Phosphate rocks may contain accessory-gangue minerals and impurities that can be hazardous to man and animal health such as arsenic, cadmium, lead, fluorine and uranium (Tokarnia *et al.*, 2000), and uranium ores in some phosphate mining sites are processed as a by-product of the fertilizer industry (USGS, 2002).

Uranium is the heaviest natural element in nature; it is hazardous to human and animal health because of both its radioactivity and chemical toxicity. In nature, uranium is more plentiful than silver (Ag) and about as abundant as molybdenum (Mo) or arsenic (As) (ASTDR, 1999). Practically every phosphate rock contains uranium, although the amounts of this and other hazardous elements vary widely among sources and even within the same deposit. Thus, mining, milling, industrializing and using phosphate products in soil and animal nutrition are anthropogenic activities increasing the potential for human exposure to uranium (Mangini *et al.,* 1979; ASTDR, 1999; FAO/IAEA, 2004).

Figure 1 provides an outline of nutrient and contaminant flows in the environment, including P flows from fertilizers and manure. Absorption of essential and toxic elements by humans and animals is mostly by oral ingestion of food, feed and water, but inhalation and dermal contact can lead to some absorption in particular cases. Workers in agriculture are more likely to be exposed to uranium, especially those applying phosphates on farmland.

The general public is also potentially exposed when eating root vegetables like potatoes grown on uranium contaminated soil. Besides the ingestion of foods, drinking uranium-contaminated potable waters is also a route for uranium to enter into the animal organism (Mangini *et al.*, 1979; ASTDR, 1999).

Studies in the 1970´s provided evidence for increasing uranium presence in rivers and ground water in regions with intensive use of fertilizers in agriculture. Uranium derived from phosphate fertilizers is likely to be adsorbed on the uppermost soil layers and its content in the water is correlated with the bicarbonate (HCO_3^-) content in the river (Mangini *et al*., 1979).

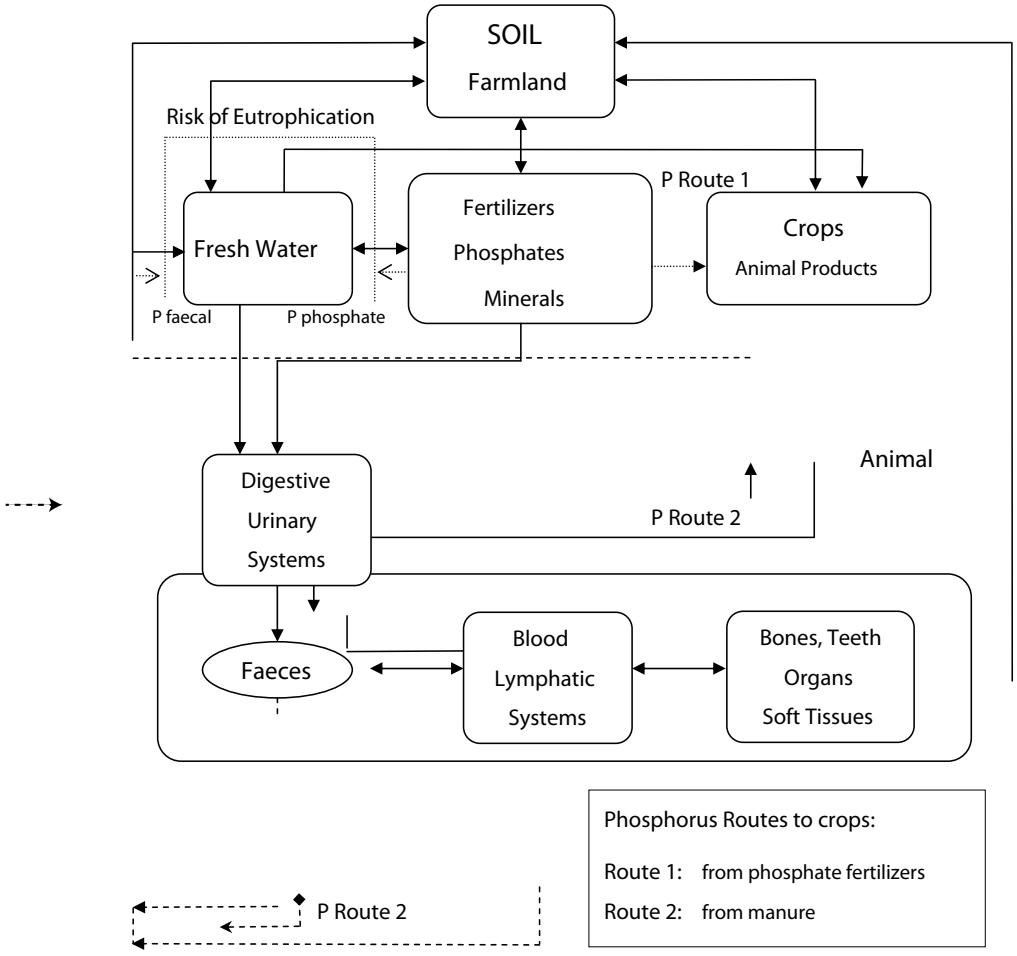

FIGURE 1. Biogeochemical flow of nutrients and contaminants in the environment, including phosphorus routes from fertilizers and manure.

Many phosphates have the ability to accumulate uranium and other toxic elements. These abilities may be used in the recovery of various useful metals from aqueous systems (El Shall *et al.,* 1993).

To face the main constraint of low inherent P in feeds, soils and plants, rock phosphates and manure are likely to be more widely applied in agriculture, raising the possibility that these sources may release contaminants from the farmland into the wider environment (Mangini *et al*., 1979; Scholten and Timmermans, 1996). Against this background, a study was made of the chemical content of selected agricultural products in Brazil.

Uranium content can be determined by some nuclear techniques including the delayed neutron technique, a precise, fast (short turnaround), sensitive, affordable and non-destructive method (DNT, 2013). The method is based on exposing the sample to neutrons in a research reactor, where fission of its uranium-235 (^{235}U) in the nucleus absorbs a neutron from the neutron flow, forming an instable, highly energetic nucleus uranium-236 (^{236}U). This unstable nucleus mostly fissions into two medium-sized nuclei emitting 2–3 neutrons as follows:

$$^{235}U_{\text{ in sample}} + \text{neutron}_{\text{ thermal, from reactor fuel}} \rightarrow {}^{236}U_{\text{ instable}} \rightarrow {}^{90}Kr + {}^{143}Ba + 3 \text{ neutrons}$$

Very quickly ($< 10^{-12}$ seconds after the fission) 99 percent of the neutrons, so-called "prompt neutrons" are emitted. The remaining neutrons are emitted from 0.0001 s up to several min later and are called "delayed-neutrons". These delayed-neutrons can be detected easily and precisely since their parameters are well known (DNT, 2013). Neutron activation analysis (NAA) was also used to measure levels of a wider range of elements. This method is based on the interaction of radiation (from the reactions occurring in the reactor) with matter (in the sample). When one natural element (present in the sample) is exposed to a neutron flux, the reaction occurs. The radionuclide formed emits gamma radiation which can be measured by suitable equipment. About 70 percent of elements have nuclides possessing properties suitable for NAA. At the Nuclear Technology Development Centre (CDTN) of the National Nuclear Energy Commission (CNEN), Belo Horizonte, Brazil, there is a TRIGA MARK I IPR-R1 nuclear reactor for application of this technique. k0- based reactor neutron activation analysis (k0-NAA), is an advanced type of NAA in which the sample is irradiated without previous chemical preparation. This specific method is based on k0 factors and some reactor radiatio n parameters. The NAA technique is more expensive than most analytical techniques and takes up to 90 d to measure long-lived elements (Avelar *et al*., 2002).

MATERIALS AND METHODS

Fertilizer samples and preparation

Phosphate fertilizers were acquired in the local market of Minas Gerais State, Brazil. Aliquots of about 100 g were taken randomly from each commercial pack and grounded to obtain a particle size of 200 Tyler mesh (75 µm) and establish 99 percent conformity of particle size of each product. An aliquot of 1.00 g ground phosphate was taken for analysis. The capsule filled with the sample was placed in a polyethylene container (vial) for the pneumatic transporting system.

Experimental animals, collection and preparation of faecal samples

Twenty-four young rabbits (30 d old) were used in the study; hard faeces samples were separated from urine and collected twice daily during the 42-d experiment, which is the average time needed for rabbits to achieve the commercial live weight of 2.0 kg.

Faeces were placed in a plastic bag (one per animal) and stored in a –20°C freezer to minimize odour and to avoid losses. A sub-sample of approximately 1 000 g from each animal was taken from the bulk manure collected during 42 d, frozen at –70°C and lyophilized. Each freeze-dried sample was powdered, homogenized and around 1.00 g was taken and sealed into polyethylene irradiation vials.

Sample analyses

Samples and standards in the vials were placed individually into the neutron flux using the pneumatic transport system of the reactor IPR-R1 at the CDTN/CNEN. The reactor was operated at 1 kW thermal power under a neutron flux of 6.6×10^{11} neutrons cm^2/s. After 60 s, samples were transported automatically out of the reactor direct to the counting room containing a measuring system consisting of a metal box filled with paraffin moderator. Six detectors (^3He filled and connected in parallel) were positioned symmetrically in order to carry out the detection. The detectors send pulses to the accompanying electronic devices, the first of which are amplified, sorted by a discriminator and the selected pulses counted in an electronic analyzer for 40 s. A decay-curve for the delayed neutrons was established as an array of 40 counts and the uranium content of samples determined by comparing their delayed-neutron intensity with those from two well-defined uranium standards from the IAEA.

For the NAA, three schemes of irradiation were undertaken: for short, medium and long half-life elements. All samples were irradiated at the CDTN/CNEN IPR-R1 reactor. After suitable decay times, gamma spectroscopy was performed in an HPGe detector with a 10 percent efficiency, connected to a multichannel analyzer. Concentrations were calculated using KayZero/Solcoy software. The only element studied with an alternative method was fluoride which was assessed by potentiometry, a well-established method (Institute of Medicine, 1997).

RESULTS

TABLE 1. Uranium content expressed as ratio of phosphorus concentration

Phosphorus Sources	Uranium Content (µg/g)
Super Simple SSP, 17% P_2O_5, Brazil	52 ± 5[a]
Dicalcium DCP, 46% P_2O_5, Brazil	181 ± 9[a]
Mono-ammonium MAP, 50% P_2O_5, Brazil	189 ± 9[a]
Triple TSP, 43% P_2O_5, Brazil	32 ± 4[a]
Phosphate Rock, 24% P_2O_5, Brazil	39 ± 4[a]
Phosphate Rock *Arad*, 31% P_2O_5, Israel	145 ± 7[a]
Phosphate Rock, 31% P_2O_5, USA	59[b]
Phosphate Rock, 33% P_2O_5, Morocco	82[b]
Phosphate Rock, 29% P_2O_5, Mali	123[b]
Phosphate Rock, 28% P_2O_5, Tanzania	390[b]
Rabbit manure (fresh content)	2.7 ± 0.5[a]

a — experimental results by DNTe, phosphates (n = 8) and rabbit manure (n = 24)

b — data from FAO/IAEA (2004)

TABLE 2. Average elemental content of rabbit manure (n = 24) and *Arad* rock phosphate (n = 8)

Elements	Rabbit Manure (µg/g)	Rock Phosphate (µg/g)
As	2.0 ± 0.5	22.5 ± 2.7
Ba	986 ± 167	17 209 ± 981
Br	1.9 ± 0.3	1.7 ± 0.3
Co	5.3 ± 0.6	14.3 ± 1.9
Cu	535 ± 48	561 ± 59
F	234 ± 112	32 500 ± 2974
Fe	3 448 ± 201	3 930 ± 208
K	5 903 ± 513	4 723 ± 455
Na	1 134 ± 101	1 100 ± 98
Th	0.54 ± 0.21	12.9 ± 1.1
Zn	244 ± 45	390 ± 52

DISCUSSION

Application of rabbit manure (Table 1) does not pose a risk to increasing the uranium concentration in farmland since the average uranium concentration in the earth's crust ranges from 2 to 4 µg/g (EPA, 1999), the same average value of the uranium content in the rabbit manure. The results also imply that from environmental standpoint, rabbit manure would be an advantageous addition to application of rock phosphates.

Concentrations of uranium were, however, quite variable in both the rock phosphates and animal manure. Differences among fertilizers (Table 1) might be due to the region of exploitation of the phosphate ores, implying different ages of mineralization, deposit types and associated accessory minerals, and by methods of industrial production.

In both rabbit manure and rock phosphates, some essential elements and some elements classified as hazards and toxic elements by the ATSDR were detected (Tables 1 and 2). These included arsenic, barium, cobalt, fluoride, thorium, uranium and zinc. Noteworthy, were the high levels of arsenic, fluoride and uranium in the rock phosphate fertilizer. The concentrations measured of these hazardous elements are at least ten times higher than those found in the rabbit manure.

Since the 1990's, Canada has placed limits on maximum acceptable cumulative metal additions to soil and maximum acceptable metal concentrations in products. For instance, the maximum acceptable zinc concentration in phosphates and manure is 1 850 mg/kg dry weight (EPA, 1999). Also, European legislation has reduced the maximum permitted level of Zn and Cu supplementation in livestock diets to minimize the environmental impact of manure disposal in the soil and waterbeds (European Commission, 2003).

CONCLUSIONS

Results indicate that the choice of fertilizers plays a key role in the control of contaminant flow in agricultural activities. In this sense, rabbit manure poses the smallest potential for being a hazard among those studied. This advantage should be even greater through time considering long-term exposure due to successive fertilizer applications over the years.

Uranium and other toxic elements in fertilizers should be investigated since these elements are normal constituents of many phosphates, and the monitoring of their presence in manure and chemical fertilizers and in applied soils should be fundamental for current and future agricultural activities in many parts of the world. Proactive measures should also be taken to avoid unnecessary exposure of humans, animals and the wider environment to these elements.

ACKNOWLEDGEMENTS AND DISCLAIMER

This project is supported by the Brazilian Agencies: CNPq and FAPEMIG. Statements and opinions expressed in this paper are those of the authors, and do not necessarily reflect those of the organizations with which they are affiliated. The authors do not endorse any product or equipment mentioned herein.

REFERENCES

ASTDR (Agency for Toxic Substances and Disease Registry of the United States). 1999. *Toxicological profile for uranium.* Washington, DC, United States Department of Health and Human Services. 379 pp.

Avelar, A.C., Veado, J.C. & Menezes, M.A.B.C. 2002. Study of essential elements in cattle tissues from a tropical country using neutron activation analysis. *Food Nutr. Bull.,* 23: 237–240.

Das, M., Ganguly, A. & Haldar, P. 2010 Nutrient analysis of grasshopper manure for soil fertility enhancement *Am. Euras. J. Agric. & Env. Sci.*, 7: 671–675.

DNPM (National Department of Mineral Production of Brazil). 2010. *Mineral Report / Informe Mineral 2010,* Brazilian Ministry of Mines and Energy, Brasilia, 871pp. (in Portuguese).

DNT (Department of Nuclear Techniques). 2013. *Determination of delayed neutron parameters.* Budapest, University of Technology and Economics. (http://www.reak.bme.hu/Wigner_Course/WignerManuals/Budapest/BpmanualPDF.PDF).

El-Shall, H., Moudgil, B.M. & Wiegel, R. 1993. *Beneficiation of phosphate: Theory and practice.* Littleton-Colorado, SME Inc.

EPA (United States Environmental Protection Agency). 1993. *Background report on fertilizer use, contaminants and regulations*. (http://www.epa.gov/oppt/pubs/fertilizer.pdf).

European Commission. 2003. *Commission Regulation (EC) No 1334/2003 of 25 July 2003 amending the conditions for authorization of a number of additives in feedingstuffs belonging to the group of trace elements*. Brussels, Official Journal European Communities L187.

FAO. 2006. *More fruits and vegetables*. (http://www.fao.org/ag/magazine/0606sp2.htm).

FAO. 2011a. *On-farm composting methods,* by R.V. Misra and R.N. Roy. (http://www.fao.org/organicag/doc/on_farm_comp_methods.pdf).

FAO. 2011b. The role of monogastric and small stock, by T.S. Dhaubhadel. In *Sustainable livestock production in the mountain eco-system of Nepal* (http://www.fao.org/DOCREP/004/T0706E/T0706E06.htm).

FAO/IAEA. 2004. *Use of phosphate rocks for sustainable agriculture.* Rome. 144 pp.

Institute of Medicine. 1997. *Dietary reference intakes for calcium, phosphorus, magnesium, vitamin D, and fluoride*. Washington, DC, National Research Council. 449 pp.

Mangini, A., Sonntag, C., Bertsch, G. & Müller, E. 1979. Evidence for a higher natural uranium content in world rivers. *Nature,* 278: 337–339.

Rashchi, F. & Finch J.A. 2000 Polyphosphates: A review of their chemistry and application with particular reference to mineral processing *Mineral. Engin.,* 13: 1019–1035.

Sauchelli, V. 1965. *Phosphate in agriculture*. Boca Raton, Reinhold Publishing Corporation. 30 pp.

Scholten, L.C. & Timmermans C.W.M. 1996. Natural radioactivity in phosphate fertilizers. *Fert. Res.,* 43: 103–107.

Shrestha, R.K. & Lal, R. 2006. Ecosystem carbon budgeting and soil carbon sequestration in reclaimed mine soil. *Environ. Intern.,* 32: 781–796.

Tokarnia, C.H., Döbereiner, J. & Peixoto, P.V. 2000 Deficiências minerais em animais de fazenda, principalmente bovinos em regime de campo *Pesq. Vet. Bras*., 20: 127–138.

USGS (United States Geological Survey). 2002 *Data set of world phosphate mines, deposits, and occurrences — Part A. Geologic data,* by C.B. Chernoff1 & G.J. Orris. Reston, VA, USGS. 352 pp.

List of abbreviations

AGRA	Alliance for a Green Revolution in Africa
ANOVA	Analysis of variance
BNF	Biological nitrogen fixation
CA	Conservation agriculture
CEC	Cation exchange capacity
CGIAR	Consultative Group on International Agricultural Research
CIAT	Centro Internacional de Agricultura Tropical
CID	Carbon isotope discrimination
COSMOS	Cosmic-ray soil moisture observing system
CR	Count ratio
CRDS	Cavity ring down spectroscopy
CRP	Coordinated research project
CSIRO	Commonwealth Scientific and Industrial Research Organization
CSSI	Compound-specific stable isotopes
CT	Conventional tillage
CWP	Crop water productivity
δ	Delta value
DAP	Days after planting
DEM	Digital elevation model
DGPS	Differential global positioning system
DI	Deficit irrigation
DOC	Dissolved organic carbon
DPM	Disintegrations per minute
DSM	Digital surface model
E	Evaporation
EA	Elemental analyzer
EC	Electrical conductivity
EPA	Environmental Protection Agency, USA
ET	Evapotranspiration
ETc	Crop evapotranspiration or actual evapotranspiration
ETo	Reference evapotranspiration
FACE	Free-air carbon dioxide enrichment
FAO	Food and Agriculture Organization
FC	Field capacity
FRN	Fallout radionuclide
FNUE	Fertilizer nitrogen use efficiency
GAP	Good agricultural practices
GC-IRMS	Gas chromatography–isotope ratio mass spectroscopy
GHG	Greenhouse gas emissions
GIS	Geographic information systems
GMWL	Global meteoric water line
GPS	Global positioning system
HI	Harvest index
IAEA	International Atomic Energy Agency
ICP-MS	Inductively coupled plasma mass spectrometry
ICT	Information and communication technology
IITA	International Institute of Tropical Agriculture
IPCC	Inter-Governmental Panel on Climate Change
IRRI	International Rice Research Institute
IT	Information technology
IMB	Isotope mass balance
ISFM	Integrated soil fertility management
KC	Crop coefficient
LADA	Land degradation assessment in drylands
LAI	Leaf area index
LMWL	Local meteoric water line
LSC	Liquid scintillation counter
LSD	Least significant difference
Ndfa	Nitrogen derived from atmosphere

Ndff	Nitrogen derived from fertilizer
Ndfs	Nitrogen derived from soil
NT	No-till
OM	Organic matter
PAE	Phosphorus acquisition efficiency
PAR	Photosynthetic available radiation
PAWC	Plant available water holding capacity
PPMV	Part per million by volume
PTFs	Pedotransfer functions
PUE	Phosphorus utilization efficiency
RH	Relative humidity
RMSE	Root mean square error
SE	Standard error
SLM	Sustainable land management
SOC	Soil organic carbon
SOM	Soil organic matter
SPAC	Soil–plant–atmosphere continuum
SSA	Sub-Saharan Africa
T	Transpiration
TDR	Time domain reflectrometry
TDS	Total dissolved solids
TE	Transpiration efficiency
TLU	Tropical livestock unit
TU	Tritium unit
USDA	United States Department of Agriculture
USLE	Universal soil loss equation
VPD	Vapour pressure deficit
VPDB	Vienna Pee Dee Belemnite
WUE	Water use efficiency

Managing Soils for Food Security and Climate Change Adaptation and Mitigation

This publication is a compilation of selected papers presented at the International Symposium on "Managing Soils for Food Security and Climate Change Adaptation and Mitigation". Six thematic topics were covered: (i) managing soils for crop production and on-farm and area-wide ecosystem service efficiency; (ii) preserving and protecting soil resources; (iii) establishing soil and water conservation zones for pollution control; (iv) managing soils for climate change adaptation and mitigation through increasing soil carbon stocks (C sequestration) and reducing greenhouse gas emissions; (v) managing agricultural water for climate change adaptation; and (vi) recent advances in nuclear techniques and applications in land management research.

It is hoped that the information presented in these Proceedings provides valuable guidance to scientists and land managers in both the public and private sectors, as well as to government and institutional policy- and decision-makers involved in addressing land management issues for climate smart agriculture and the conservation of natural resources for agricultural productivity and food security.

IAEA
Joint FAO/IAEA Programme
Nuclear Techniques in Food and Agriculture

ISBN 978-92-5-108552-3

I4035E/1/09.14